APPLICATIONS OF STATE DEPENDENT MODELS IN FINANCE

Bo Guan

A thesis submitted to Cardiff University in partial fulfillment of the requirements for the degree of

Doctor of Philosophy

Cardiff Business School

Wales, United Kingdom

September 2020

DECLARATION

STATEMENT 1 This thesis is being submitted in partial fulfilment of the requirements for the degree of … (*insert PhD, MD, MPhil, etc., as appropriate*)

Signed _____

Date _____

STATEMENT 2

This work has not been submitted in substance for any other degree or award at this or any other university or place of learning, nor is it being submitted concurrently for any other degree or award (outside of any formal collaboration agreement between the University and a partner organisation)

Signed _____

Date _____

STATEMENT 3

I hereby give consent for my thesis, if accepted, to be available in the University's Open Access repository (or, where approved, to be available in the University's library and for inter-library loan), and for the title and summary to be made available to outside organisations, subject to the expiry of a University-approved bar on access if applicable.

Signed _____

Date. _____

DECLARATION

This thesis is the result of my own independent work, except where otherwise stated, and the views expressed are my own. Other sources are acknowledged by explicit references. The thesis has not been edited by a third party beyond what is permitted by Cardiff University's Use of Third Party Editors by Research Degree Students Procedure.

Signed _____

Date _____

WORD COUNT 34465 words

(Excluding summary, acknowledgements, declarations, contents pages, appendices, tables, diagrams and figures, references, bibliography, footnotes and endnotes

ACKNOWLEDGEMENTS

I would like to express my deepest gratitude to my supervisory team, and especially to Professor Saeed Heravi. He provided me with excellent supervision in every aspect of the research process, such as discussing methodological and empirical points, and the structure of this thesis. The thesis would not have reached its present form without his support, and the huge amount of time he dedicated to supervising me. I enjoyed every single moment under his supervision and learned a huge amount from him.

I am also grateful to Professor Atanu Ghoshray and Professor Arman Eshraghi for examining my thesis and for their valuable comments and kind suggestions.

I would also like to thank Professor Khelifa Mazouz and Dr. Joshy Easaw for providing me with support and guidance throughout my Ph.D. I would further like to thank Dr. Peter Morgan for conducting a regular review process with the supervisory team for me.

Last but not least, I wish to thank my parents for supporting me and motivating me throughout the past few years. With their care and nurturing, I was able to concentrate comfortably throughout my Ph.D journey with nothing to worry about.

ABSTRACT

The State-Dependent Model (SDM) prescribes specific types of nonlinearity with linearity as special cases and can identify structural breaks within a time series. In a simulation study of various time series models, the SDM technique was able to capture the true type of linearity/non-linearity in the data. This thesis makes among the first attempts to apply the SDM to business, economics, and financial data. Its application to business cycle indicators suggests the presence of significant nonlinearity in most industrial production sectors, but the results are inconclusive in terms of symmetric or asymmetric nonlinearity. The SDM was also used to test Purchasing Power Parity. The study found that the real exchange rates (against the US dollar) for the Pound, Euro, Yen, are globally mean reverting with ESTAR characteristics, Brazilian Real as random walk, and that the PPP holds consistently for GBP/USD and JPY/USD. Additional analysis indicated that the higher the uncertainty level, the higher the degree of mean-reverting these real exchange rates have, and uncertainty events result in instantaneous shocks in real exchange rates before mean reversion took place. Finally, the forecasting performance of the SDM models was investigated and compared with the linear ARIMA, ETS, and Neural Network Autoregressive models. Employing two sets of real data, the study found that the SDM models possess superior forecasting ability in long-term forecasts for industrial production and Japanese tourism data.

Table of Contents

This page intentionally left blank

Introduction

This thesis contains a collection of applications of the general State Dependent Model (SDM) in the fields of business, finance, and economics. Chapter 1 provides a general introduction to linear models and different classes of nonlinear models. Chapter 2 presents the methodology of the traditional recursive autoregressive SDM. These chapters are then followed by four empirical chapters. Chapter 3 applies the SDM to simulated data from various linear and non-linear time series models. Chapter 4 examines the nonlinearity and structural breaks in business cycle indicators. Chapter 5 applies the SDM model to a multivariate form by testing Purchasing Power Parity conditions and exploring how real exchange rates for GBP/USD, EUR/USD, JPY/USD, and BRL/USD behave at different levels of global uncertainty. Chapter 6 evaluates the forecasting performance of the SDM. The SDM models were extended by incorporating a smoothed and unsmoothed grid-search method and examining the forecasting ability of the three variants of the SDM models. Chapter 7 provides a discussion and concludes the thesis.

This page intentionally left blank

Chapter 1 Linear and Nonlinear Time Series Processes

1.1 Introduction

Linear time series models provide the basic building blocks of time series analysis. A good understanding of linear techniques is a crucial step towards analysing nonlinear time series methods. The first part of this chapter provides an overview of linear time series models, typically the general class of Autoregressive Integrated Moving Average (ARIMA) models, then the second part introduces nonlinear processes, including the Smooth Transition Autoregressive (STAR) models, Artificial Neural Network (ANN), Singular Spectrum Analysis (SSA), etc. One advantage of the State-Dependent Model is that it is general, and it does not have a priori assumptions in linearity or nonlinearity, and it nests all models listed in Chapter 1.2, except for SSA and ANN which considered as nonparametric and machine learning methods. This chapter aims to provide a background and to set the scene about nonlinear models. The details of the functional forms of the SDM coefficients will be discussed in Chapter 2.2.

1.1 Linear Time Series Models

1.1.1 Stochastic processes

A stochastic process is a sequence of random variables (X_t) represented in time order. Random variables can either be discrete or continuous. Gross Domestic Product and industrial production index are examples of discrete time series, whereas a series of readings recorded by an electrocardiogram over time form an example of a continuous random variable. The single realisation of a univariate time series over time provides the information needed to analyse the nature of a stochastic process.

A special type of stochastic process is Gaussian white noise, in which the errors, ϵ_t , follow an independently, identically, and normally distributed process with a mean of zero and a constant variance of σ^2. The covariance between such errors in different time periods is zero. A white noise process does not contain any information which forecasters can use to predict future values using linear models (Franses and Dijk, 2000).

1.1.2 Stationarity

Stationarity is necessary in making predictions from historic data. The term refers to a "statistical equilibrium" (Woodward, Gray and Elliott, 2017) in which the behaviour of a time series has fixed characteristics. A strictly stationary time series implies that the moments of the time series (not just the mean and the variance) are unchanged over time, an assumption which may be too strict for many time series data. A second order stationarity, or covariance stationarity, assumes a weak stationarity in which the first two moments (i.e., the mean and the variance) of X_t do not change, and the covariance between X_t and X_{t-j} depends only on the lag j between time periods. As variance is assumed to be finite, stationary time series always revert to the mean and have a constant amplitude; these characteristics facilitate better predictions. A smaller autocovariance indicates a faster speed of mean reversion (Gujarati and Porter, 2009).

Therefore, under second order stationarity, the following are all constant:

$$\mathrm{E}(X_t) = \mu$$

$$\mathrm{Var}(X_t) = E[(X_t - \mu)^2] = \sigma^2$$

$$Cov(X_t, X_{t+k}) = E[(X_t - \mu)(X_{t+k} - \mu)]$$

1.1.3 Non-stationary and stationary stochastic processes

Random Walk without Drift

Supposing ϵ_t is white noise with $\epsilon_t \sim N(0, \sigma^2)$, a random walk with no drift can be expressed via the following equation:

$$X_t = X_{t-1} + \epsilon_t$$

Under this random walk process, the mean of X_t is equal to X_0, and the variance of X_t is $t\sigma^2$. This means that the further into the future, the larger the variance. Therefore, the variance of X_t in such a process is not finite.

It is generally accepted in finance that asset prices, foreign exchange rates, and share prices follow a random walk process (Gujarati and Porter, 2009), and are therefore nonstationary. The random walk process implies that tomorrow's price is a combination of today's price and a random error. The efficient market hypothesis suggests that asset prices follow random walk processes, and that therefore, it is neither possible to predict the future realisation of a time series nor to generate consistent abnormal profit. A coefficient of 1 associated with X_{t-1} indicates that a random walk process has a unit root and is nonstationary (i.e., the shocks in the random walk process do not die away). However, to make this type of time series stationary, a first differencing is sufficient. By taking the difference between X_t and X_{t-1}, the resultant series ΔX_t is stationary (i.e., any random walk process with no drift is always first order homogeneous).

Random Walk with Drift

The equation for a random walk with drift is as follows:

$$X_t = \delta + X_{t-1} + \epsilon_t$$

Here, the mean of X_t either drifts upwards or downwards, depending on the value of δ.

$$E(X_t) = X_0 + t\delta$$

$$Var(X_t) = t\sigma^2$$

These equations indicate that both the mean and the variance increase over time, making the stochastic process nonstationary.

Autoregressive Processes

As the name suggests, autoregressive (AR) processes involve the different lags of a time series of a dependent variable. The formula expressing an AR(k) process can be presented as follows:

$$X_t + \alpha_1 X_{t-1} + \alpha_2 X_{t-2} + \ldots + \alpha_k X_{t-k} = \varepsilon_t$$

where ε_t is white noise with mean of zero and a variance of σ^2. As the shorthand notation AR(k) suggests, the model is an autoregressive model of order *k*.

Selecting the order of AR(k) using Information Criteria

We can choose the best order for the model by minimising Akaike's Information Criterion (AIC), or Schwarz's Bayesian Information Criterion (BIC or SIC), or the Hannan and Quinn Criterion (HQC).

$$AIC = N \log\left(\frac{SSE}{N}\right) + 2(k+2)$$

$$BIC = N \log\left(\frac{SSE}{N}\right) + (k+2)\log(N)$$

$$HQC = N \log\left(\frac{SSE}{N}\right) + 2k \log\log(N)$$

In the above equations, N is the number of observations, k is the order of the autoregressive model, and SSE is the sum of the squared residuals. The three models all penalise the information criteria when extra predictor variables are added. Compared with AIC, BIC always selects a model with equal or fewer parameters. HQC and BIC model selection penalise additional parameters more severely than AIC. There is no universal consensus regarding the best criteria to employ for model selection. Statisticians prefer BIC to AIC when there are enough observations to attempt to fit the true model (Hyndman and Athanasopoulos, 2018). AIC and corrected AIC model selection methods are preferred by Hyndman and Athanasopoulos (2018) who argued that models selected using these information criteria can also produce better forecasts. On the other hand, Liew (2004) found that when the sample size is small, the above-mentioned models can capture the correct order of model at least 60% of the time, while BIC and HQC are better at modelling with sample sizes above 200.

Parameter Estimation of AR(k) through Ordinary Least Squares Method

One method of parameter estimation for a linear AR(k) model is through using the Ordinary Least Square (OLS) technique. The method is described, for example, by Gujarati and Porter (2009).

In the matrix notation, the relation between the independent and dependent variables of the AR(k) model can be expressed as $\boldsymbol{Y} = \boldsymbol{X}\widehat{\boldsymbol{\alpha}} + \boldsymbol{\epsilon}$. Slightly different from multiple regression equations, the independent variables are replaced by lags of the original time series:

$$\begin{bmatrix} X_{k+1} \\ X_{k+2} \\ X_{k+3} \\ \cdots \\ X_n \end{bmatrix} = \begin{bmatrix} X_k & X_{k-1} \cdots & X_1 \\ X_{k+1} & X_k & \cdots & X_2 \\ X_{k+2} & X_{k+1} & \cdots & X_3 \\ \cdots & \cdots & \cdots & \cdots \\ X_{n-1} & X_{n-2} & \cdots & X_{n-k} \end{bmatrix} \begin{bmatrix} \hat{\alpha}_1 \\ \hat{\alpha}_2 \\ \hat{\alpha}_3 \\ \cdots \\ \hat{\alpha}_k \end{bmatrix} + \begin{bmatrix} \epsilon_1 \\ \epsilon_2 \\ \epsilon_3 \\ \cdots \\ \epsilon_n \end{bmatrix}$$

Using the OLS method, the parameters are estimated using the equation $\widehat{\boldsymbol{\alpha}} = (\boldsymbol{X'X})^{-1}\boldsymbol{X'Y}$. This method is easy to compute and has the property of BLUE (Best Linear Unbiased Estimate), and it also minimises the residual sum of squares (RSS).

1.1.4 State space representations of linear time series models

The state space representation of a linear autoregressive time series can be expressed in the following form, which provides a very compact description of the model:

$$\boldsymbol{x_{t+1}} = \boldsymbol{F x_t} + \boldsymbol{\varepsilon_{t+1}}$$

$$X_t = \boldsymbol{H x_t}$$

Here, $\boldsymbol{x_t} = (X_{t-k+1}, \dots, X_t)'$, which is called the state vector, and ***F, H*** are appropriately defined matrices, as follows:

$$\boldsymbol{F} = \begin{pmatrix} 0 & 1 & \cdots & 0 & 0 \\ 0 & 0 & 1 & 0 & 0 \\ \cdots & \cdots & \cdots & \cdots & \cdots \\ \cdots & \cdots & \cdots & \cdots & 1 \\ -a_n & -a_{n-1} & \cdots & \dots & -a_1 \end{pmatrix}$$

$\boldsymbol{H} = (0, 0, 0, \dots, 1)$ and $\boldsymbol{\epsilon_t} = (0, 0, \dots, \epsilon_t)$

The above representation is not necessarily unique, as there are several "canonical forms" of minimal realisations of linear time series models (Kalman, 1963).

1.2 Nonlinear Time Series Models

Many real-life situations exhibit non-linear behaviour, and thus assumption of linearity is misleading. Thus employing a linear time series model would not give us accurate

forecasts. Nonlinear time series models can in many situations improve the modelling or forecasting results from linear time series models (Franses and van Dijk, 2005).

Based on formal statistical tests, ample empirical evidence suggests that financial time series of stocks and exchange rates are non-linear (see: Hinich and Patterson (1985); Hsieh (1989); Scheinkman and LeBaron (1989); Hsieh (1991); Crato and de Lima (1994); Brooks (1996), etc.). The behaviour of these time series is dynamic and complex. Vast literature related to financial time series such as Franses and Dijk (2000), Hinich and Patterson (1985) suggests that nonlinear models should be used in fitting and forecasting returns and volatility. Many believe that traditional linear models are no longer adequate to describe or forecast financial time series. Substantial evidence has suggested that the non-linear models perform well in modelling both real and simulated time series, and that they can be directly applied in time series forecasting (see Tong and Lim (1980); Gabr and Rao (1981); Haggan and Ozaki (1981); Ozaki (1981)).

This section provides an introduction to some of the typical non-linear time series models, namely the exponential time series, threshold autoregressive, non-linear threshold autoregressive, logistic smooth transition autoregressive (LSTAR), exponential smooth transition autoregressive (ESTAR), bilinear models, artificial neural networks (ANN), and singular spectrum analysis (SSA). Each of these are discussed in turn in the sub-sections which follow.

1.2.1 Exponential autoregressive (EXPAR)

The Exponential autoregressive model was introduced by Ozaki (1978) and further developed by Haggan and Ozaki (1981):

$$X_t + (\theta_1 + \pi_1 e^{-\gamma X_{t-1}^2})X_{t-1} + \ldots + (\theta_k + \pi_k e^{-\gamma X_{t-1}^2})X_{t-k} = \varepsilon_t$$

The model is an extension of the linear AR model, in which the coefficients are exponential functions of X_{t-1}. Its applications can be seen in modelling and forecasting rainfall data (Gurung, 2013). This model can accommodate amplitude-dependent frequency, jump phenomena, and limit cycle behaviours, which are only present in nonlinear processes. It is an appropriate approach to fit and describe time series processes with an underlying self-exciting mechanism (Haggan and Ozaki, 1981). However, this model is not widely employed on Financial data. EXPAR models with conditional heteroscedasticity models have been successfully applied in modelling and forecasting nonlinear behaviours for financial and economic data (Katsiampa, 2015). The SDM contains a broad range of models including the functional form of a general EXPAR model and can be modified to account for heteroscedasticity. It can also serve as a preliminary step in the model fitting before confirming if EXPAR models are appropriate to these time series.

1.2.2 Threshold autoregressive model

The threshold autoregressive models were introduced by Tong (1978) and Tong and Lim (1980). It is a regime-switching model, and the regimes separate by a threshold value. As the threshold depends on its lag, this type of models is called Self-Exciting Threshold autoregressive models (SETAR).

$$\begin{cases} X_t + \alpha_1^{(1)} X_{t-1} + \cdots + \alpha_k^{(1)} X_{t-k}, & \text{if } X_{t-1} \leq c \\ X_t + \alpha_1^{(2)} X_{t-1} + \cdots + \alpha_k^{(2)} X_{t-k}, & \text{if } X_{t-1} > c \end{cases}$$

The resultant model is a step-function of α_u, with more than one regime. In this case, there is a sudden change in coefficients, which depends on whether X_{t-1} is higher or lower than a threshold value of c.

This type of model performs well in modelling "cyclical" data and the fitted model can exhibit limit cycle behaviour. In principle this model applies the piecewise linearization. SETAR models can capture jump resonance, amplitude-frequency dependency, limit cycles, subharmonics and higher harmonics, which are typical phenomena in nonlinear processes. Linear models, generally, fail to capture these types of nonlinear characteristics. Studies also show that Self-exciting TAR (SETAR) models can reduce Root Mean Squared Error by 10% relative to linear models in forecasting (Tong, 1980). The TAR models have been applied on simulated data, Sunspot data and Canadian lynx data and meteorological data (Tsay, 1989).

However, the SETAR models work when the number of regimes is pre-specified. Under this model, the structural change(s) is sudden and abrupt. The SDM can handle multiple regimes well without pre-specification. We can observe multiple structural breaks by plotting the SDM coefficients against time. The SDM works well for time series data with structural breaks, both with abrupt or smooth chnages, and we let the data speak. We can decide if SETAR is indeed appropriate by fitting an SDM model to the time series as a preliminary step.

1.2.3 Non-linear threshold autoregressive model

The non-linear threshold autoregressive model is a modified threshold autoregressive model, and was proposed by Ozaki (1981), with the general formula of:

$$\begin{cases} X_t + (\phi_1 + \pi_1|X_{t-1}|)X_{t-1} + \cdots + (\phi_k + \pi_k|X_{t-k}|)X_{t-k} = \varepsilon_t, & \text{if} |X_{t-1}| \le c \\ X_t + (\phi_1 + \pi_1 c)X_{t-1} + \cdots + (\phi_k + \pi_k c)X_{t-k} = \varepsilon_t, & \text{if} |X_{t-1}| > c \end{cases}$$

The model is more flexible than the TAR models, as the parameters of this model are not step-functions of its lag. The nonlinear TAR can also capture amplitude-dependent frequency shift phenomena, jump phenomena and limit cycle behaviours.

Methodological improvements to linear and non-linear Threshold Autoregressive models have been widely applied in empirical economics (Hansen, 2011), in areas such as output growth (Pesaran and Potter, 1997), forecasting unemployment rates (Rothman, 1998), modelling interest rates (Pfann, Schotman and Tschernig, 1996), price indices (Yadav, Pope and Paudyal, 1994), stock returns (Cao and Tsay, 1992) and exchange rates (Sarno, Taylor and Chowdhury, 2004).

When compared with nonlinear autoregressive models, the SDM is even more flexible. It not only can model this nonlinearity but also prescribe the exact nonlinear behaviours through SDM model fitting. If the nonlinear form looks similar to that of an NLAR model, we can then fit this model into that time series.

1.2.4 Smooth Transition Autoregressive (STAR) models

This family of models includes both exponential and logistic threshold autoregressive models and can accommodate time series data. The Smooth Transition Autoregressive (STAR) model is a type of regime switching model which allows a time series to vary between regimes in a smooth manner. Applications of STAR models have been seen in industrial production modelling (Zhou, 2010), the successful forecasting of macroeconomic variables (Teräsvirta, van Dijk and Medeiros, 2005), exchange rate modelling (Sarantis, 1999) and forecasting (Michael, Nobay and Peel, 1997), etc. Variants of smooth transition models are applied in exchange rate forecasting (Pippenger and Goering, 1998).

The following formula of a STAR model was expressed by Dijk, Teräsvirta and Franses (2000):

$$X_t + (\alpha_0 + \alpha_1 X_{t-1} + \ldots + \alpha_k X_{t-k})\big(1 - G(\boldsymbol{x_{t-d}}; \gamma, c)\big) + (\beta_0 + \beta_1 X_{t-1} + \ldots + \beta_k X_{t-k}) G(\boldsymbol{x_{t-d}}; \gamma, c) = \varepsilon_t$$

Which they also conveniently expressed as:

$$X_t + \boldsymbol{\alpha x_t}\big(1 - G(\boldsymbol{x_{t-d}}; \gamma, c)\big) + \boldsymbol{\beta x_t} G(\boldsymbol{x_{t-d}}; \gamma, c) = \varepsilon_t$$

Or

$$X_t + \boldsymbol{\alpha x_t} + (\boldsymbol{\beta} - \boldsymbol{\alpha}) \boldsymbol{x_t}\, G(\boldsymbol{x_{t-d}}; \gamma, c) = \varepsilon_t$$

The $\boldsymbol{\alpha}$ and $\boldsymbol{\beta}$ are the coefficients of the autoregressive processes. The transition function G is bounded between zero and one, such that based on the above formula, each smoothed realization X_t is a weighted average of two different autoregressive (AR) models. The transition function G can either be a logistic function or an exponential function. The transition function can either be a function of $\boldsymbol{x_{t-d}}$, or an exogenous variable $\boldsymbol{z_t}$. When $\boldsymbol{z_t}$ is involved, the models are called Smooth Transition Regression models.

1.2.4.1 Logistic Smooth Transition Autoregressive models

The transition function can take a logistic form:

$$G(\boldsymbol{x_{t-d}}; \gamma, c) = (1 + e^{-\gamma(\boldsymbol{x_{t-d}} - c)})^{-1}$$

Figure 1-1 Plot of three different logistic functions against $\boldsymbol{x_{t-1}}$

The figure below illustrates a plot of three functions $G(\boldsymbol{x_{t-d}}; \gamma, c) = (1 + e^{-\gamma(\boldsymbol{x_{t-d}} - c)})^{-1}$ with γ = 1, 5, and 20. In this figure, the value of c is set at zero. The larger the value of γ, the steeper the logistic curve.

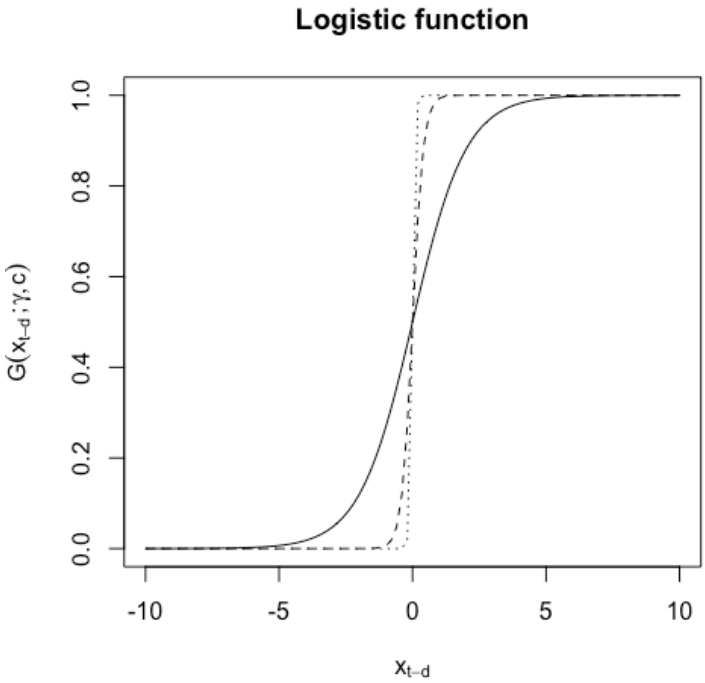

In this equation, c is the threshold between the regimes. The value of γ determines the smoothness of the transition between the regimes. When γ approaches infinity, the logistic STAR model (LSTAR) approaches the form of a Threshold Autoregressive (TAR) model, with a sudden jump between the regimes at $X_{t-d} = c$.

1.2.4.2 Exponential Smooth Transition Autoregressive model

Another type of transition function takes an exponential form:

$$G(\boldsymbol{x_{t-d}}; \gamma, c) = 1 - e^{-\gamma(x_{t-d}-c)^2}$$

This type of STAR model is called an Exponential Smooth Transition Autoregressive (ESTAR) model. A higher value of γ reflects a faster speed of transition. Therefore, in Figure 1-2, the slowest transition takes place at γ = 1.

Figure 1-2 Plot of three different exponential functions against x_{t-d}

This figure shows a plot of the exponential functions $G(x_{t-d}; \gamma, c) = 1 - e^{-\gamma(x_{t-d}-c)^2}$ against $\boldsymbol{x_{t-d}}$ with γ = 1, 5, and 20. Again, the value of c is set at zero. The larger γ is, the faster the speed of the transition between the two regimes becomes.

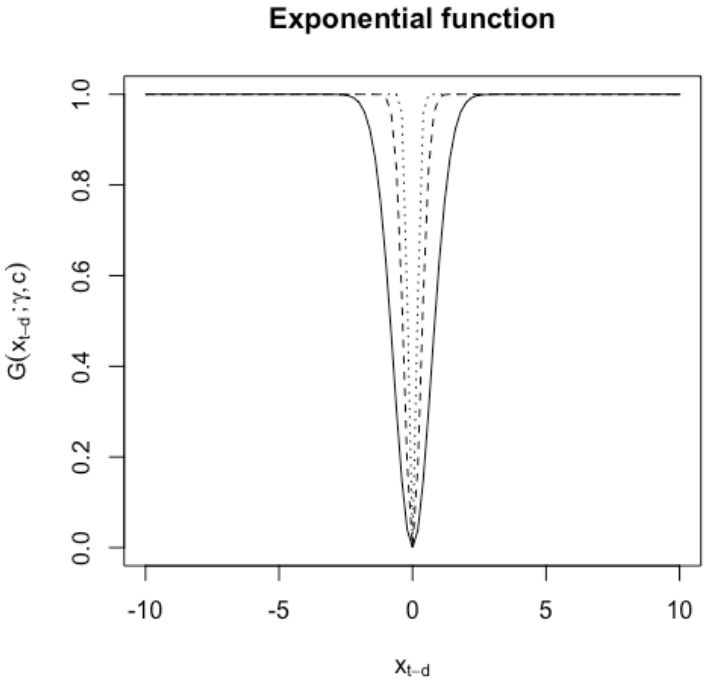

The STAR models include TAR (SETAR self-exciting threshold autoregressive) models as a special case. Therefore, it can capture abrupt and gradual transitions through parameters produced by STAR. However, in STAR model fitting, one has to fix and assume that the shape of the parameters follows an exponential or logistic function, which is not justifiable without a strong theory to support it. Secondly, the basic STAR model allows only two regimes. The SDM is advantageous in that its functional form of (non)linearity is not just limited to LSTAR or ESTAR but can be open to other non-linear functional forms. The SDM can also accommodate more than two regimes. Through an exploration of the plots of parameters against state and time, we may see unexpected and interesting findings. The SDM can serve as a preliminary step to test if a two regime

STAR model is appropriate. If the shape of nonlinearity is STAR with regime shifts, we then proceed to model fitting using specific STAR models (e.g. multiple regime STAR models, general two-regime STAR models, or vector STAR models). Therefore, the SDM is more general and flexible than the STAR models.

1.2.5 Bilinear model

The bilinear model was introduced by Mohler (1973) and Brockett (1976). Its applications in time series have been discussed by Granger and Anderson (1978) and Gabr and Rao (1981). The model can be written in the following form:

$$X_t + \alpha_1 X_{t-1} + \cdots + \alpha_k X_{t-k} = \epsilon_t + \beta_1 \varepsilon_{t-1} + \cdots + \beta_j \varepsilon_{t-l} + \sum_{i=1}^{m}\sum_{j=1}^{p} \gamma_{ij} \epsilon_{t-i} X_{t-j}$$

When the coefficients γ_{ij} are all zero, it reduces to an ARMA(k, l) model as a special case. The terms $\varepsilon_{t-i} X_{t-j}$ make the model non-linear. Applications of bilinear models can be found in control theory, and have also been seen in the contexts of distillation columns in chemistry (España and Landau, 1978), immunology (Mohler, 2005), and employed by Granger and Andersen (1978) in time series econometrics.

One advantage of bilinear models is that it is parsimonious, and can approximate general Volterra expansions with excellent accuracy (Rao, 1981). Though not widely applied in financial and economic time series, the model is includes in the SDM as special case.

1.2.6 Artificial Neural Network (ANN)

The Artificial Neural Network (ANN) is a more recent model for forecasting. Successful applications of ANN can mainly be found in forecasting foreign exchange rates (Kuan and Liu, 1995). This method is more complicated than traditional econometric and time series models. The process of model fitting and forecasting mimics how the neurons in

human brains learn and adapt. The ANN does not require a time series process to follow a certain probability distribution, and it can perform reliable forecasting even with missing observations and noisy data. It does not require a process to be linear, and can accurately forecast in highly complicated and dynamic situations (Vellido, Lisboa and Vaughan, 1999). However, the ANN also suffers from a number of drawbacks. First, it operates in a "black-box" way which is not easy to understand, especially in the presence of hidden nodes. Second, there is no universal way to determine which variables should be inputs to the ANN, or how many hidden nodes the ANN should have. However, the evidence suggests that the ANN can perform much better than traditional regression methods in fields such as tourism demand forecasting (Burger *et al.*, 2001).

The ANN architecture generally consists of an input layer, one or two hidden layers, and an output layer. Lags of k explanatory variables serve as inputs to the neural network structure. This makes the ANN autoregressive (also known as Neural Network AR), which is analogous to independent variables in traditional linear regressions. The processes of feedforward and backward propagation are applied to the multilayer perceptrons (MLP). The output layer has dependent variables, while the hidden layers contain unobservable units. Every input is coupled with a corresponding output unit through a feedforward process. The nodes of different layers are connected through mathematical functions. Each input is multiplied by relevant weights, which are summed and fed forward to the next node. If the next node is the intermediate layer – a hidden layer, the outputs from the input layer become the inputs of the next layer and are fed forward to the output layer. The inputs of the hidden layer are compressed into a logistic function. The relevant weights of the inputs are determined by minimising the sum of squares.

1.2.7 Singular Spectrum Analysis (SSA)

Singular Spectrum Analysis (SSA) is a new technique in time series analysis and forecasting. It is a non-parametric method which has many advantages, and which performs well regardless of the presence of linearity or stationarity in a time series. This is a great step forward, as it had generally been claimed that the restrictive assumptions of stationarity, normality, and linearity do not always provide good forecasting results (Hassani and Thomakos, 2010). The SSA requires few assumptions in relation to the time series and can cope with a small number of observations. It has been successfully applied in many areas, including classical time series analysis, multivariate time series analysis, multivariate geometry, dynamical systems, signal processing, etc. (Zhigljavsky, 2010). Forecasting SSA is a promising area, as the SSA has also been successfully applied in forecasting areas such as the climate, meteorology, geophysics, engineering, medicine, etc. It has also been introduced to forecasting econometric time series (Zhigljavsky, 2010). Other applications of SSA include foreign exchange (Drogobetskii, 2005; Drogobetskii and Smolynsky, 2008), forecasting tourist demand (Hassani *et al.*, 2015), and modelling and forecasting European industrial production (Hassani, Heravi and Zhigljavsky, 2009).

The Algorithm of Basic SSA

The methodology of SSA aims to decompose a time series of interest into different types of components: trends, oscillatory (sinusoidal) components, and random noise (Zhigljavsky, 2010). SSA has not only been applied in forecasting, but also for the purposes of smoothing, noise reduction, and filtering. The basic SSA aims to extract the deterministic component from a time series. The SSA has two stages: decomposition and

reconstruction. The reconstructed series satisfies the linear recurrent formula and is used in forecasting (Zhigljavsky, 2010).

Empirical studies on SSA

SSA has been shown to perform well in both modelling and forecasting financial and economic time series. Hassani, Heravi and Zhigljavsky (2009) applied it in forecasting 24 series of European industrial production indices, and found superior forecasting performance on the part of SSA in a long-term horizon compared with ARIMA and Holt-Winters methods. Lisi and Medio (1997) applied a multichannel SSA to the exchange rates of major currencies and found statistically significant and superior performance compared to the Random Walk model. Furthermore, Thomakos, Wang and Wille (2002) used SSA to model futures returns and found that SSA could decompose volatility series and model market trends and periodicities very well. They suggested using SSA as a tool for practitioners.

Hassani, Soofi and Zhigljavsky (2010) employed univariate and multivariate singular spectrum analyses to predict the value and signs of changes in the daily sterling/dollar exchange rate, and found that multivariate SSA forecast better than the random walk model in predicting the value and direction of change in these exchange rates, and that it was also superior to the vector error-correction (VEC) model. Silva, Hassani and Heravi (2018) employed multivariate singular spectrum analysis (MSSA) to evaluate forecasts for 24 non-seasonally adjusted industrial production series, and found that the optimised MSSA produced superior forecasts in more than 70% of cases.

1.3 Discussion and conclusion

Nonlinearity in time series is important, as linear time series processes assume symmetry and constancy in parameter, which does not capture the dynamic behaviour of time series processes. Nonlinear models allow more accurate model fitting and forecasting in many

real life situations. The SDM is general, without prior assumptions, it nests nonlinear models described in sections 1.2.1 - 1.2.5, and the linear model as a special case. Priori, it does not prescribe a specific type of nonlinearity and can serve as a preliminary step before any specific model is fitted. Fitting SDM helps us discover any types of nonlinearities through exploring plots of SDM coefficients against state vector and show structural breaks by plotting the parameters against time.

This chapter provided a comprehensive background in time series analysis through introducing linear and various non-linear time series models. The chapter started from simple linear time series models as the basic building block, building towards nonlinear models. These individual linear and nonlinear models have their advantages and disadvantages. The chapter described the advantages of the SDM over other models and also provided the state-space representation of linear time series models, which is a steppingstone towards nonlinear state-space representations explained in Section 2.3.

The next chapter introduces the State-Dependent Model, explains the details of estimation procedure and shows that linear and nonlinear time series models can be considered as special cases of this general model. Chapter 2.2 will explain how the SDM encompasses most specific nonlinear models described in Chapter 1.2 through expressing these models in their distinct functional forms.

Chapter 2 The State-Dependent Model

2.1 Introduction

The State Dependent Model (SDM) was introduced by Priestley (1980). It is a functional coefficient model where the coefficients depend on the past state of the time series. It generally includes most special non-linear time-series models, such as bilinear models, threshold autoregressive models, exponential autoregressive models, non-linear threshold autoregressive models, and logistic and exponential smooth transition autoregressive models (see sections 1.2.1 - 1.2.5). It also includes linear ARMA models as a special case. Without any prior assumptions regarding the type of model to be fit to the time series (Cartwright, 1985a), the SDM operates like a dictionary, as it can provide an overview of the specific type of non-linearity of the time series and indicate which model is most appropriate for a specific set of time series data (Heravi, 1985). The SDM algorithm can also point out structural breaks based on the plots of coefficients against time.

Much of the literature on SDM was produced by Priestley (1980). Haggan *et al.* (1984) extended the SDM scheme and successfully applied it to both real and simulated data. Cartwright (1985b) also applied the SDM to predict missing values in the Wolfer sunspot series by using one-step forecasts to replace them in the time series. In a similar vein, Cartwright and Newbold (1982) and Cartwright (1985a) also investigated the forecasting performance of SDM using the grid-search method.

Cartwright and Newbold (1982) also applied state-dependent models to predict North Sea oil discoveries and found that non-linear forecasting methods performed significantly

better than linear models. Cartwright (1985a) compared the forecasting performance of linear ARMA models, non-linear models such as bilinear models, and SDMs on the Wolfer sunspot series and IBM Daily Stock prices and found that non-linear forecasting models, especially the SDM, could significantly improve forecasting errors when compared with linear models. In a recent paper, Dixon, Easaw and Heravi (2019) investigated inflation gap persistence using the SDM model.

The Functional Coefficient Autoregressive model (FCAR) was introduced by Chen and Tsay (1993). This model belongs to the family of state-dependent models, and the identification and estimation of FCAR is easier than in SDM models. However, embedded within this method is a non-parametric smoothing through an arranged local regression. This method may not perform well in identifying points of abrupt structural changes. Chen and Tsay (1993) showed that due to the overlapping of windows, the FCAR cannot model Threshold Autoregressive models well. The SDM, in contrast, may perform better in capturing different degrees of transitions in models, and can contain TAR models as special cases.

Particle filtering provides a different approach to Kalman Filtering in estimating the coefficients of an AR process, as it is based on creating simulated particles through Monte Carlo methods and assigning weights to them, then updating through Importance Sampling (IS). Unlike Kalman Filtering, the parameter distributions do not need to follow a Gaussian distribution; nor does the data need to be linear (Lopes and Tsay, 2011). Despite its flexibility this method, which is based on Monto-Carlo sampling techniques, is more computationally cumbersome and costly (Lopes and Tsay, 2011). Dixon, Easaw

and Heravi (2019) also found that in the long run, particle filtering and Kalman filtering produce similar results in estimating coefficients.

Studies in SDM show that broader models such as SDM are better in forecasting (Cartwright and Newbold, 1982; Cartwright, 1985a). Furthermore, practitioners face difficulty choosing a nonlinear model for analysis (Franses and Dijk, 2000). It is beneficial to use a general SDM in model fitting and forecasting. The SDM can be applied as a preliminary step before fitting specific (non)linear models.

Consider the linear ARMA (k, l) model:

$$X_t + \phi_1 X_{t-1} + \cdots + \phi_k X_{t-k} = \mu + \varepsilon_t + \varphi_1 \varepsilon_{t-1} + \cdots \varphi_l \varepsilon_{t-l}$$

The general nonlinear model is just an extension of the linear ARMA model, which can be expressed by the following equation:

$$X_t + \phi_1(\boldsymbol{x_{t-1}})X_{t-1} + \cdots + \phi_k(\boldsymbol{x_{t-1}})X_{t-k} = \mu(\boldsymbol{x_{t-1}}) + \epsilon_t + \psi_1(\boldsymbol{x_{t-1}})\epsilon_{t-1} + \cdots + \psi_l(\boldsymbol{x_{t-1}})\epsilon_{t-l}$$

This model is called a state-dependent model of order (k, l). This general formula shows a non-linear model because the coefficients ϕ_u and ψ_u are functions of the state vector, $\boldsymbol{x_{t-1}}$. The coefficients ϕ_u and ψ_u are represented "locally" by a linear ARMA model. This means that the process involving these coefficients allows small deviations from the current state of the process. The model nests different types of special non-linear models. A linear ARMA model is also a special case of this type of model when ϕ_u and ψ_u are constant and independent from $\boldsymbol{x_{t-1}}$.

2.2 Non-linear models encompassed by the SDM

The following section shows how different types of models are encompassed by the SDM by using particular forms of $\phi_1, \phi_2, \dots, \phi_k, \psi_1, \psi_2, \dots, \psi_l$.

(a) Linear Models

Take $\{\phi_1, \phi_2, \dots, \phi_k\}$,$\{\psi_1, \psi_2, \dots, \psi_l\}$ to be constant and independent of $\boldsymbol{x_{t-1}}$.

(b) Exponential AR models

Take $\{\psi_1, \psi_2, \dots, \psi_l\} = 0$, and

$$\phi_u(\boldsymbol{x_{t-1}}) = \theta_u + \pi_u e^{-\gamma x_{t-1}^2}$$

(c) Threshold AR models

Take $\{\psi_1, \psi_2, \dots, \psi_l\} = 0$, and

$$\phi_u(\boldsymbol{x_{t-1}}) = \begin{cases} \alpha_u^{(1)}, & \text{if } X_{t-d} \le c \\ \alpha_u^{(2)}, & \text{if } X_{t-d} > c \end{cases}$$

(d) Non-linear Threshold AR

Take $\{\psi_1, \psi_2, \dots, \psi_l\} = 0$, and

$$\phi_u(\boldsymbol{x_{t-1}}) = \begin{cases} \theta_u + \pi_u |X_{t-d}|, & \text{if } X_{t-d} \le c \\ \theta_u + \pi_u c, & \text{if } X_{t-d} > c \end{cases}$$

(e) Logistic Smooth Transition models (LSTAR)

Take $\{\psi_1, \psi_2, \dots, \psi_l\} = 0$, and

$$\phi_u(\boldsymbol{x_{t-1}}) = \alpha_u + (\beta_u - \alpha_u)\left[1 + e^{-\gamma(X_{t-1}-c)}\right]^{-1}$$

(f) Exponential Smooth Transition models (ESTAR)

Take $\{\psi_1, \psi_2, \dots, \psi_l\} = 0$, and

$$\phi_u(\boldsymbol{x_{t-1}}) = \alpha_u + (\beta_u - \alpha_u)[1 - e^{-\gamma(X_{t-1}-c)^2}]$$

(g) Bilinear models

Take $\{\phi_1, \phi_2, \dots, \phi_k\} = 0$ as constants, and choose:

$$\psi_u(\boldsymbol{x_{t-1}}) = b_u + \sum_{j=1}^{p} c_{uj} X_{t-j}$$

2.3 State Space Representations of the State-Dependent Model

The state-space representation of the SDM was expressed by Haggan, Heravi and Priestley (1984) as follows:

$$\boldsymbol{x_{t+1}} = \{\boldsymbol{F}(\boldsymbol{x_t})\}\boldsymbol{x_t} + \boldsymbol{\epsilon_{t+1}}$$

$$\boldsymbol{X_t} = \boldsymbol{H}\boldsymbol{x_t}$$

In the above equations, F is a transition matrix and is an analytic function of $\boldsymbol{x_t}$.

$$\boldsymbol{x_t} = (1, \epsilon_{t-l+1}, \dots, \epsilon_t, X_{t-k+1}, \dots, X_t)'$$

$$\boldsymbol{H} = (0, 0, \dots, 0, 0, \dots, 1)'$$

$$\boldsymbol{\epsilon_t} = \epsilon_t(0, 0, \dots, 1, 0, \dots, 1)$$

$$\boldsymbol{F}(\boldsymbol{x_t}) = \begin{pmatrix} 1 & 0 & 1 & \cdots & 0 & 0 & 0 & 0 & 0 \\ 0 & 0 & 0 & \cdots & 0 & 0 & 0 & 0 & 0 \\ 0 & 0 & 0 & \cdots & 1 & 0 & 0 & 0 & 0 \\ 0 & 0 & 0 & \cdots & 0 & 1 & 0 & 0 & 0 \\ 0 & 0 & 0 & \cdots & 0 & 0 & 1 & 0 & 0 \\ 0 & 0 & 0 & \cdots & 0 & 0 & 0 & 1 & 0 \\ 0 & 0 & 0 & \cdots & 0 & 0 & 0 & 0 & 1 \\ \mu & \psi_l & \psi_{l-1} & \cdots & \psi_1 & -\phi_k & -\phi_{k-1} & \cdots & -\phi_1 \end{pmatrix}$$

2.4 Parameter Estimation of the AR-SDM model

In this section, the parameter estimation for the AR-SDM model is described.

Consider the following AR-SDM model:

$$X_t + \phi_1(\boldsymbol{x_{t-1}})X_{t-1} + \cdots + \phi_k(\boldsymbol{x_{t-1}})X_{t-k} = \mu(\boldsymbol{x_{t-1}}) + \epsilon_t$$

The state vector $\boldsymbol{x_{t-1}}$ is given by:

$$\boldsymbol{x_{t-1}} = (1, X_{t-k+1}, \ldots, X_t)'$$

In order to fit an SDM model, the parameters μ, ϕ_1, …, ϕ_k need to be estimated, which depend on the state vector $\boldsymbol{x_{t-1}}$. The estimation procedure involves a recursive method similar to Harrison and Stevens (1976), but the coefficients are state-dependent instead of time-dependent. Priestley (1980) implemented an extended version of the Kalman Filter algorithm to estimate the parameters for the SDM model. This algorithm assumes that all the coefficients in the process are linear functions of the state vector $\boldsymbol{x_t}$. Therefore,

$$\mu(\boldsymbol{x_t}) = \mu^{(0)} + \boldsymbol{x_t\alpha}$$

$$\phi_u(\boldsymbol{x_t}) = \phi_u^{(0)} + \boldsymbol{x_t\beta_u}$$

The $\boldsymbol{\alpha}$, $\boldsymbol{\beta_u}$ are gradient parameters. μ, ϕ_u are represented locally as a smooth and linear functions of $\boldsymbol{x_t}$. The updated equations can be expressed as:

$\mu(\boldsymbol{x_{t+1}}) = \mu(\boldsymbol{x_t}) + \boldsymbol{\Delta x_{t+1}\alpha^{(t+1)}}$ (for the local intercept)

$\phi_u(\boldsymbol{x_{t+1}}) = \phi_u(\boldsymbol{x_t}) + \boldsymbol{\Delta x_{t+1}\beta_u^{(t+1)}}$(for the slope coefficients)

Where $\boldsymbol{\Delta x_{t+1}} = \boldsymbol{x_{t+1}} - \boldsymbol{x_t}$

In matrix form, the random walk model for the gradients can be written as:

$$\boldsymbol{B_{t+1}} = \boldsymbol{B_t} + \boldsymbol{V_{t+1}}$$

In this equation, $\boldsymbol{B_t} = (\boldsymbol{\alpha^{(t)}}, \boldsymbol{\beta_1^{(t)}}, \cdots, \boldsymbol{\beta_k^{(t)}})$ are unknown. These parameters are determined by minimising the difference between the observed value X_t and the fitted value of $\widehat{X}_t$. $\{\boldsymbol{V_t}\}$ is a sequence of matrix random variables with a multivariate normal distribution, a mean of zero, and a standard deviation of Σ_{v}. The choice of Σ_{v} depends on the smoothness of the parameter, and the diagonal elements of Σ_{v} are set relative to σ_ε^2 in order to capture rapid changes in the models' parameters.

Priestley (1980) gave a reformulation of the SDM model in a state-space form in which the state-vector $\boldsymbol{\theta_t}$ includes all the current parameters:

$$\boldsymbol{\theta_t} = \boldsymbol{F_{t-1}\theta_{t-1}} + \boldsymbol{W_t}$$

$$X_t = \boldsymbol{H_t\theta_t} + \epsilon_t$$

Where:

$$\boldsymbol{H_t} = (1, -X_{t-1}, \cdots, -X_{t-k}; 0,0, \cdots, 0)'$$

$$\boldsymbol{\theta_t} = \left(\mu_{t-1}, \phi_1^{(t-1)}, \cdots, \phi_k^{(t-1)}; \alpha^{(t)'}, \beta_1^{(\mathrm{t})'}, \cdots, \beta_k^{(\mathrm{t})'}\right)$$

$$\boldsymbol{W_t} = (0,0,0, \cdots, 0, \boldsymbol{v_{1,t}}, \cdots, \boldsymbol{v_{k+1,t}})$$

Where $v_{1,t}, \cdots, v_{k+1,t}$ are columns of $\boldsymbol{V_t}$.

Applying the Kalman algorithm to the reformulated equations gives the following recursion equations:

$$\widehat{\boldsymbol{\theta}}_{\boldsymbol{t}} = \boldsymbol{F_{t-1}}\widehat{\boldsymbol{\theta}}_{\boldsymbol{t-1}} + \boldsymbol{K_t}\{\boldsymbol{X_t} - \boldsymbol{H_tF_{t-1}}\widehat{\boldsymbol{\theta}}_{\boldsymbol{t-1}}\}$$

$$\boldsymbol{\Phi_t} = \boldsymbol{F_{t-1}C_{t-1}}(\boldsymbol{F_{t-1}})' + \Sigma_{\mathrm{w}}$$

$$\boldsymbol{K_t} = \boldsymbol{\Phi_t}(\boldsymbol{H_t})'[\boldsymbol{H_t\Phi_t}(\boldsymbol{H_t})' + \sigma_\epsilon^2]^{-1}$$

$$\boldsymbol{C_t} = \boldsymbol{\Phi_t} - \boldsymbol{K_t}[\boldsymbol{H_t\Phi_t}(\boldsymbol{H_t})' + \sigma_\varepsilon^2](\boldsymbol{K_t})'$$

Where $\boldsymbol{K_t}$ is called "Kalman Gain", $\boldsymbol{\Phi}$ is the variance-covariance matrix of the one-step ahead prediction errors of $\boldsymbol{\theta_t}$, and $\boldsymbol{C_t}$ is the variance-covariance matrix of $(\boldsymbol{\theta_t} - \widehat{\boldsymbol{\theta}}_{\boldsymbol{t}})$, i.e.:

$$\boldsymbol{\Phi_t} = \boldsymbol{E}[(\boldsymbol{\theta_t} - \boldsymbol{F}^*_{\boldsymbol{t-1}}\widehat{\boldsymbol{\theta}}_{\boldsymbol{t-1}})(\boldsymbol{\theta_t} - \boldsymbol{F}^*_{\boldsymbol{t-1}}\widehat{\boldsymbol{\theta}}_{\boldsymbol{t-1}})']$$

$$\boldsymbol{C_t} = \boldsymbol{E}[(\boldsymbol{\theta_t} - \widehat{\boldsymbol{\theta}}_{\boldsymbol{t}})(\boldsymbol{\theta_t} - \widehat{\boldsymbol{\theta}}_{\boldsymbol{t}})']$$

$$\boldsymbol{\Sigma_w} = \begin{pmatrix} 0 & 0 \\ 0 & \boldsymbol{\Sigma_v} \end{pmatrix}$$

And the transition matrix is defined as follows:

$$\boldsymbol{F_{t-1}} = \begin{pmatrix} & \boldsymbol{\Delta x'_{t-1}} & 0 & 0 \\ I_{k+1} & 0 & \ddots & 0 \\ & 0 & 0 & \boldsymbol{\Delta x'_{t-1}} \\ 0 & & \mathrm{I}_{k(k+1)} & \end{pmatrix}$$

Where, $\boldsymbol{\Delta x'_{t-1}} = (X_{t-1} - X_{t-2}, \dots, X_{t-k} - X_{t-k-1})$.

As was explained above, the time series are assumed to exhibit small departures from their current states. Therefore, all the intercept and slope coefficients are smooth functions of the state vector $\boldsymbol{x_t}$. To start the recursion, initial estimates are needed for the intercept coefficient, the slope coefficients, the variance-covariance matrix of parameters, and the variance of residuals, σ_ϵ^2. It is believed that an AR(k) model can provide a reasonably good fit and good starting values for the local behaviour of the AR-SDM model. The first stretch of observations is used and an AR(k) is fitted to create the initial estimates required for the SDM algorithms. The initial "gradient" parameters are also set to be zero. Thus:

$$\hat{\theta}_{\mathrm{t}_0-1} = (\hat{\mu}, \hat{\phi}_1, \cdots, \hat{\phi}_k, 0, \cdots, 0)'$$

$$C_{t_0-1} = \begin{pmatrix} \hat{R}_{\mu,\phi} & 0 \\ 0 & 0 \end{pmatrix}$$

$\hat{R}_{\mu,\phi}$ is the estimated variance and covariance matrix of the parameters $(\hat{\mu}, \hat{\phi}_1, \dots, \hat{\phi}_k)$, obtained from the initial AR(k) model fitting. The estimation procedure for ARMA-

SDM is similar to that for AR-SDM estimation, and can be found in Haggan *et al.* (1984).

2.5 Conclusion

This chapter has presented the theories underpinning linear, non-linear, and state-dependent models. The next chapters set out several applications of SDM on simulated data, modelling and testing on real data, and an assessment of the forecasting performance of the State-Dependent Model. The SDM is general, and can be fitted without any priori assumptions on the functional form of (non-)linearity, with a linear model as special cases. It is based on an extended-Kalman Filter algorithm that is fast and efficient. A summary table on the models SDM nests and how these models link to SDM is presented in Table 2-1. The SDM can serve as a necessary preliminary step before a specific class of nonlinear models fitted to time series data. Although SDM serves as a preliminary analysis, it may direct the researchers to develop new specific types of non-linearity in a real life situation. Allow more informed understanding of nonlinearity, as the SDM is general and more flexible than an individual model. SDM can direct the researchers to choose the most suitable type of model for the selected time series data and then best specific non-linear (linear) model to be fitted, taking advantage of good properties of each nonlinear model.

Table 2-1 Comparisons between SDM and the model it nests

Model	General expressions and functional forms	Comparison with SDM and the roles of SDM
General SDM	$X_t + \phi_1(\boldsymbol{x_{t-1}})X_{t-1} + \cdots + \phi_k(\boldsymbol{x_{t-1}})X_{t-k} = \mu(\boldsymbol{x_{t-1}}) + \epsilon_t + \psi_1(\boldsymbol{x_{t-1}})\epsilon_{t-1} + \cdots + \psi_l(\boldsymbol{x_{t-1}})\epsilon_{t-l}$	The SDM serves as a preliminary model before fitting specific time series models. Also it may direct the researchers to develop new specific types of non-linearity in a real life situation. The SDM can be directly used as a forecasting model for its strong forecasting ability.
Linear	Take $\{\phi_1, \phi_2, \dots, \phi_k\}$,$\{\psi_1, \psi_2, \dots, \psi_l\}$ to be constant and independent of $\boldsymbol{x_{t-1}}$	The SDM can capture nonlinear behaviour, which a linear model cannot. The SDM captures linear behaviours as a special case. Use SDM as a preliminary step to decide if a linear model is adequate.
EXPAR	Take $\{\psi_1, \psi_2, \dots, \psi_l\} = 0$, and $\phi_u(\boldsymbol{x_{t-1}}) = \theta_u + \pi_u e^{-\gamma x_{t-1}^2}$	The SDM contains a functional form of a general EXPAR model and can be modified to account for heteroskedasticity. Use SDM as a preliminary step to decide if EXPAR is appropriate
TAR	Take $\{\psi_1, \psi_2, \dots, \psi_l\} = 0$, and $\phi_u(\boldsymbol{x_{t-1}}) = \begin{cases} \alpha_u^{(1)}, & \text{if } X_{t-d} \le c \\ \alpha_u^{(2)}, & \text{if } X_{t-d} > c \end{cases}$	The SDM handles multiple regimes well without pre-specification and we can observe multiple regimes through plotting the SDM coefficients against time. The SDM works well irrespective of breaks in data are smooth or abrupt. Use SDM as a preliminary step to decide if SETAR is appropriate. SDM gives an indication of the threshold values.

NLTAR	Take $\{\psi_1, \psi_2, \dots, \psi_l\} = 0$, and $\phi_{\mathrm{u}}(\boldsymbol{x_{t-1}}) = \begin{cases} \theta_{\mathrm{u}} + \pi_u \lvert X_{t-d} \rvert, & \text{if } X_{t-d} \le c \\ \theta_{\mathrm{u}} + \pi_u c, & \text{if } X_{t-d} > c \end{cases}$	The SDM is even more flexible than NLAR. It not only can model non-linearity in autoregressive processes but also prescribe the exact nonlinear behaviours. Use SDM as a preliminary step to decide if NLAR is appropriate and locate the threshold values.
STAR	LSTAR: Take $\{\psi_1, \psi_2, \dots, \psi_l\} = 0$, and $\phi_u(\boldsymbol{x_{t-1}}) = \alpha_u + (\beta_u - \alpha_u)\left[1 + e^{-\gamma(X_{t-1}-c)}\right]^{-1}$ ESTAR: Take $\{\psi_1, \psi_2, \dots, \psi_l\} = 0$, and $\phi_u(\boldsymbol{x_{t-1}}) = \alpha_u + (\beta_u - \alpha_u)[1 - e^{-\gamma(X_{t-1}-c)^2}]$	The STAR models contain SETAR, STR or TAR as a special case, and widely used in economics and finance. SDM is more general than STAR, can handle more than two regimes. When there no strong theories to support LSTAR or ESTAR, the SDM is better as it has no a priori assumptions. In SDM the functional form of (non)linearity is not just limited to LSTAR or ESTAR but can contain other functional forms. Through this process, we allow new nonlinear forms to be discovered. SDM direct researchers to discover and develop new specific nonlinear time series models. The SDM here can serve as a preliminary step to test if a two-regime STAR model is appropriate, or should we use a multi-regime STAR
Bilinear	Take $\{\phi_1, \phi_2, \dots, \phi_k\} = 0$ as constants, and choose: $\psi_u(\boldsymbol{x_{t-1}}) = b_u + \sum_{j=1}^{p} \mathrm{c}_{uj} X_{t-j}$	Bilinear models are parsimonious and can approximate general Volterra expansions with good accuracy (Rao, 1981). The Bilinear model is contained in the SDM general expression.

		Use SDM as a preliminary step to decide if a bilinear model is appropriate

Chapter 3 Numerical Examples on Simulated Data

3.1 Introduction

In this chapter, the State Dependent Model (SDM) algorithm is run on simulated time series data. Data were generated from linear and various specific non-linear models to test the ability of the SDM method to correctly estimate (reproduce) the true linear/non-linear models. The aim of this simulation chapter is to test the theory of SDM and to see if SDM can distinguish these different nonlinear models. To do this, the true functional form of the parameters of the model were then graphically compared with those estimated by SDM algorithm. The questions I aim to address include: Firstly, whether the SDM can capture specific forms of nonlinearity pre-specified in the simulated data. Secondly, if the SDM can recognise and capture different shifts in the mean of the time series. Of course, distinguishing the true nonlinear form of the model and accurate estimation of the parameters are essential in producing good forecasts. In fact, the results in Chapter 6 (forecasting chapter) show improved forecasting accuracy using the SDM algorithm over classical forecasting and machine learning methods. Therefore, this chapter contributes to the theory and the literature by investigating the reliability and validity of the SDM using simulations from various linear and non-linear time series models.

The present analysis began by providing a literature review on simulated studies. This study simulates data from the linear models, logistic smooth transition autoregressive (LSTAR) models, and an exponential smooth transition autoregressive (ESTAR) model. Then, the SDM is used to fit the simulated data in order to verify the ability of the SDM to capture the behaviour of the simulated models. Subsequently, the SDM is implemented in simulated time varying coefficient models with different degrees of change in the

intercept coefficient. The results show that the SDM algorithm can accurately prescribe the linear and specific non-linear form of a simulated time series, and capture the time varying behaviour of the intercept terms.

3.2 Review of simulated studies on SDM, gaps in the research, and the contribution of the present study

There has been a tremendous surge of interest in studying nonlinearity in economic time series (Koop and Potter, 1998). Koop and Potter (2001) argued that in macroeconomics, many policy debates and modelling rely on whether a time series is linear or nonlinear. Therefore, it is important to work out specific linear/non-linear forms to aid the modelling and policymaking processes.

A limited study of State-Dependent Model fitting using simulation data was provided in Haggan, Heravi and Priestley (1984), who generated positive and interesting results. However, no prior simulated studies have applied SDM algorithms on logistic STAR models or on Exponential STAR models, or on time-varying smooth transition intercept models. Industrial production indices can be modelled using STAR/STR models (Teräsvirta and Anderson, 1992), and the relationship between US GNP and leading indicators can be explored using STR models (Granger and Teräsvirta, 1993). There seems to be a need for STAR models in the literature. However, these studies made a prior assumption about STAR/STR models before model fitting. SDM is therefore important to check the nature of potential nonlinearity for these economic data, and to see how SDM works in simulated STAR models. This study first seeks to study whether the SDM can replicate linearity or specific nonlinearity expressed in simulated models. It

also seeks to analyse intercepts of different speeds of smooth transitions can be modelled and captured by SDM algorithms.

This study fills the abovementioned research gaps and provides a new set of extensive empirical evidence using simulated data with which to evaluate the theory of the State-Dependent Models.

3.3 Numerical Examples on Simulated Series

In order to investigate how the SDM algorithm fits different classes of time series models, the SDM was applied to simulated time series with typical linear and non-linear characteristics. For each simulation, 500 observations were generated. The scatter plot of estimated parameters was smoothed using LOWESS smoothing techniques (Cleveland, 1979; Cleveland *et al.*, 1981; Becker, Chambers and Wilks, 1988). The LOWESS smoother employs a locally weighted polynomial regression in smoothing plots, where a local linear polynomial fit or a local constant fit are used. A weighted least square method was employed. The distance to the $(f \times n)^{\text{th}}$ nearest neighbour was used for local fitting. Here, the value f is the proportion of data influencing a smoothed point. The larger the value of f, the smoother the LOWESS is. The estimated parameters were plotted against their corresponding Y_{t-1}, and compared with their theoretical functions. The estimates were also plotted against time. Then, the true values of the simulated parameters and the fitted values produced by SDM were graphically presented and compared.

This section considers several different simulations, including a linear $AR(2)$ process, LSTAR processes, and an ESTAR process. In an $AR(2)$ process, the coefficients are constant, and for LSTAR and ESTAR processes, the coefficients are logistic and

exponential functions, respectively. The state-dependent model (SDM) algorithms were applied and model fittings investigated. Then, time-varying coefficient models with different speed of transition were simulated to verify the ability of the SDM to capture the varying degrees of transition in the intercept.

In the following section, the solid lines in each graph represent the functional form of the parameter for the true (non)linear model. The dash lines represent the parameter estimated from SDM. The theory of SMD is tested by graphical comparison of the true functional form of the parameter (solid line) with the estimated parameter (dash line) computed by the SDM algorithm.

3.3.1 Linear model simulation

In this simulation study, 500 observations from the following linear $AR(2)$ process were generated:

$$Y_t = 0.4Y_{t-1} - 0.7Y_{t-2} + \epsilon_t$$

where $\{\epsilon_t\}$ is a sequence of independently and normally distributed random numbers with a mean of zero and a standard deviation of one. In this case, the first 50 observations were used and an $AR(2)$ model was fitted to produce the initial values.

Figure 3-1 Plot of μ, θ_1, θ_2 against y_{t-1}

The following figure contains graphs of μ, θ_1, θ_2 estimated from SDM plotted against delay Y_{t-1} , in dashed lines, for simulated equation $Y_t = 0.4Y_{t-1} - 0.7Y_{t-2} + \epsilon_t$. The solid lines represent the true values simulated. The value of the smoothing parameter in the SDM algorithm was set to 0.01%.

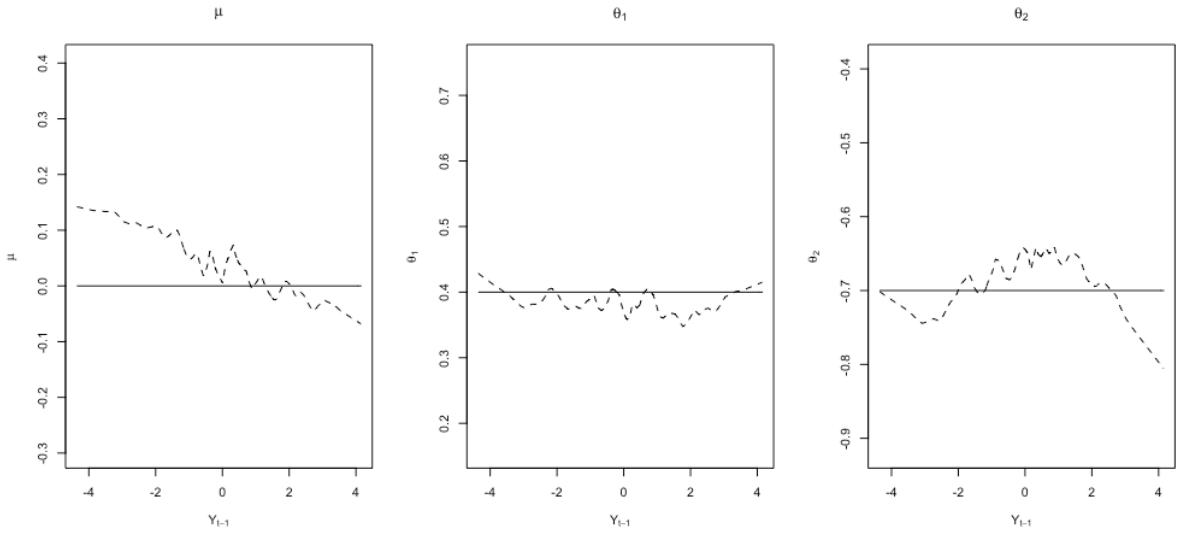

If the SDM fits this $AR(2)$ process well, the plotted values for μ in Figure 3-1 should be near zero, θ_1 should be constant and close to 0.40, and θ_2 should be flat and close to -0.70. The initialisation procedure from linear AR(2) produced the following estimates:

μ = 0.0483, θ_1 = 0.518, θ_2 = -0.672,

Variance-covariance matrix = $\begin{pmatrix} 0.0224 & -0.000491 & -0.000282 \\ -0.000491 & 0.0110 & -0.00332 \\ -0.000282 & -0.00332 & 0.0109 \end{pmatrix}$

σ_ϵ^2 = 1.07

The SDM algorithm was applied and the initial estimates were then updated over time through Kalman Filtering. The recursion started from $t = 26$. From a visual inspection of the μ, θ_1, and θ_2 in Figure 3-1, it was observed that μ stayed close to 0.00; θ_1 was very

close to 0.40, and θ_2 fluctuated mildly around -0.70. These figures indicate that the SDM algorithm can reproduce the true shape of the parameters of the simulated linear $AR(2)$ process. Therefore, based on the data only, the SDM model provided strong evidence that the series was generated by a linear model.

3.3.2 Logistic Smooth Transition Autoregressive (LSTAR) simulations

This section describes how the data simulated from two LSTAR process were generated, and model fitting was investigated. The difference between the two simulations was that in the first LSTAR simulation, the slope coefficient was positive and increasing, while for the second simulation, the simulated slope coefficient was a negative and decreasing function of the state vector. Again, 500 observations were generated. The first 50 observations were used for initialisation, and the recursion of the SDM started from $t = 26$.

a) Simulation with a Positive Slope Curve

The first LSTAR simulation has the following form:

$$Y_t = 0.4(1 + e^{-Y_{t-1}})^{-1} Y_{t-1} + \epsilon_t$$

In this equation, the gamma (speed of transition) is 1.00.

If Y_t is written in the form $Y_t = h(Y_{t-1}) + \epsilon_t$, and differentiating h with respect to Y_{t-1}, it can be seen that the true functional form of θ should be as follows:

$$\theta(Y_{t-1}) = \frac{2(1 + e^{-Y_{t-1}} + Y_{t-1}e^{-Y_{t-1}})}{5(e^{Y_{t-1}} + 1)^2}$$

This function was plotted in solid line, to represent the true values of θ. The smoothing parameter f was set to 10%. If the fitting is good, the two lines should be as close to each

other as possible. The range of θ in this case was between approximately 0.00 and 0.40, and the dashed line and solid line intersected at (0.00,0.20).

Figure 3-2 Plot of θ against Y_{t-1}

The following figure contains a graph of θ estimated using SDM plotted against Y_{t-1} for the simulated equation $Y_t = 0.4(1 + e^{-Y_{t-1}})^{-1}Y_{t-1} + \epsilon_t$ as plotted via a dashed line. The solid line represents the true values' functional form.

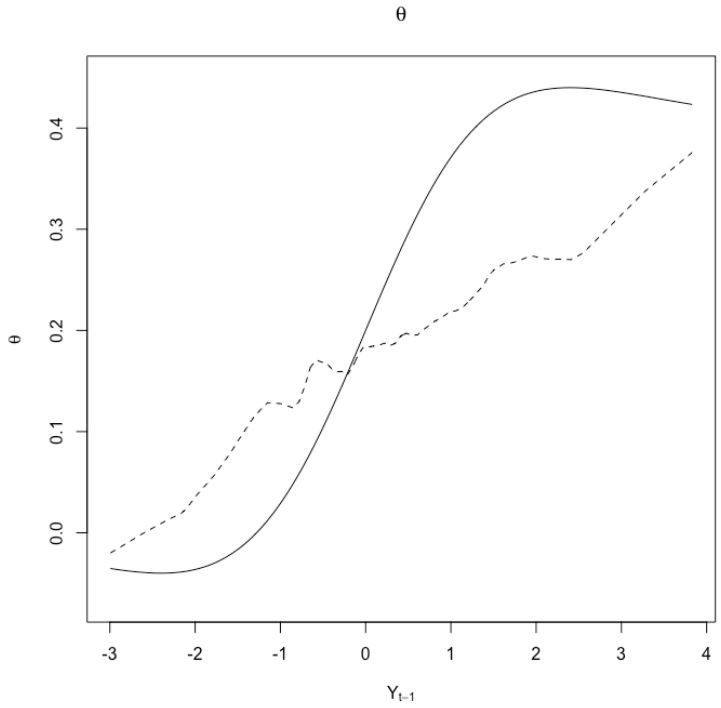

The preliminary estimates were:

$\theta = 0.161$,

Variance-covariance matrix = $\begin{pmatrix} 0.0151 & -0.00372 \\ -0.00372 & 0.0198 \end{pmatrix}$

σ_ϵ^2=0.708

In Figure 3-2, the estimated line (in dashed form) produced by the SDM algorithm fitted the actual θ parameter well. The range of fitted θ values were approximately the same as

the true parameter, which ranged from 0.00 and 0.40 and showed the same upward slope. These figures all indicate that the SDM algorithm confirmed that the series was generated by a LSTAR model.

b) Simulation with a Negative Slope Curve

The second LSTAR simulation has the following equation:

$$Y_t = -0.5(1 + e^{-Y_{t-1}})^{-1}\mathrm{Y}_{t-1} + \epsilon_t$$

The first derivative of the function with respect to Y_{t-1} is:

$$\theta(Y_{t-1}) = -\frac{1 + \mathrm{e}^{-Y_{t-1}} + \mathrm{Y}_{t-1}e^{-Y_{t-1}}}{2(e^{-Y_{t-1}} + 1)^2}$$

The curve has a range of approximately -0.50 to 0.00, and passes the point (0.00, -0.25).

Figure 3-3 Plot of θ against Y_{t-1}

The following figure contains a graph of θ estimated using SDM plotted against delay Y_{t-1}, smoothed in dashed lines, for simulated equation $Y_t = -0.5(1 + e^{-Y_{t-1}})^{-1}Y_{t-1} + \epsilon_t$. The solid lines represent the true values simulated.

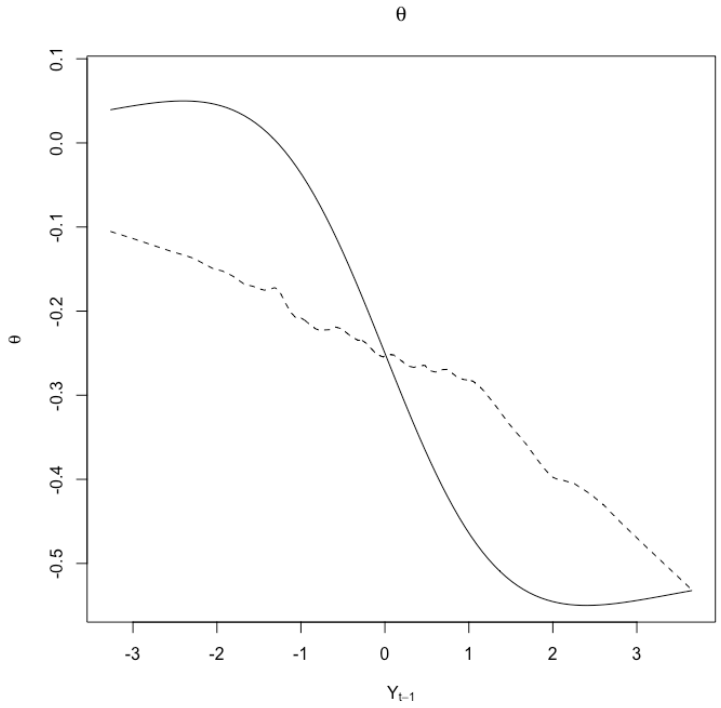

Based on Figure 3-3, the curve fitting is good, which indicates that the series was generated by an LSTAR model. Similar to the curve fitting for the first LSTAR simulation, the fitted curve is not as steep as the true functional form of the parameter.

3.3.3 Exponential Smooth Transition Autoregressive (ESTAR) simulations

In this example, 500 observations were generated using the following model:

$$Y_t = 0.7\left(1 - e^{-1.1Y_{t-1}^2}\right)Y_{t-1} + \epsilon_t$$

The SDM algorithm was run to produce a plot of estimated θ against Y_{t-1}. The first 50 observations were used to produce initial values of μ, θ, the variance-covariance matrix,

and σ_ϵ^2. Recursion started from $t = 26$. The smoothing parameter for SDM was set to 0.001, and the proportion of data influencing a single point in the LOWESS smoothing was 20%.

Figure 3-4 Plot of θ against Y_{t-1}

The following figure contains a graph of θ estimated via SDM, and plotted against delay Y_{t-1}, smoothed in dashed lines, for simulated equation $Y_t = 0.7\left(1 - e^{-1.1Y_{t-1}^2}\right)Y_{t-1} + \epsilon_t$. The solid lines represent the true values simulated.

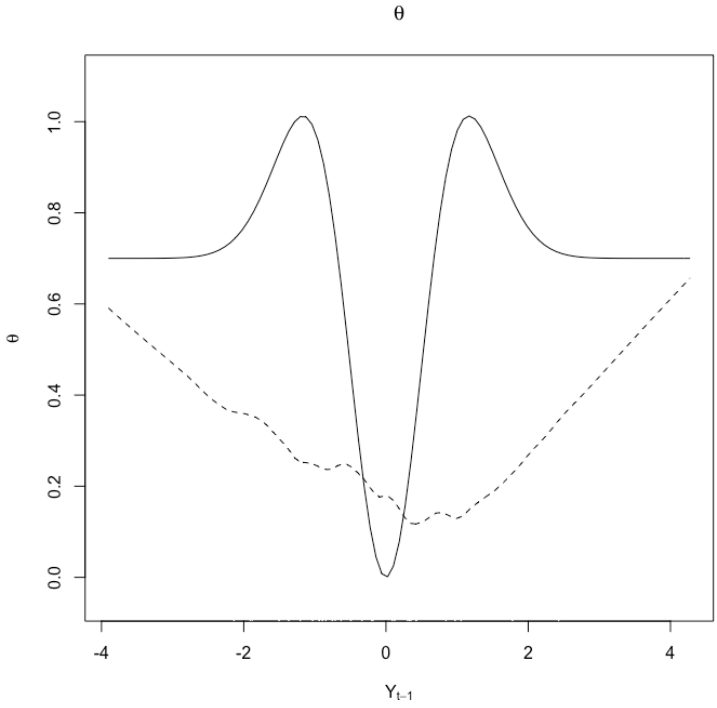

The actual θ values should vary according to the first derivative of the ESTAR model, i.e.

$$\theta(Y_{t-1}) = \frac{e^{-1.1Y_{t-1}^2}(35e^{1.1Y_{t-1}^2} + 77Y_{t-1}^2 - 35)}{50}$$

The preliminary estimates of the model are shown below:

μ = 0.314, θ = 0.327

Variance-covariance matrix = $\begin{pmatrix} 0.0282 & -0.00731 \\ -0.00731 & 0.0170 \end{pmatrix}$

σ_ϵ^2=1.229

Figure 3-4 shows that the fitted curve has very similar characteristics with the true value of θ. The values of θ at both the left-hand side and the right-hand side are very close to the expected value, 0.70, and the minimum of the fitted curve also occurs near the point where $Y_{t-1} = 0.00$. Therefore, the SDM was able to provide a very good fit through prescribing the right non-linear shape and the right range of values. In particular, the symmetrical appearance of Figure 3-4 is obviously different from the graphs for LSTAR models, and this is an important feature of the parameters for ESTAR models.

3.3.4 Simulations with time varying intercept coefficients

Having examined model fittings for the linear time series, and non-linear LSTAR and ESTAR models, the following section investigates whether the SDM algorithm can capture shifts in the intercept parameter, μ.

Three simulations from models with time varying intercept parameters were produced. A total of 500 observations were simulated. The first 50 observations were used to provide initial values, and a linear model was used to provide initialised values of μ, θ, the variance-covariance matrix, and σ_ϵ^2. The SDM algorithm was applied and recursion started from $t = 26$. Plots of the three simulated series are presented below:

Figure 3-5 Plots of the simulated time series for γ = 0.5, γ = 1.0 and γ = 10.0

The following figure presents the time series plots with equation $Y_t = (1 + e^{-\gamma z})^{-1} + 0.6Y_{t-1} + \epsilon_t$, with $\gamma = 0.50$, 1.00 and 10.0, where γ represents the adjustment in the logistic function. z takes its value from -5 to 5 at equal intervals of 0.02 (for 500 observations).

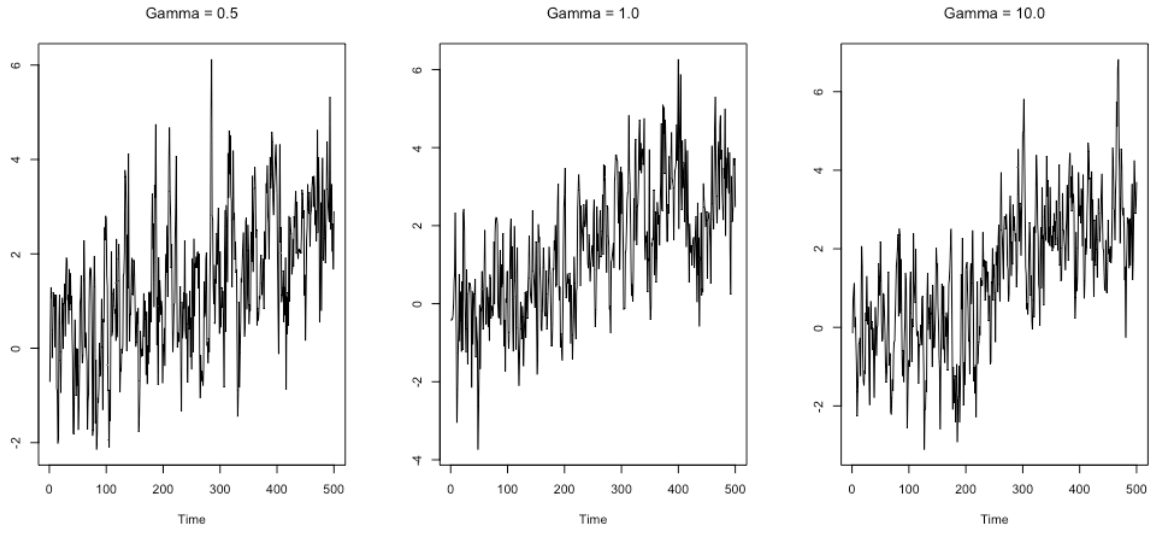

It can be observed from Figure 3-5 that the first series had the most gradual transition in level, and the third series had the most abrupt change in level.

a) Smooth shift in the level (mean) of time series ($\gamma = 0.50$)

The first simulation equation was as follows:

$$Y_t = (1 + e^{-0.5z})^{-1} + 0.6Y_{t-1} + \epsilon_t$$

In this equation, z sequentially takes values from -5 to 5 at equal intervals. The coefficient γ is 0.50, which represents the speed of adjustment. After using the first 50 observations to initialise values of μ, θ, variance-covariance matrix and σ_ϵ^2, in SDM algorithm, a Kalman filter was run. The recursion started from $t = 26$ and the SDM

reported estimated values for μ and θ. The smoothing parameter used in the SDM algorithm was 0.001, and the smoothing proportion of the LOWESS smoothing was 20%.

Figure 3-6 Plot of μ against time, and plot of θ against Y_{t-1} with γ = 0.50

This figure contains the graphs of μ estimated from SDM plotted against time, and θ estimated from SDM plotted against delay Y_{t-1}, smoothed in dashed lines, for simulated equation $Y_t = (1 + e^{-0.5z})^{-1} + 0.6Y_{t-1} + \epsilon_t$. The solid lines represent the true values simulated.

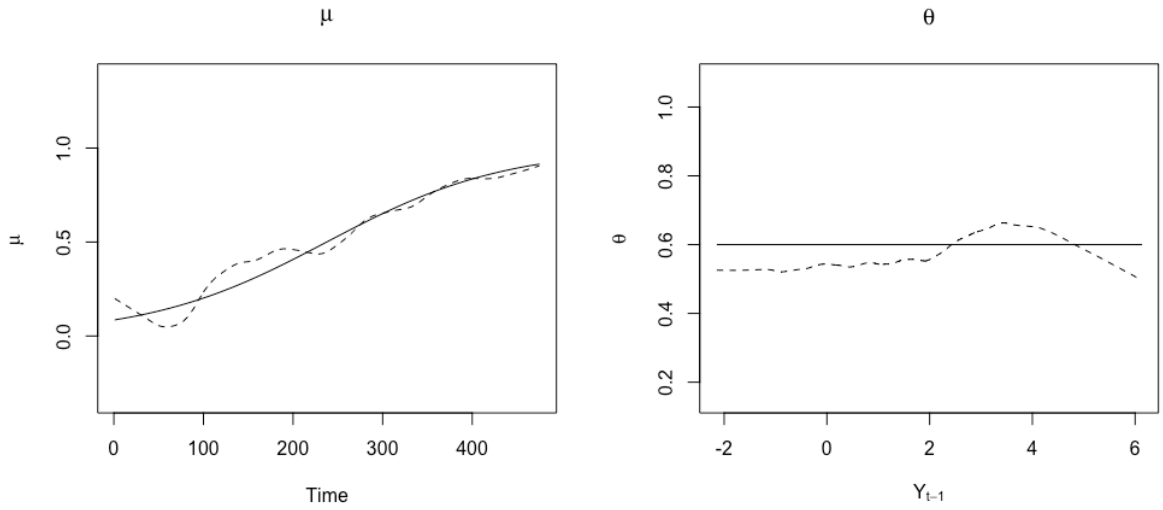

The preliminary estimates of the simulated time series were as follows:

μ = 0.153, θ = 0.575,

Variance-covariance matrix = $\begin{pmatrix} 0.0152 & -0.00433 \\ -0.00433 & 0.0133 \end{pmatrix}$.

$\sigma_\epsilon^2 = 0.676$

Figure 3-6 demonstrates an excellent fit between the estimated and true intercept parameters. Not only does μ behave in a logistic transition manner, but the dashed lines in the graph almost perfectly fit the simulated parameters. The second graph also shows excellent behaviour of the θ parameters which vary very closely around 0.60 against different values of Y_{t-1}.

b) Smooth shift in the level (mean) of time series ($\gamma = 1.00$)

The second simulation used the following equation:

$$Y_t = (1 + e^{-1.00z})^{-1} + 0.6Y_{t-1} + \epsilon_t$$

Also, in this equation, z took sequential values from -5 to 5 at equal intervals in time. The SDM algorithm was run using the Kalman filter algorithm on the simulated time series. The smoothing technique was LOWESS, with the proportion influencing the smoothness set to 20%, and the smoothing parameter used in the SDM algorithm was 0.1%. The solid lines were true simulated μ and θ and the dashed lines were smoothed parameters. The first 50 observations were used for initialisation, and recursion started from $t = 26$.

Figure 3-7 Plot of μ against time and plot of θ against Y_{t-1} with γ = 1.00

The following figure contains the graphs for μ estimated using SDM plotted against time, and θ estimated using SDM plotted against delay Y_{t-1}, smoothed in dashed lines, for simulated equation $Y_t = (1 + e^{-z})^{-1} + 0.6Y_{t-1} + \epsilon_t$. The solid lines represent the true values simulated.

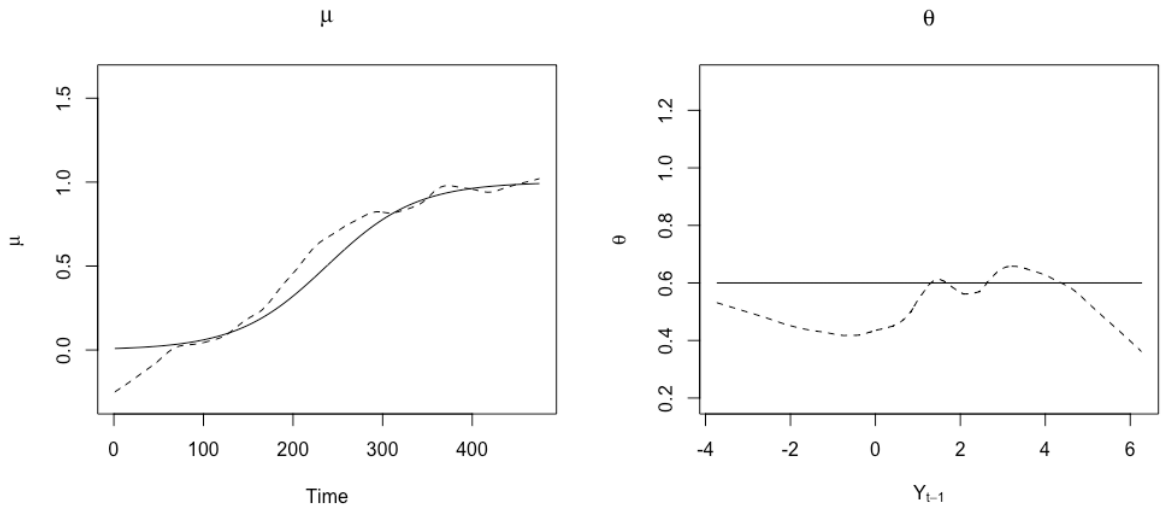

The preliminary estimates of the simulated time series are given below:

$\mu = -0.169$, θ =0.460,

Variance-covariance matrix = $\begin{pmatrix} 0.0272 & 0.00450 \\ 0.00450 & 0.0165 \end{pmatrix}$

σ_ϵ^2=1.27

The plot of μ against time in Figure 3-7 shows the clear logistic and rising behaviour of the estimated μ parameter produced by the SDM algorithm. The fit is excellent, and the speed of transition is slightly faster than that of the simulated data, with γ = 0.50. The plot of θ against Y_{t-1} also shows that θ is very close to 0.60. These figures show that the SDM algorithm can capture the time varying level shift, and that it is able to produce consistent slope estimates very close to that of the simulated.

c) Smooth shift in the level (mean) of time series ($\gamma = 10.0$)

Having examined the actual and fitted values for logistic mean shifts for γ = 0.50 and γ = 1.00, another time series was simulated. Here, the coefficient γ was changed to be 10.0 and there was a rapid change in mean. As γ is the steepness of the logistic curve, if the SDM can capture the increase in steepness, it is expected that the estimated μ against time for this simulation should have the steepest shape of all three of the simulations.

$$Y_t = (1 + e^{-10.0z})^{-1} + 0.6Y_{t-1} + \epsilon_t$$

Again, z took sequential values from -5 to 5 at equal intervals in time.

Figure 3-8 Plot of μ against time and plot of θ against Y_{t-1} with γ = 10.0

The following figure contains graphs of μ estimated from SDM plotted against time, and θ estimated from SDM plotted against delay Y_{t-1}, smoothed in dashed lines, for simulated equation $Y_t = (1 + e^{-10z})^{-1} + 0.6Y_{t-1} + \epsilon_t$. The solid lines represent the true values simulated.

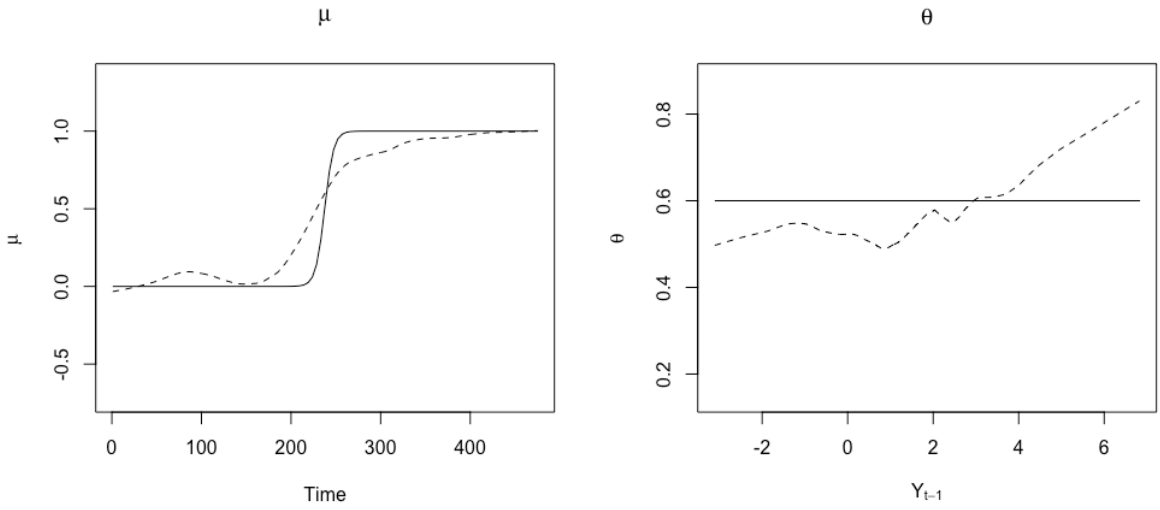

The preliminary estimation gave the following results:

μ = -0.00580, θ = 0.615,

Variance-covariance matrix = $\begin{pmatrix} 0.0146 & 0.00208 \\ 0.00208 & 0.0150 \end{pmatrix}$

σ_ϵ^2 = 0.700

Figure 3-8 shows a faster speed of adjustment than that in Figure 3-6 and Figure 3-7. This clearly indicates that the SDM algorithm can correctly pick up further increases in the value of γ. The second graph in Figure 3-8 demonstrates that estimates of θ vary around the simulated value of 0.6. This shows that reliable estimates can be produced on the intercept and slope coefficient around pre-specified values from the simulated model. The previous examples provide strong evidence that the data is generated from a linear model with a time varying mean.

3.4 Discussion and Conclusion

Limited simulation study have been reported in Haggan, Heravi and Priestley (1984), Heravi (1985). This study fills the gap by extending the Monte Carlo Simulation study. In this Chapter, data from various linear and nonlinear models were generated to test the theory of the State Dependent Models. As the STAR family of models are widely seen and applied in finance and economics, the ability to identify LSTAR and ESTAR models will be very useful in the field. Therefore, specifically, data were generated from LSTAR and ESTAR processes to test the SDM.

The results of the SDM model fitting in this chapter show the capability of the SDM to prescribe (non)linearity in simulated data. This implies that given data from a particular time series model, the SDM can prescribe its (non)linear form. The simulation study shows that the SDM can distinguish between different nonlinear models without any prior assumptions. The results from simulation study indicated that the SDM is a reliable exploratory analysis and can indicate which family of nonlinear model is most appropriate to fit, or if a linear model is equally satisfactory. SDM could also help the researchers to develop new and interesting nonlinear models. Thus it is interesting to apply the SDM in order to find the most suitable model in real life situations. With a

good understanding of the type of nonlinearity in the real and simulated time series, we will be able to further understand the economic phenomena such as business cycle, mean-reverting behaviours of real exchange rates, and also to forecast real time series processes well.

This chapter has contributed a thorough examination of the modelling ability of State Dependent Models using data generated from linear and non-linear models. The results in this chapter gave strong evidence that the State-Dependent Model can prescribe linearity in the parameters and identify specific non-linearity in different simulated models. The SDM can also accurately capture varying degrees of smooth transition in intercepts and slope parameters. The intercept parameter estimated from applying the SDM model and plotted against time provides information about the behaviour of the time series. This also reveals the capability of the SDM algorithm in confirming the true generated model. In the following chapters, the SDM algorithm is applied to modelling, testing, and forecasting financial, economic and tourism data.

Chapter 4 Application of State-Dependent Models to Industrial Production Data

4.1 Introduction

The previous chapter showed that the State Dependent Model has an excellent ability to correctly identify the specific form of (non-)linearity in simulated data. The present chapter represents among the first attempts to use the SDM model to examine (non-)linearity and structural breaks in real business data. First, it presents an overview of non-linearity in business cycles. Then, the motivations for, and contributions of, using the state dependent model in modelling UK industrial production indices are explained. Data are presented, methodologies are described, and then the results are analysed and evaluated. This chapter ends with an evaluation, limitations and discussions.

4.2 An Overview of Non-linearity in Business Cycles and Industrial Production Data

The study of (non-)linearity in business cycle indicators enables various interested parties such as investors, producers, and governments to anticipate the momentum of business situations and the timing of turning points. It can also help in identifying the state of the business cycles which they are currently in – such as upturns, downturns, or neither, so that they can develop steps in policy making such as strategic planning and funding decisions. Understanding the (non-)linearity of business cycles can help tremendously in understanding their nature, and thus to anticipate and make informed decisions.

The seminal work by Mitchell (1927, pp. 407 - 412) showed that business cycles in economic and business time series are asymmetric. Further studies conducted by Keynes

(1936) and more recently by Artis, Kontolemis and Osborn (1997) suggested a potential nonlinearity in European business cycles, with downturns generally being more short-lived than upturns. Peel and Speight (1996) also found non-linearity in the growth rates of all macroeconomic series, including industrial production, unit labour costs, unemployment, and consumer prices, and reported that all of these time series exhibit non-linearity.

The characteristics of non-linearity have very important implications for these economic time series. Firstly, they mean that traditional linear time series models may provide incorrect descriptions of business cycles, as these models assume symmetric cyclical fluctuations in business cycles which do not in fact occur in reality (Teräsvirta and Anderson, 1992). These linear models are thus potentially incorrect and misleading in their specification and representation (Bradley and Jansen, 2004) of business cycle characteristics. Inaccurate model specifications potentially have negative implications for forecasting (Teräsvirta and Anderson, 1992), which have led to increased attention being paid to investigating non-linearity in business cycles. Therefore, there is a need to explore linearity/nonlinearity in business cycle indicators.

In business, economics and finance, it is generally found that asset returns are asymmetric (Franses and van Dijk, 2005), and commodity prices are also asymmetric (Ghoshray, 2019). Large negative returns are generally be found with higher volatilities, while large positive returns are less so. This is probably due to investor react more violently to downturns than upturns, which may be linked to the prospect theory. It has motivated this study to test if all business cycles indicators are indeed asymmetric.

4.3 Mixed Evidence in Empirical Applications on Business Cycle Indicators

There is plenty of evidence supporting nonlinearity and asymmetry in business cycle indicators. The Smooth Transition Autoregressive (STAR) model was employed to model non-linearity in business cycle time series by Teräsvirta and Anderson (1992). They fitted STAR models to the quarterly difference in logarithms of industrial productions of OECD industrial output series. They found that both models fit well and captured sharp transitions from expansion to contraction phases, but they also discovered no mechanisms from expansion towards recession (Teräsvirta and Anderson, 1992).

Öcal and Osborn (2000) analysed the UK's real consumer expenditure and industrial production, and reported superior forecasts using two-transition STAR models in comparison to other models in periods of economic contraction. Franses and van Dijk (2005) compared forecast performance for quarterly seasonality unadjusted industrial production indices for 18 OECD countries, and found that the non-linear TVD-STAR and TV-STAR models performed much better than other types of linear and non-linear models. Further, Hassani, Heravi and Zhigljavsky (2009) investigated German, French and British industrial production time series and found that the Singular Spectrum Analysis model produced much better longer-term forecasts than the linear ARIMA and Holt-Winters forecasts. The non-linear neural network model fitted to the industrial production data of Germany, France, and the UK yielded very good results in predicting the direction of change (Heravi, Osborn and Birchenhall, 2004).

However, evidence against nonlinearity and asymmetry has also been presented. Delong and Summers (1986) investigated a possible asymmetry issue with skewness coefficients

and concluded that detrended business cycle indicators in relation to pre- and post-war GNP and industrial production data displayed cyclical oscillations with a rising trend. Westlund and Öhlén (1991) employed detrended seasonally adjusted industrial production and unemployment as business cycle indicators which ranged from 1960Q1 to 1988Q1, and also found no evidence of asymmetry.

Therefore, the prior evidence is mixed regarding the symmetry and (non-)linearity of business cycles.

4.4 Motivations and Contributions

As can be inferred from the literature reviewed above, there is no consensus in terms of linearity or symmetry in business cycle indicators, and modelling business cycle indicators by forcing a pre-assumed non-linear model may produce incorrect estimates.

One major advantage of the SDM is that it is general, and as such, encapsulates all types of specific nonlinear models without assuming (non-)linearity. If industrial production were linear, the SDM would be able to reflect this result too. The SDM can also potentially prescribe specific types of non-linearity and capture various different structural breaks in these time series.

The SDM model can serve as a useful tool with which to diagnose (non-)linearity and asymmetry. It was successfully applied to a model in a multivariate approach to describe US consumption as non-linear functions of sentiment and income (Heravi, Easaw and Golinelli, 2016). Easaw, Heravi and Dixon (2015) also applied the SDM to model the non-linear persistence of the inflation gap using professional forecasts, and found strong

state dependence and time-dependence in CPI-inflation. Therefore, it is reasonable as a first attempt to apply the SDM algorithm to modelling business cycle indicators.

Therefore, this study aims to graphically describe and explore the true nature of (non-)linearity in industrial production time series, and to answer the research question of what types of non-linearities are present in industrial productions time series, if there are any; and to identify where the significant changes in structures in these time series are, as structural breaks are present in these industrial production indices. The study seeks to let the data speak for itself, in checking if a linear model is sufficient for modelling the data.

As the SDM has been successfully implemented in modelling non-linear inflation gap estimation and US consumption from income and sentiment, this project extends the SDM algorithm in the same spirit to check and diagnose (non-)linearity in the industrial production series.

4.5 Data

Industrial production is a significant component of a country's Gross Domestic Product (Skalin and Teräsvirta, 1999). Therefore, it is a good indicator with which to reflect the behaviour of business cycles (Hamilton and Lin, 1996), and previous studies have employed industrial production indices as indicators of business cycles (Teräsvirta and Anderson, 1992; Öcal and Osborn, 2000; Heravi, Osborn and Birchenhall, 2004; Franses and van Dijk, 2005; Hassani, Heravi and Zhigljavsky, 2009; Silva, Hassani and Heravi, 2018).

The present data consists of industrial production indices with respect to the UK. The sample period for each of the eight sectors of UK industrial production indices starts in

January 1998 and ends in August 2017[1]. The start date for the data was chosen based on the availability of consistent data for these series in Datastream. Eight sectors are examined, namely: Electrical and Electronic, Vehicles, Chemical, Basic Metal, Food, Gas, Machinery, and Fabricated Metal. The sectors covered are distinct types of industries with a variety of sub-sectors. The selection of sectors follows that of Heravi, Osborn and Birchenhall (2004), Osborn, Heravi and Birchenhall (1999), and Hassani, Heravi and Zhigljavsky (2013). It has been reported that for the UK, these eight sectors selected contributed majority (Hassani, Heravi and Zhigljavsky, 2013) of total industrial productions in the UK. For the same reason, the same sectors were chosen for this study. The frequency of the data is monthly. Each of the eight series are annual percentage changes in seasonally unadjusted industrial production data for each important sector. A more precise definition of each sector is provided in Appendix Table A.1.

This chapter presents the analysis of applying the State Dependent Model to data for the eight UK industrial production sectors. Osborn, Heravi and Birchenhall (1999) argued that it is appropriate to analyse economic time series after taking logarithms. In the same spirit, the variables used in the analyses are annual differences in logarithmic industrial production indices for each of the eight sectors. The process of taking logarithms and calculating annual differences is followed to remove seasonality and ensure that the series is stationary. This transformation means that the data studied in this chapter represent annual growth.

[1] For empirical evidence of the same categorisation of industrial production data as that employed in this study, see Osborn, Heravi and Birchenhall (1999); Heravi, Osborn and Birchenhall (2004); Hassani, Heravi and Zhigljavsky (2009) and Zhigljavsky, Hassani and Heravi (2009).

4.6 Descriptive Properties of the Data

Based on a visual inspection of the eight series shown in Figure 4-1, industrial production for the Food sector has an increasing trend, while the Electric & Electronic and Basic Metal sectors have downward trends. Most of the UK industrial production sectors have structural breaks at around 2008-2010 which are represented by a sudden change in direction and structure of the time series, except for the Gas sector. The timing of the structural break is in the wake of the impact of the credit crunch, the European sovereign debt crisis, and the global financial crisis. In this chapter, the SDM algorithm is used to identify multiple structural breaks.

Figure 4-1 Time plot of industrial production sectors for the United Kingdom

This figure shows monthly time series plots of industrial production indices for eight industrial sectors of the United Kingdom, namely Electric & Electronic, Vehicles, Chemical, Basic Metal, Food, Gas, Machinery, and Fabricated Metal, for the time period between 1998.01 and 2017.08.

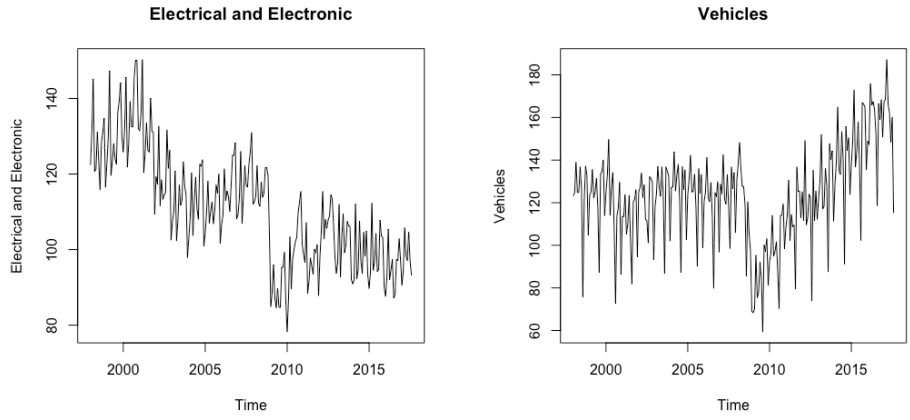

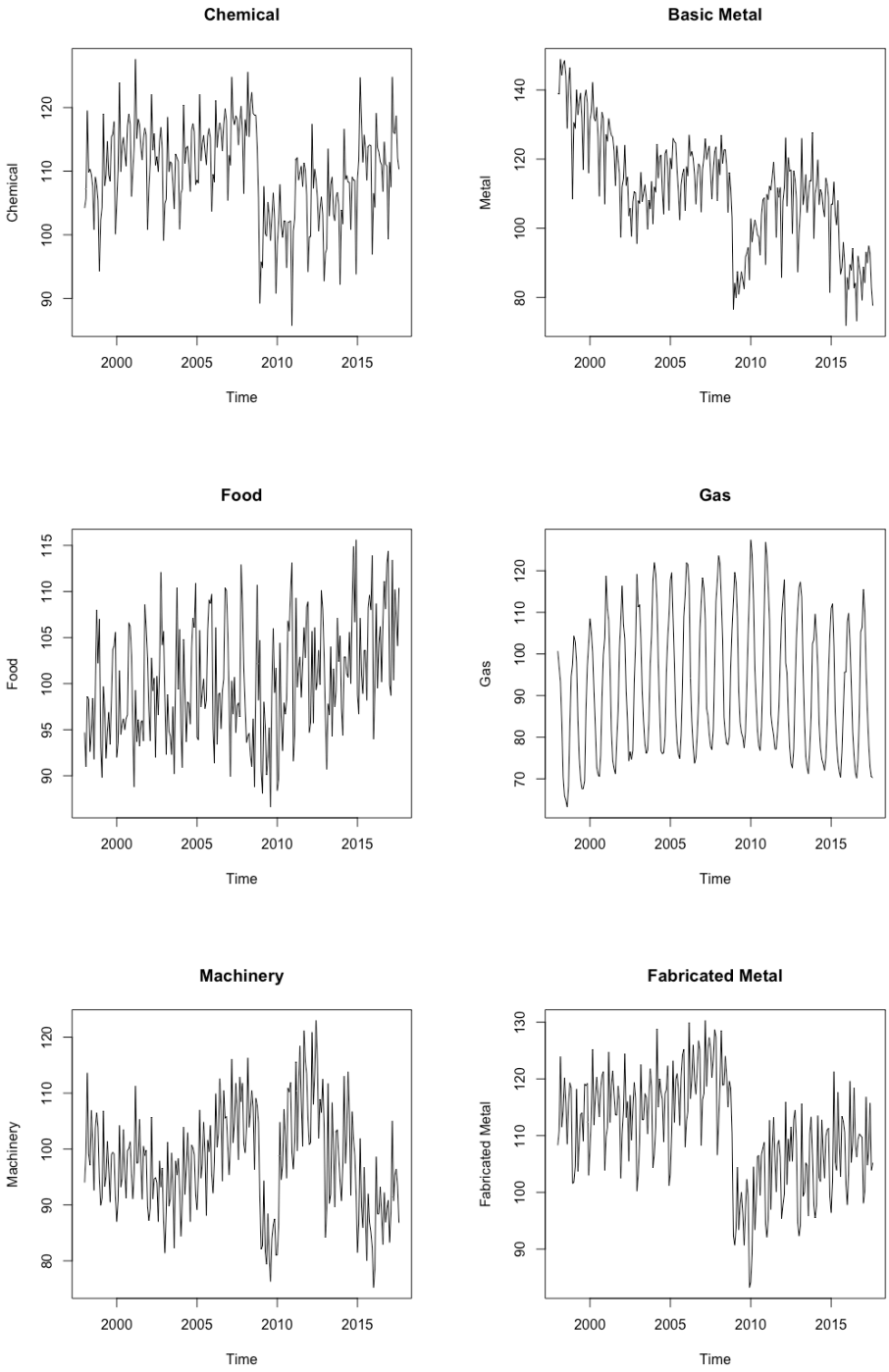

In this section, as the first step, an AR(k) model was fitted to each time series to select the lag k by minimising the Bayesian Information criterion (BIC). The AR(k) was used to provide initial estimates of μ, θ and σ_ϵ^2. The first 30 observations were used to provide initial values, and the recursion started from $t = 6$. To examine the existence of non-

linearity and structural breaks, the parameters were then plotted against the data with a lag of one, and the parameters were also plotted against time.

Escribano and Jordá (1997)'s method was employed to choose whether an ESTAR or an LSTAR model would be more appropriate to characterise the specific time series, or alternatively, if a linear model would be sufficient. Following their method, if the p-value for an even lag of the auxiliary polynomial equation is the smallest, then ESTAR is an appropriate model for the data. However, if the smallest p-value belongs to the odd power of the auxiliary polynomial equation, LSTAR is more appropriate to describe the time series. If the p-values of neither even nor odd powers are significant, this indicates that a linear model is most appropriate to describe the time series.

In order to investigate non-linearity and structural breaks, logistic and exponential smooth transition autoregressive models (LSTAR & ESTAR) were fitted. Logistic and Exponential Time-varying autoregressive (TVAR) models were also applied, and the threshold values were recorded and compared with those identified by the SDM algorithm. The test for structural breaks constructed by Bai and Perron (2003) was also applied to the eight data series for UK industrial production sectors to explore if the SDM and the Bai & Perron test were consistent in the identification of structural breaks.

4.7 Empirical Results for UK Industrial Production Data

4.7.1 Parameter estimation of optimal AR(k) models

Using the BIC, the optimal linear time series were obtained and are presented in Table 4-1.

Table 4-1 Parameter estimation

This table presents the parameter estimation for each of the industrial production indices of the United Kingdom after an $AR(k)$ model was fitted. The AR models were selected by minimising Bayesian Information Criterion when order $k = 1, 2, 3$ were used.

	μ	θ_1	θ_2	θ_3	Model selected
Electricals	-0.0117	0.855			AR(1)
	(0.576)	(0.000)			
Vehicles	0.0136	0.636	0.207		AR(2)
	(0.686)	(0.000)	(0.00147)		
Chemical	0.00306	0.628	0.230		AR(2)
	(0.818)	(0.000)	(0.000)		
Basic Metal	-0.0236	0.631	0.240		AR(2)
	(0.421)	(0.000)	(0.000)		
Food	0.00534	0.00662	0.168	0.555	AR(3)
	(0.470)	(0.904)	(0.00188)	(0.000)	
Gas	0.00478	0.524			AR(1)
	(0.441)	(0.000)			
Machinery	-0.00482	0.899			AR(1)
	(0.853)	(0.000)			
Fabricated Metal	-0.00584	0.583	0.291		AR(2)
	(0.735)	(0.000)	(0.000)		

4.7.2 Test of non-linearity and ESTAR/LSTAR model selection

The Escribano & Jordá test results are presented in Table 4-2. The p-values for ESTAR and LSTAR suggest that only six of the eight series were significant at a 10% significance level. These were: Electricals, Vehicles, Chemical, Gas, Machinery, and Fabricated Metal. According to Table 4-2, Electricals, Vehicles, Chemical, and Gas exhibited LSTAR nonlinearity, while Machinery and Fabricated metal followed ESTAR, and Basic Metal and Food were linear. For Gas, both ESTAR and LSTAR were significant, but LSTAR had a lower p-value for odd power than for even power, meaning LSTAR is a better model.

Table 4-2 Escribano & Jordá Model Selection Results

This table shows the results of a test proposed by Escribano and Jordá (1997). This test is used for two reasons. First, it compares relative strength in rejecting the null hypotheses of $H_{0E}: \beta_2 = \beta_4 = 0$ and $H_{0L}: \beta_1 = \beta_3 = 0$. If the odd power has the minimum p-value and is statistically significant, an LSTAR is more appropriate than the linear alternatives. Otherwise, an ESTAR is more appropriate if it is statistically significant against the linear alternatives. Secondly, if neither H_{0E} nor H_{0L} are significant, a linear model is more appropriate to model the time series. Here, the delay was set to lag one of the dependent variables.

Sectors	H_E (p-values)	H_L (p-values)	Result
Electricals	0.204	0.0661	LSTAR
Vehicles	0.401	0.0449	LSTAR
Chemical	0.601	0.0437	LSTAR
Basic Metal	0.667	0.972	Linear
Food	0.428	0.149	Linear
Gas	0.0858	0.00576	LSTAR
Machinery	0.0619	0.941	ESTAR

Fabricated Metal	0.0988	0.928	ESTAR

4.7.3 Bai & Perron's structural break test

Table 4-3 Results for the Bai & Perron structural break test with minimised BIC for eight selected industrial production sectors of the United Kingdom

The table below shows the results when Bai & Perron's structural break test was employed to examine the presence of m structural breaks from $m + 1$ segments in our time series. The test assesses deviations from stability. The breakpoints from models with minimised residual sum of squares (RSS) are reported in the table below. This method was applied to the industrial production sector data to identify the timing of specific structural breaks.

Sectors	Timing of structural breaks identified by Bai & Perron Test					
Electricals	2001(9)	2004(8)	2007(5)	2010(2)	2012(12)	-
Vehicles	-	-	2007(1)	2009(10)	-	-
Chemical	2001(9)	2004(6)	2008(3)	2010(12)	-	-
Basic Metal	-	2003(5)	2007(2)	2009(11)	-	2014(2)
Food	-	-	-	2010(1)	-	-
Gas	-	2004(5)	-	-	-	-
Machinery	-	2003(9)	2007(3)	2009(12)	2012(9)	-
Fabricated Metal	-	-	2007(8)	2010(5)	-	-

For seven of the data series, there were structural breaks at around 2009/2010, and for six series there were structural breaks near 2007/2008. Also, five series showed structural breaks in 2003/2004. Six out of the eight series had more than one structural break, which indicates a strong possibility of nonlinearity.

4.7.4 Fitting logistic and exponential time varying models

The results of the non-linear model fitting are presented in Table 4-4. When these two models were fitted, most of the series showed identified structural breaks at 2009/10. For the Vehicle, Chemical, Machinery and Fabricated Metal sectors, both models fitted a point of structural breaks near 2009/10. All series except one had a threshold which is highly significant at 1%.

Table 4-4 Fitting Logistic TVAR and Exponential TVAR

The following table displays the results of employing a logistic and an exponential time-varying autoregressive model. The model replaced a state-dependent transition variable with a time dependent variable from the general formula for a STAR model. For a logistic model, $G(\bar{t};\gamma,c) = (1+e^{-\gamma(\bar{t}-c)})^{-1}$, and $G(\bar{t};\gamma,c) = 1-e^{-\gamma(\bar{t}-c)^2}$ for Exponential TVAR model. $\bar{t}$ is normalised so that $\bar{t} = \frac{t'}{T}$. Estimates and statistical significance of Gamma and threshold c are reported. ***, ** and * represents statistical significance at 1%, 5% and 10%.

Sectors	Model	Estimate of Gamma	Estimate of Threshold	Time
Electricals	LTVAR	200	0.744***	2012(11)
	ETVAR	200**	0.558***	2009(5)
Vehicle	LTVAR	200	0.575***	2009(9)
	ETVAR	200***	0.547***	2009(4)
Chemical	LTVAR	200	0.576***	2009(9)
	ETVAR	200**	0.551***	2009(4)
Basic Metal	LTVAR	200	0.674***	2011(7)
	ETVAR	42.8	0.564***	2009(6)
Food	LTVAR	43.3	0.936***	2016(5)
	ETVAR	156*	0.638***	2006(11)
Gas	LTVAR	200	0.288	2004(5)
	ETVAR	198	0.210***	2002(11)
Machinery	LTVAR	200	0.642***	2010(12)
	ETVAR	163*	0.622***	2010(7)
Fabricated Metal	LTVAR	200	0.578***	2009(9)
	ETVAR	175***	0.556***	2009(5)

4.7.5 SDM estimations for sectors

For the methodology of the parameter estimation using the State Dependent Model, please refer to Chapter 2.

4.7.5.1 Electric and electronic

An AR(1) model was fitted using the first 30 observations:

μ = 0.0233, θ_1= 0.688,

Variance-covariance matrix = $\begin{pmatrix} 0.0000491 & -0.000712 \\ -0.000712 & 0.0222 \end{pmatrix}$

σ_ϵ^2 = 1.07

Figure 4-2 Plot of μ and θ_1 against the transition variable for Electricals

The following graphs plot μ and θ_1 against the transition variable for the Electricals sector. The transition variable is annual growth with one lag.

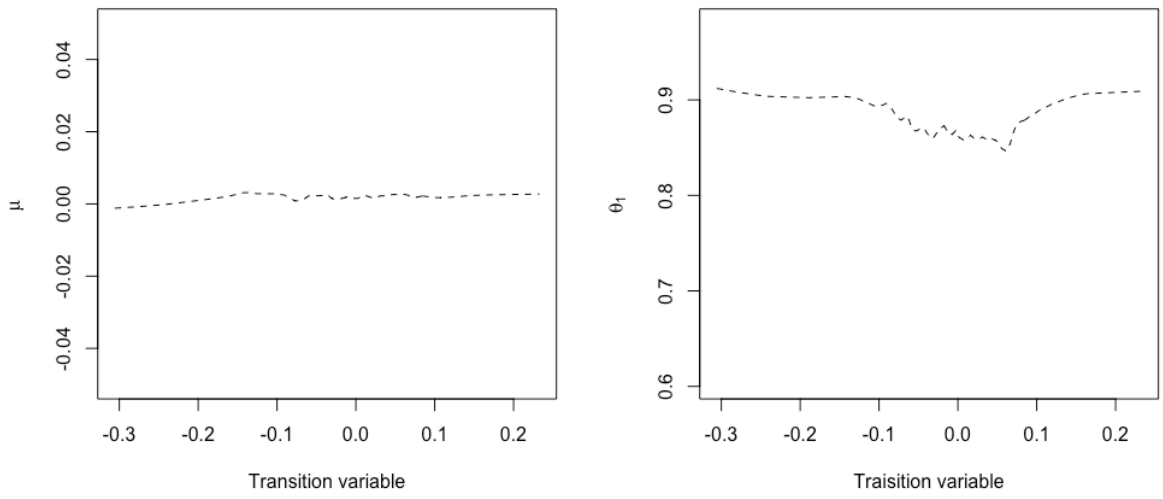

Figure 4-3 Plot of μ and θ_1 against time for UK Electricals

The following graphs plot μ and θ_1 against time for the UK Electricals sector. The purpose was to check for (non-)linearity and structural breaks collectively from the time varying coefficients prescribed by the SDM model.

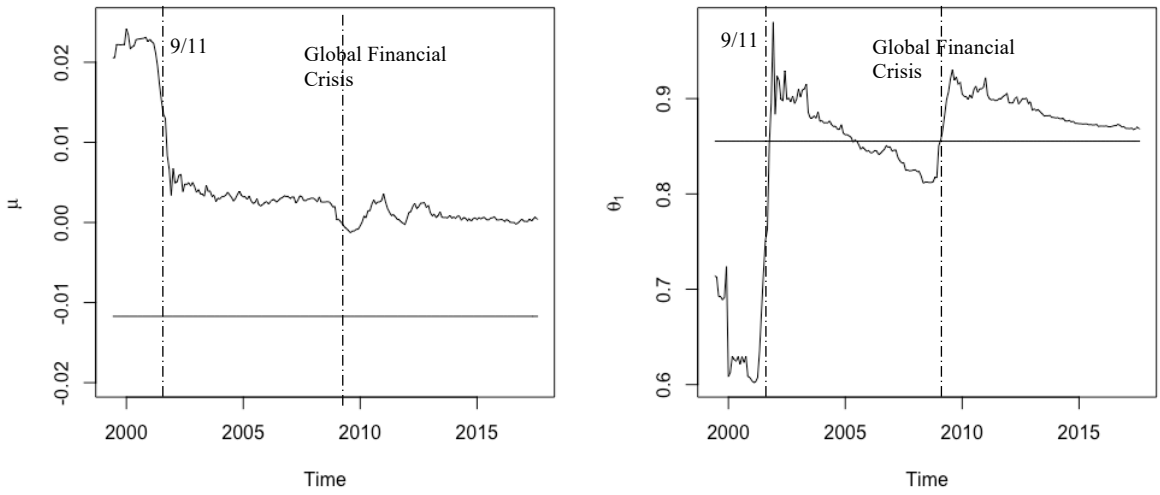

The shape of μ and θ_1 plotted against the transition variable in Figure 4-2 appear to be globally linear, with μ flat at around 0.00 and θ_1 flat at around 0.90. Figure 4-3 presents μ and θ_1 plotted against time. It can be observed that the θ_1 estimate fluctuates around the AR estimate overall, especially after 2002. Two obvious structural breaks were identified by the SDM; one at around 2001 and the other at around 2009. These are consistent with the structural breaks observed from the time series, and also with the two structural breaks captured by Bai & Perron's test in 2001(9) and 2010(2). The SDM also picked up the structural breaks identified in 2009(5) by the Exponential TVAR model. Therefore, judging from μ and θ_1 for the Electric and Electronic data, the series may be globally linear but with structural breaks, consistent with Bai & Perron's test and the Exponential TVAR model.

4.7.5.2 Vehicles sector

An AR(2) model was fitted using the first 30 observations:

μ = -0.0452, θ_1= 0.408, θ_2= 0.262,

Variance-covariance matrix = $\begin{pmatrix} 0.000274 & 0.000724 & 0.000489 \\ 0.000724 & 0.0330 & -0.0191 \\ 0.000489 & -0.0191 & 0.0340 \end{pmatrix}$

σ_ϵ^2 = 0.00621

Figure 4-4 Plot of μ, θ_1 and θ_2 against the transition variable for the UK Vehicles sector

The following graphs plot μ, θ_1 and θ_2 against the transition variable for the UK Vehicles sector. The transition variable is lag 1 of the dependent variable.

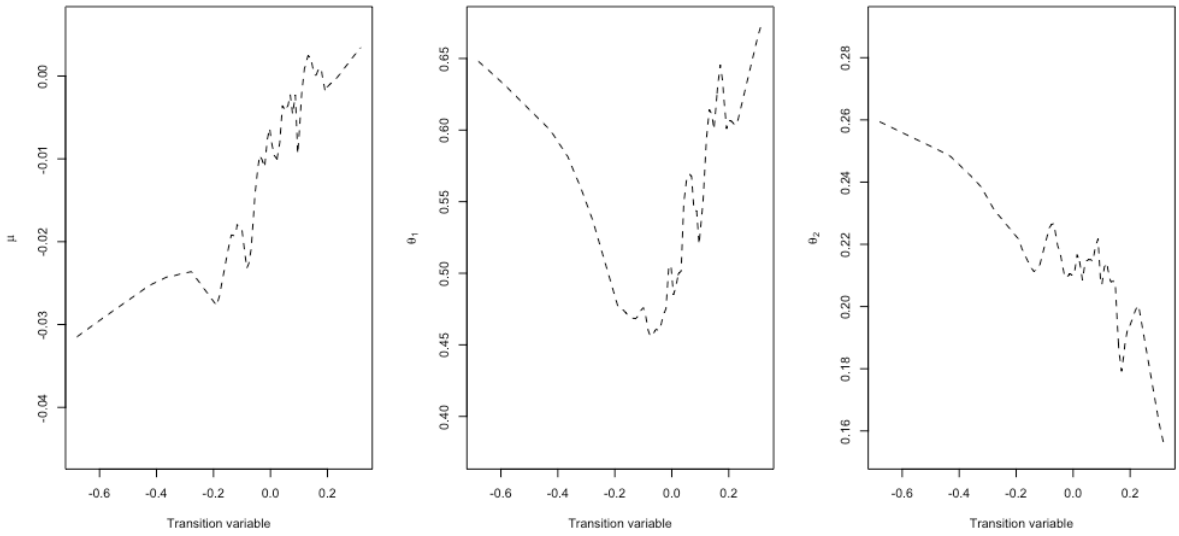

Figure 4-5 Plot of μ, θ_1 and θ_2 against time for the UK Vehicles sector

The following graphs plot μ, θ_1 and θ_2 against time for the UK Vehicles sector. The purpose was to check for (non-)linearity and structural breaks collectively from the time varying coefficients prescribed by the SDM model.

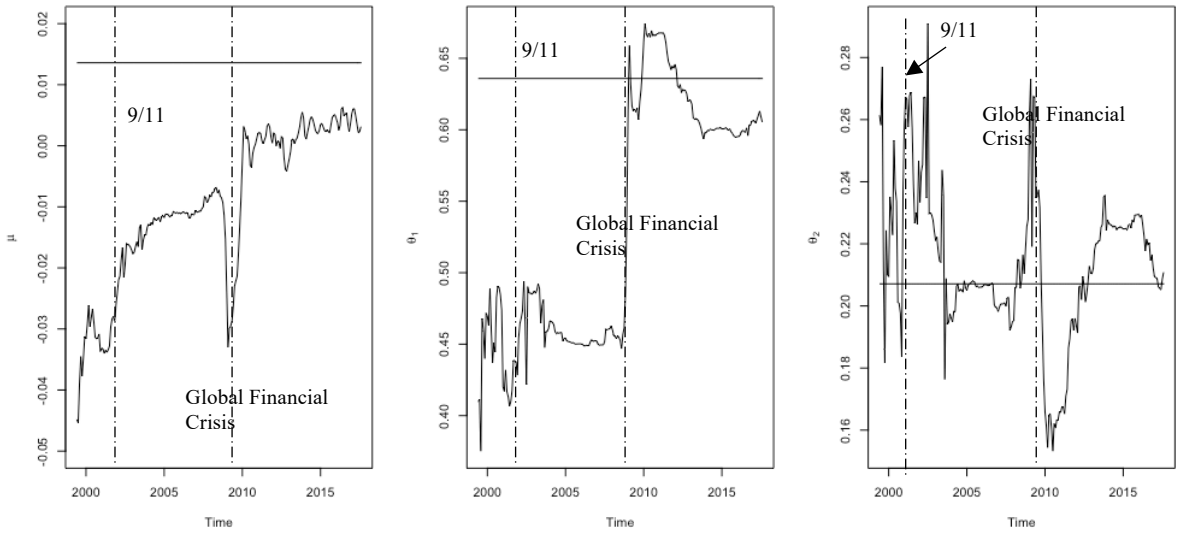

Here, θ_1 and θ_2 are both significant. Although θ_1 is the most significant parameter, the shape of θ_2 as indicated in Figure 4-4 is more consistent with the Escribano and Jordá (1997) model's selection results, for which LSTAR is selected. Overall, the shapes of the SDM estimates indicate significant non-linearity. Figure 4-5 shows μ, θ_1, θ_2 plotted against time. The straight lines show the coefficient estimates after fitting an AR(2) model. μ was underestimated by SDM by about 0.05, and θ_1 and θ_2 fluctuated around the respective AR(2) estimates. A clear structural break could be identified in 2009 by θ_1, which is consistent not only with the time plot, but also with the break identified by Bai & Perron's structural break test at 2009(10). This was also supported by the structural breaks identified when Logistic TVAR and Exponential TVAR were fitted. The structural breaks identified were at 2009(9) by Logistic TVAR and at 2009(2) by Exponential TVAR, respectively. The estimated values of θ_2 also fluctuated around the estimated value of 0.207 in the linear model.

4.7.5.3 Chemicals

An AR(2) model was fitted using the first 30 observations:

μ = 0.0262, θ_1= 0.409, θ_2= 0.256,

Variance-covariance matrix = $\begin{pmatrix} 0.0000496 & -0.000566 & -0.000372 \\ -0.000566 & 0.0329 & -0.0166 \\ -0.000372 & -0.0166 & 0.0297 \end{pmatrix}$

σ_ϵ^2 = 0.000553

Figure 4-6 Plot of μ, θ_1 and θ_2 against the transition variable for the UK Chemicals sector

The following graphs plot μ, θ_1 and θ_2 against the transition variable for the UK Chemicals sector. The transition variable is lag 1 of the dependent variable.

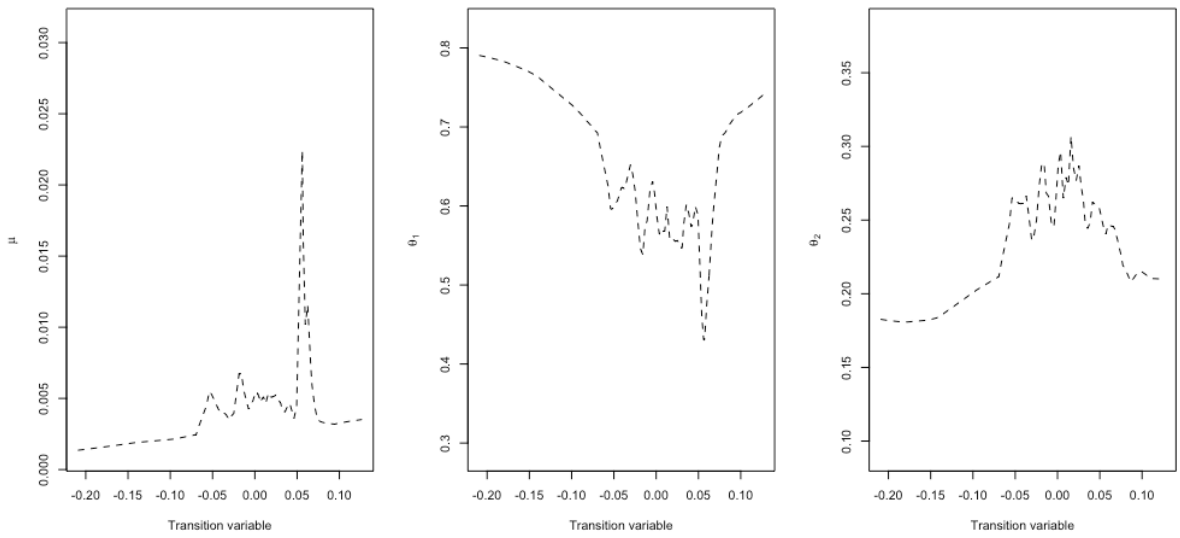

Figure 4-7 Plot of μ, θ_1 and θ_2 against time for the UK Chemicals sector

The following graphs plot μ, θ_1 and θ_2 against time for the UK Chemicals sector. The purpose was to check for (non-)linearity and structural breaks collectively from the time varying coefficients prescribed by the SDM model.

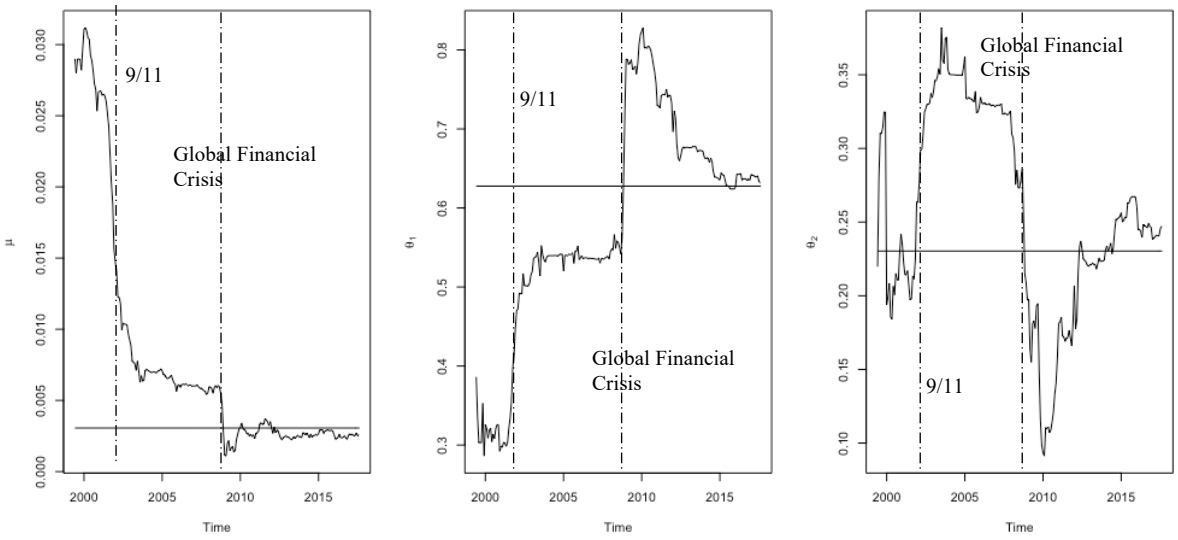

Based on the observation of Figure 4-6, θ_1 showed significant non-linearity in decreasing from 0.800 to 0.400, except near the end. This is consistent with the LSTAR selected by Escribano and Jordá (1997). As Figure 4-7 shows, θ_2 wanders around the linear AR estimates. The two structural breaks were collectively identified by the SDM coefficient estimates, near 2002 and near 2009. These structural breaks were consistent with two of the structural breaks identified by Bai & Perron's test, which they identified as 2001(9) and 2008(3). The structural break identified by SDM in 2009 was consistent with those identified by Logistic TVAR in 2009(9) and Exponential TVAR in 2009(4).

4.7.5.4 Basic metals

An AR(2) model was fitted using the first 30 observations to initialise:

μ = -0.0455, θ_1= 0.507, θ_2= 0.161,

Variance-covariance matrix = $\begin{pmatrix} 0.0000788 & 0.000515 & 0.000567 \\ 0.000515 & 0.0355 & -0.0224 \\ 0.000567 & -0.0224 & 0.0352 \end{pmatrix}$

σ_ϵ^2 = 0.000941

Figure 4-8 Plot of μ, θ_1 and θ_2 against the transition variable for the UK Basic Metals sector

The following graphs plots μ and θ_1 and θ_2 against transition variable for the UK's Basic Metals sector. The transition variable is lag 1 of the dependent variable.

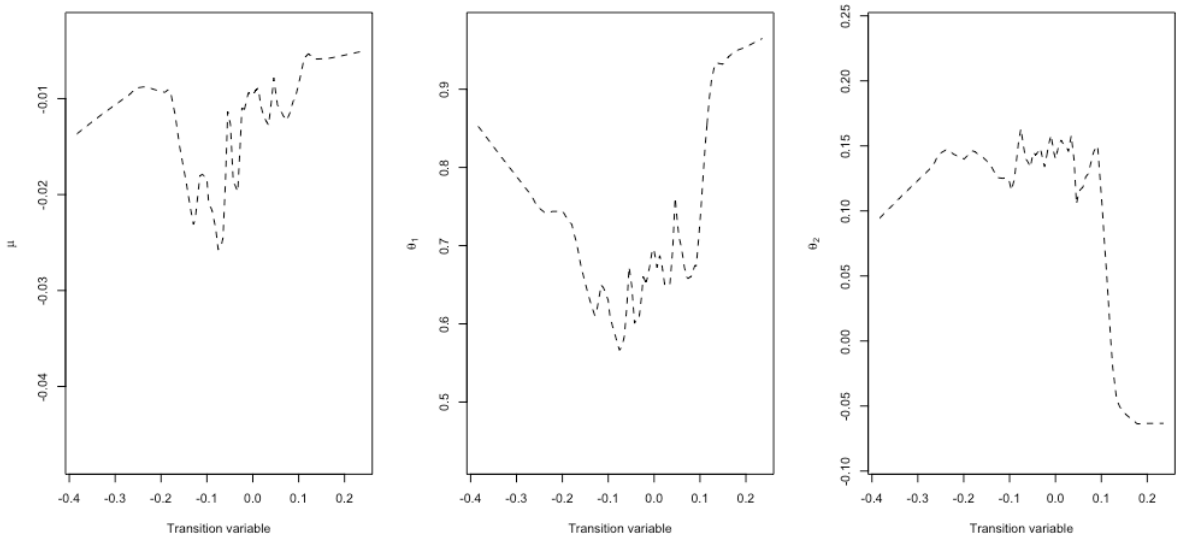

Figure 4-9 Plot of μ,θ_1 and θ_2 against time for the UK Basic Metals sector

The following graphs plot μ, θ_1 and θ_2 against time for the UK Basic Metals sector. The purpose was to check for (non-)linearity and structural breaks collectively from the time varying coefficients prescribed by the SDM model.

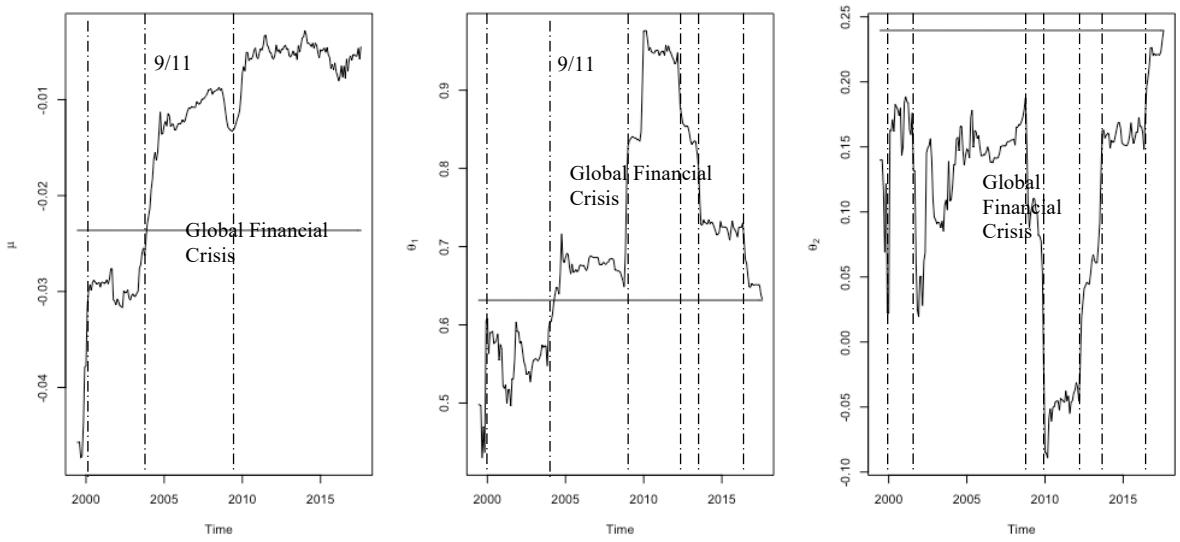

θ_1 was the most significant parameter when AR(2) is fitted. θ_1 was therefore the most effective parameter. As can be seen in Figure 4-8, the shapes of θ_1 and θ_2 were not constant, so were not linear. This was not consistent with the linear model selected using the Escribano and Jordá (1997) method.

For the two θ_s that were significant, θ_1 had approximately an ESTAR shape, and θ_2 had approximately an LSTAR shape. However, based on Escribano and Jordá (1997)'s model selection method, neither ESTAR nor LSTAR were significant. The minimum point of θ_1 against the transition variable was in approximately the same place as that identified by the ESTAR model. Significant non-linearity was observed for the Basic Metal sector after applying SDM.

For the time plots of μ, θ_1 and θ_2 produced by the SDM algorithm in Figure 4-9, θ_2 values were lower than the linear AR estimate. Although Escribano and Jordá's test statistics showed linearity in the basic metal sector, when θs are plotted against time, several main structural breaks can be observed - in 2000, 2004, 2009, 2010, 2013, 2014, and 2016. The structural breaks identified by SDM were consistent with all the structural breaks identified by the Bai & Perron test: at 2003(5), 2007(2), 2009(11) and 2014(2). The structural breaks identified by SDM were also consistent with the breaks identified by the Logistic TVAR model in 2011(7), and by the Exponential TVAR model in 2009(6).

4.7.5.5 Food

An AR(3) model was fitted using the first 30 observations to initialise:

μ = 0.00219, θ_1= -0.303, θ_2= 0.000460, θ_3 = 0.397

Variance-covariance matrix = $\begin{pmatrix} 0.0000165 & 0.0000154 & 0.0000377 & 0.0000407 \\ 0.0000154 & 0.0326 & 0.0126 & 0.00561 \\ 0.0000377 & 0.0126 & 0.0358 & 0.0119 \\ 0.0000407 & 0.00561 & 0.0119 & 0.0315 \end{pmatrix}$

σ_ϵ^2 = 0.000443

Figure 4-10 Plot of μ, θ_1 and θ_2 , θ_3 against the transition variable for the UK Food sector

The following graphs plot μ and θ_1, θ_2 and θ_3 against the transition variable for the UK Food sector. The transition variable is lag 1 of the dependent variable.

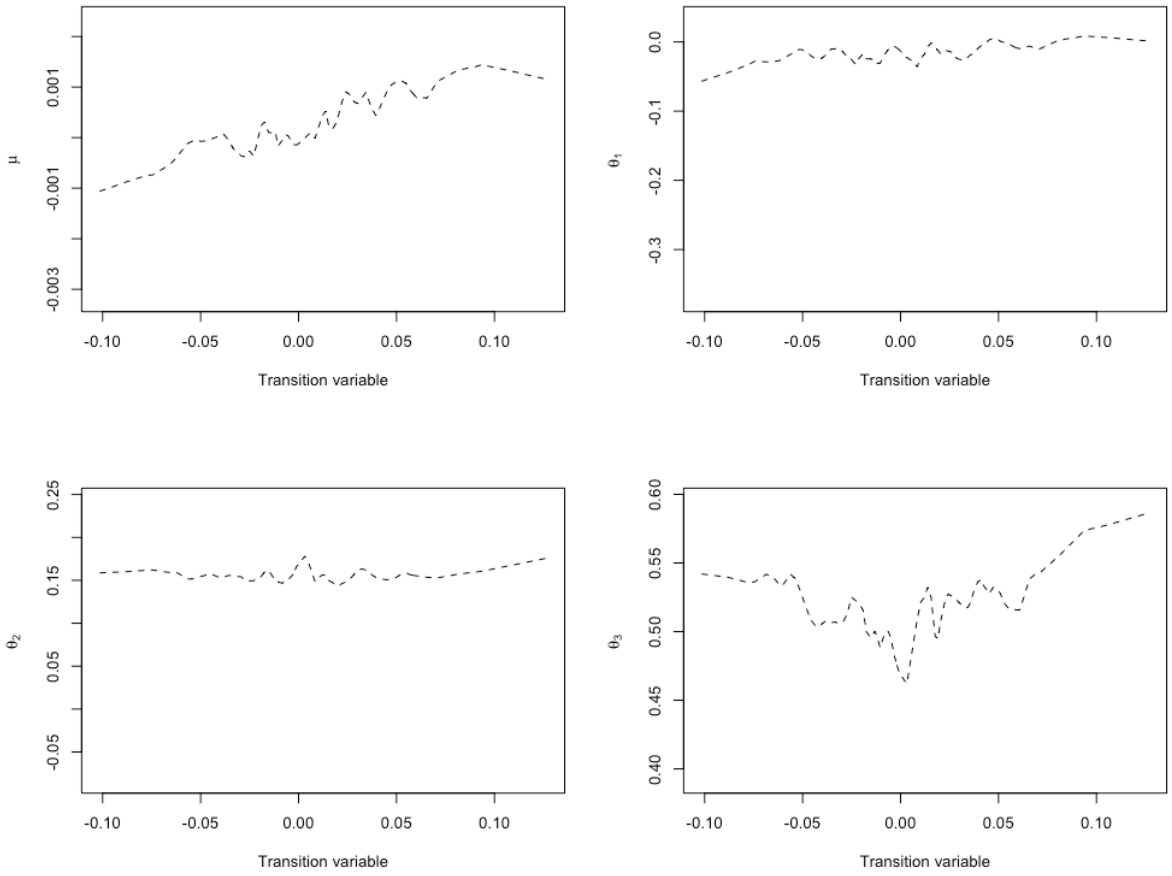

From the plots of θs against the transition function shown in Figure 4-10, θ_1 and θ_2 were approximately constant. θ_3 was the most significant parameter; the shape of the SDM estimation for θ_3 resembled an ESTAR model and was symmetric around zero. The shape produced by the SDM was consistent with Escribano and Jordá's model selection, where neither LSTAR nor ESTAR models were selected. θ_3 ranged between 0.47 and 0.58. The shape of θ_1 and θ_2 were more consistent with the model selection results from Escribano and Jordá's method. The food sector data was therefore, on the whole, linear.

Figure 4-11 Plot of μ, θ_1, θ_2, and θ_3 against time for the UK Food sector

The following graphs plot μ, θ_1, θ_2, and θ_3 against time for the UK Food sector. The purpose was to check for (non-)linearity and structural breaks collectively from the time varying coefficients prescribed by the SDM model.

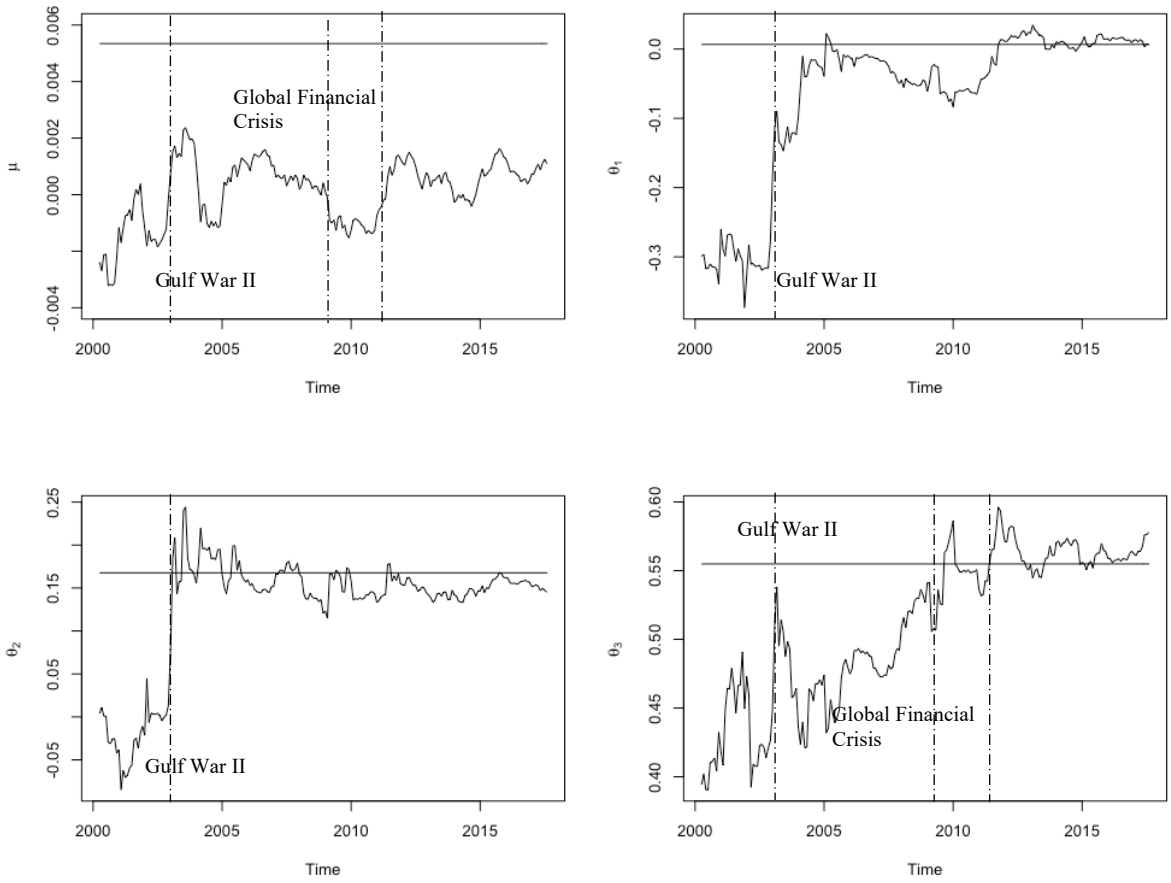

From Figure 4-11, it can be observed that $\theta_1, \theta_2, \theta_3$ varied around their respective AR estimates after fitting the first initial proportion of the data. A clear structural break is identifiable at around 2003. In the time plot of the series, some changes in the structure are also observable during this time. The graph of θ_3 shows an increasing trend, with small breaks at 2009 and 2011. The structural breaks identified at 2009 and 2011 were near those identified by the Bai & Perron structural break test in 2010(1). The SDM captured an additional structural break near 2003. The structural breaks identified by SDM were also consistent with those identified by the Exponential TVAR model at 2010(11).

4.7.5.6 Gas

An AR(1) model was fitted using the first 30 observations:

μ = 0.0453, θ_1= -0.0414,

Variance-covariance matrix = $\begin{pmatrix} 0.0000964 & -0.00163 \\ -0.00163 & 0.0353 \end{pmatrix}$

σ_ϵ^2 = 0.000616

Figure 4-12 Plot of μ and θ_1 against the transition variable for the UK Gas sector

The following graphs plot μ and θ_1 against the transition variable for the UK Gas sector. The transition variable is lag 1 of the dependent variable.

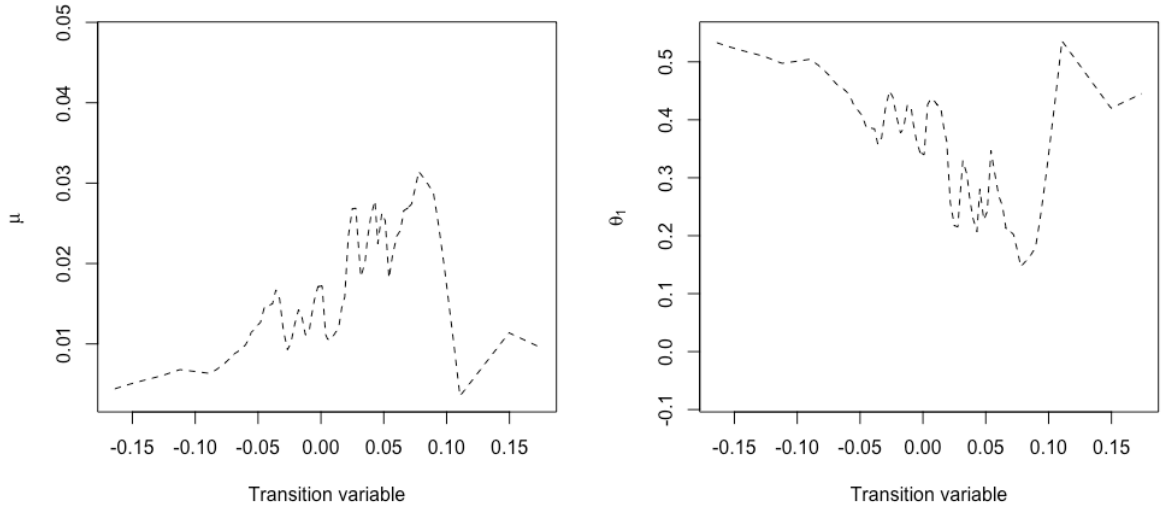

Figure 4-13 Plot of μ and θ_1 against time for the UK Gas sector

The following graphs plot μ and θ_1 against time for the UK Gas sector. The purpose was to check for (non-)linearity and structural breaks collectively from the time varying coefficients prescribed by the SDM model.

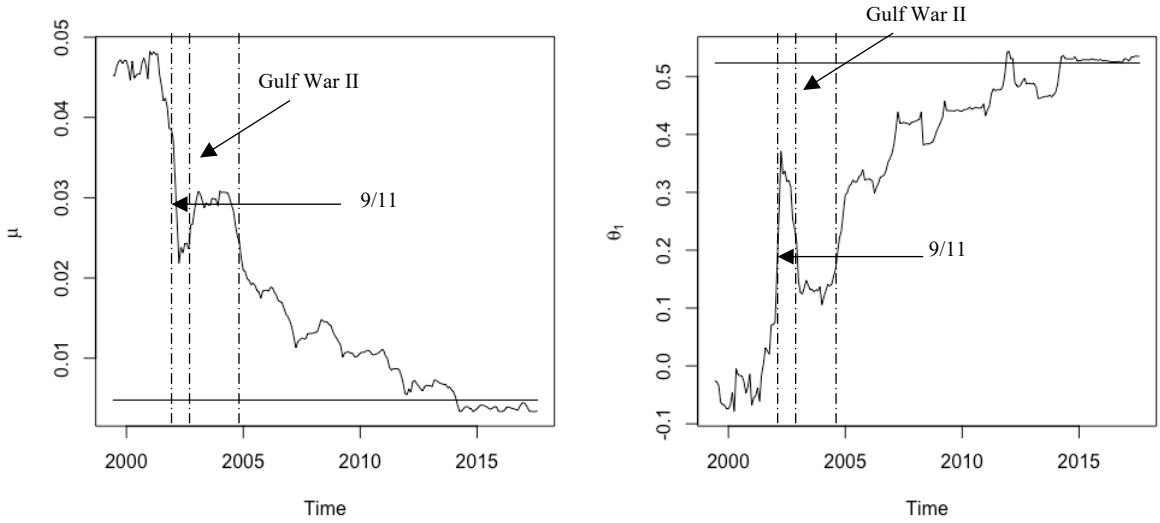

From Figure 4-12, it can be observed that firstly, θ_1 was non-linear, as it did not look constant. This is consistent with the results of Escribano and Jordá's non-linearity test. Secondly, the "true shape" of θ_1 against transition variable resembled that of an LSTAR model, consistent with the selected LSTAR model by applying Escribano and Jordá's method. Non-linearity was therefore present for the Gas sector data.

Figure 4-13 shows the plot of θs produced by the SDM algorithm presented against time. It can be seen that θs initially deviate from the initial linear AR(1) estimates, before becoming very close to the respective initial AR(1) estimates from around 2012 onwards. The SDM algorithm has thus captured the structural breaks identified by the Bai & Perron structural break test at 2004(5). The SDM was also consistent with the structural breaks identified by the Logistic TVAR model at 2004(5).

4.7.5.7 Machinery

An AR(1) model was fitted using first 30 observations:

μ = -0.0110, θ_1= 0.861,

Variance-covariance matrix = $\begin{pmatrix} 0.0000140 & 0.0000891 \\ 0.0000891 & 0.00819 \end{pmatrix}$

σ_ϵ^2 = 0.000379

Figure 4-14 Plot of μ and θ_1 against the transition variable for the UK Machinery sector

The following graphs plot μ and θ_1 against the transition variable for the UK Machinery sector. The transition variable is lag 1 of the dependent variable.

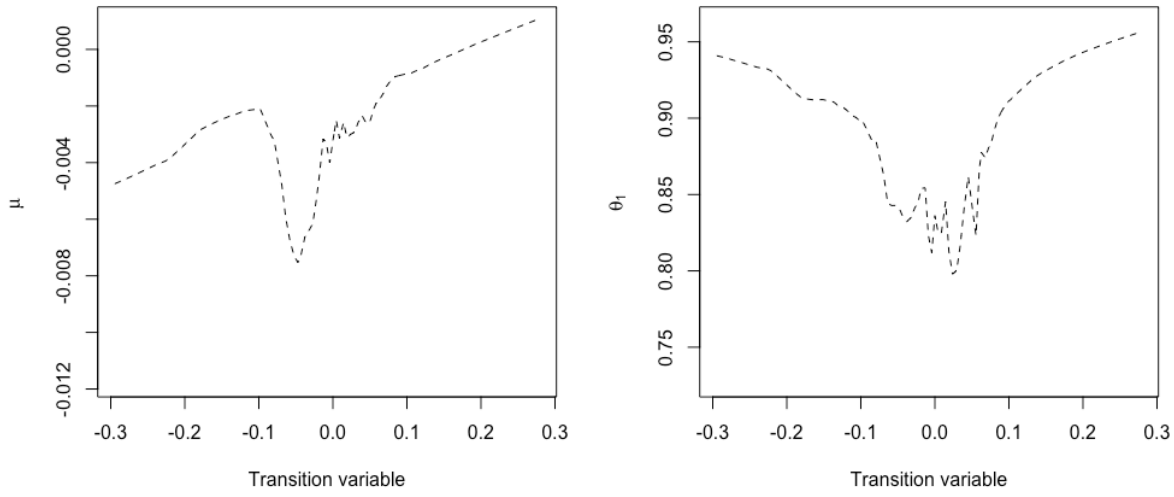

Figure 4-15 Plot of μ and θ_1 against time for the UK Machinery sector

The following graphs plot μ and θ_1 against time for the UK Machinery sector. The purpose was to check for (non-)linearity and structural breaks collectively from time varying coefficients prescribed by the SDM model.

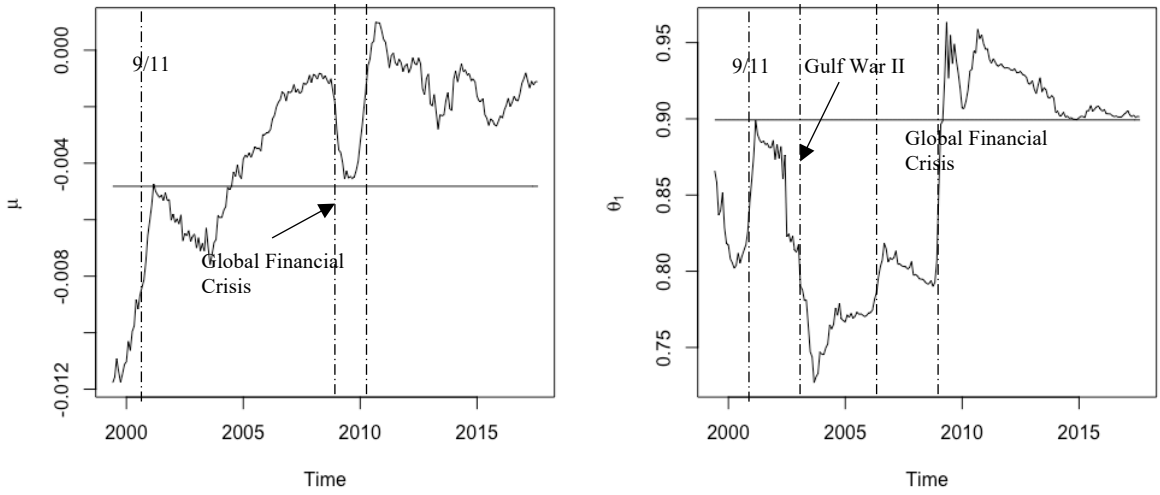

Based on θ_1 plotted against the transition variable in Figure 4-14, this parameter appeared symmetric at around zero. This was consistent with the model selected from applying Escribano and Jordá's method, where ESTAR was selected. Significant nonlinearity was seen to be present in Machinery sector. From Figure 4-15, the θ_1 generated by the SDM fluctuated around the linear AR(1) coefficient estimates. While the Bai & Perron test captured several structural breaks in 2003(9), 2007(3), 2009(12), and 2012(9), the SDM not only managed to identify these structural breaks, but also to show the relative degree of structural change. The SDM also captured the structural breaks identified when fitting a Logistic TVAR in 2010(12) and when fitting an Exponential TVAR model in 2010(7).

4.7.5.8 Fabricated metal

An AR(2) model was fitted using the first 30 observations:

μ = -0.00539, θ_1= 0.723, θ_2= 0.162,

Variance-covariance matrix = $\begin{pmatrix} 0.0000162 & -0.000136 & 0.0000539 \\ -0.000136 & 0.0340 & -0.0276 \\ 0.0000539 & -0.0276 & 0.0308 \end{pmatrix}$

σ_ϵ^2 = 0.000428

From fitting a linear AR(2) model to the UK fabricated metal sector, θ_1 and θ_2 were found to be significant. In Figure 4-16, θ_1 appeared linear at around 0.550, and θ_2 had an LSTAR shape. Based on Escribano & Jorda's method of model selection, ESTAR was marginally significant, but LSTAR was not significant. The results were therefore not quite consistent with the shape produced by the SDM algorithm.

Figure 4-16 Plot of μ, θ_1 and θ_2 against the transition variable for the UK Fabricated Metal sector

The following graphs plot μ and θ_1 and θ_2 against the transition variable for UK Fabricated Metals. The transition variable is lag 1 of the dependent variable.

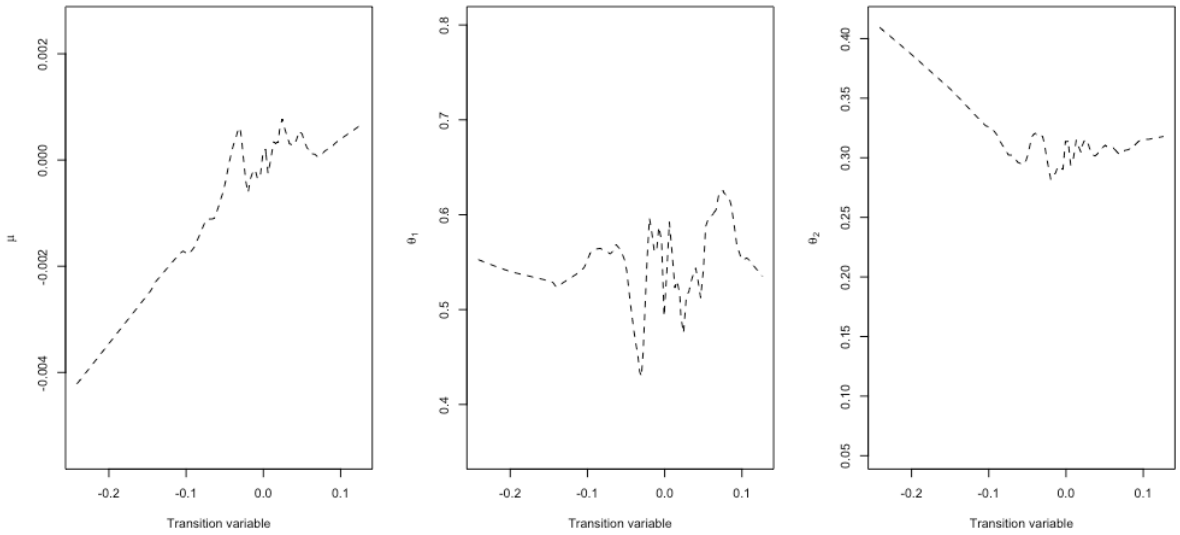

Figure 4-17 Plot of μ, θ_1 and θ_2 against time for the UK fabricated metal sector

The following graphs plot μ, θ_1 and θ_2 against time for the UK Fabricated Metals sector. The purpose was to check for (non-)linearity and structural breaks collectively from the time varying coefficients prescribed by the SDM model.

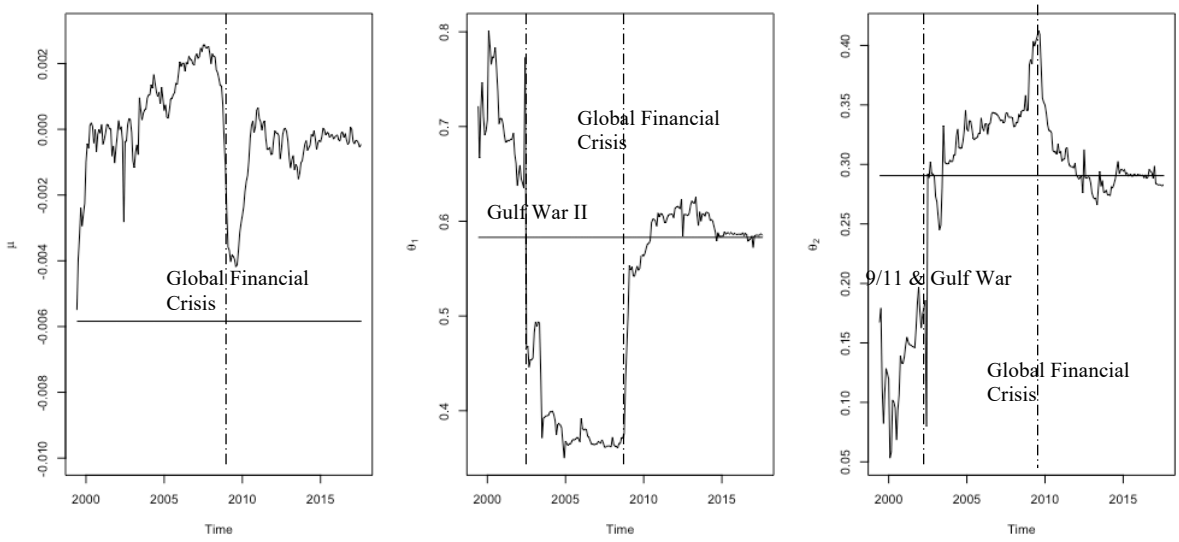

From Figure 4-17, it can be observed that θ_1 and θ_2 vary around linear AR(2) estimates. Several structural breaks can be identified collectively, in 2002/2003, 2004, and 2009/10. The SDM was therefore consistent with one of the two structural breaks captured by the Bai & Perron structural break test in 2010(5), but not the break in 2007/2008 identified by the Bai & Perron test. The SDM was also consistent with the structural breaks found when a Logistic TVAR and an Exponential TVAR were fitted. The Logistic TVAR found a structural break in 2009(9) and the Exponential TVAR provided a break in 2009(5).

4.8 Summary of Findings and Learnings

Figure 4-18 present the findings of this chapter. Based on the SDM modelling, the Food and Electricals sectors show linearity in business cycles. This tells us that Food and Electricals sector have simple dynamics, and the other sectors have nonlinear behaviours.

Sector	SDM Findings	Linearity Test Result	Structural Breaks	(As)symmetry
Electrical and Electronic	Linear	LSTAR	SDM 2001 and 2009; consistent with BP 2001(9) and 2010(2); consistent with TVAR 2009(5)	Symmetric
Vehicles	LSTAR and ESTAR in two parameters, but significant nonlinearity	LSTAR	SDM 2009; consistent with BP 2009(10); TVAR 2009(9) and 2009(2)	Inconclusive
Chemicals	Significant nonlinearity	LSTAR	SDM 2002 and 2009; BP 2001(9) and 2008(3); TVAR 2009(9) and 2009(4)	Symmetric
Basic Metal	LSTAR and ESTAR in two parameters, significant nonlinearity	Linear	SDM 2004,2009,2010,2013,2014; BP 2003(5), 2007(2), 2009(11), 2014(2); TVAR 2011(7), 2009(6)	Inconclusive
Food	Linear	Linear	SDM: 2003, 2009, 2011; BP 2010(1); TVAR 2010(11)	Symmetric
Gas	LSTAR, Nonlinear	LSTAR	BP: 2004(5); TVAR 2004(5)	Asymmetric
Machinery	ESTAR, nonlinearity	ESTAR	BP: 2003(9); 2007(3); 2009(12); 2012(9); TVAR: 2010(12), 2010(7)	Symmetric
Fabricated Metal	LSTAR, generally nonlinear	ESTAR	SDM: 2002/2003, 2004, 2009/10	Asymmetric

Figure 4-18 Summary of Findings Related to Business Cycles

For the Chemical, and Machinery sectors, all models as well as the SDM concluded significant nonlinearity. But they did not agree in terms of symmetry or asymmetry. For the Gas sector, the models all agree with LSTAR with asymmetric business cycles. For Fabricated Metals, the SDM disagreed with the linearity test results. It is noted for Vehicles and Basic Metals, they both were modelled by AR(2) models. The two slope parameters indicated nonlinearity in the series, however, the functional form of one parameter was consistent with ESTAR and one with LSTAR model. This is the superiority of the SDM algorithm over other methods. SDM results also suggest that researchers need to develop a new mixed ESTAT/ LSTAR model to capture this form of nonlinearity.

An interesting observation overall is that structural breaks identified by the coefficients estimated from the SDM model happen during negative and uncertain events, such as the 9/11 terrorist attack, Gulf War II, and 2008 global financial meltdown. These show that wars, terrorist activities and crises can have catastrophic impacts on the industrial productions.

This chapter shows significant nonlinearity present in many of the business cycle indicators. This implies that a linear AR model, which shows a constant coefficient across the whole sample period may not be appropriate in modelling the business cycle. The SDM and STAR models generally agree on the presence of significant nonlinearity in vehicles, chemicals, gas, machinery, fabricated metal sectors. In terms of nonlinearity, the SDM is in general in agreement with LSTAR and ESTAR models in nonlinearity. This study shows that for different industrial production sectors, we observe different forms of (non)linearity. This may also lead to inconclusive evidence in symmetric or asymmetric

business cycles indicators and the need for development of a new type of nonlinear models.

The SDM can also show relative magnitude in structural breaks that are consistent with the time plot of the industrial production indices as demonstrated by Electricals, Vehicles, Chemical, Basic Metal, Food. The SDM also captured smooth transitions in the gas sector, which is consistent with its behaviour.

In summary, we found significant nonlinearity in 6 out of 8 series, and for different industrial production sectors, we observed all types of behaviours - linear, symmetric nonlinear, asymmetric linear. This may provide evidence that for different sectors, we do not always observe asymmetric nonlinear business cycles as mentioned in the literature.

4.9 Limitations to Other Models

In this chapter, several assumptions were made, which may be their limitations. First, I assumed that the series is I(0) for the purpose of the linearity test. It is a reasonable assumption, as seen from the linear and SDM regression that these models did not produce explosive behaviours. Harvey, Leybourne and Xiao (2008)'s suggested linearity test can be a robust alternative to the Escribano and Jordá (1997) model used in this thesis. But Escribano and Jordá (1997) is a reasonable test, as it tests the null of linearity against STAR nonlinear alternatives. The second assumption is that in testing structural breaks, the shocks in the series were I(0), as Sobreira and Nunes (2016) mentioned should be a necessary condition. As I have already performed seasonal differences to the time series. Therefore, the dependent and independent variables for the business cycle chapter can assume to be I(0). Sobreira and Nunes (2016) could also be used as a robust structural break test, as it can handle shocks that are I(0) or I(1). The prediction error was

computed in a standard way, which could be improved by using a Newey West method to account for heteroscedasticity (Newey and West, 2014).

4.10 Discussions and Conclusions

Lumsdaine and Papell (1997) claimed that allowing for only one structural break may not be the best characterisation of macroeconomic time series. Therefore, as models such as logistic and exponential smooth transition autoregressive models, time-varying autoregressive models, linear and nonlinear threshold autoregressive models assume to have two regimes. Following studies by Harvey, Leybourne and Taylor (2009), Sobreira and Nunes (2016) allowed more breaks and claimed to have found the same large sample property between multiple trend breaks and a single break. However, the model they employed requires either the number of breaks, m, or break fractions to be known (Sobreira and Nunes, 2016). The model they proposed also assumes there is at least one structural break in the series. Most structural break tests suffer from nonmonotonic power functions when the number of breaks is large and errors are serially correlated (Kejriwal and Perron, 2010). The SDM comparatively, is more flexible and can tackle time series with no structural breaks. State-Dependent Model is advantageous and can capture multiple structural breaks without pre-specifying the number of structural breaks. It can perform reasonably good model fitting without the need for a priori knowledge of the location of structural breaks. Through SDM, we can simultaneously test the structural breaks and non-linearity and obtain the relative magnitudes between the structural breaks. The SDM can offer more than linear AR(k) models, as it offers information about the type of nonlinearity in the business cycle and indicate if it is symmetric or asymmetric

. The results of Escribano and Jordá (1997) is helpful but only tests between linear and STAR alternatives. which is not as flexible because SDM. tests against general nonlinearity.

The structural break results by the SDM were generally consistent with those identified by Bai & Perron test. The economic reasons to explain the structural breaks identified in 2007 to 2009 are mainly due to the Global Financial Crisis, European Sovereign Debt Crisis and Credit Crunch. The common structural breaks in productions in 2002-2004 are probably related to recovery from the impact of the 9.11 terrorist attack and Gulf War II on outputs. The Bai and Perron (2003) test do not reveal the relative differences in the magnitude of the structural breaks, but the SDM method can manage well.

Harvey, Leybourne and Xiao (2008) suggested a linearity test that can be a robust alternative to the Escribano and Jordá (1997) model used in this thesis. Sobreira and Nunes (2016) could also be used as a robust structural break test, as it can handle shocks that are I(0) or I(1). To improve these tests Newey and West (2014) method could also be used to account for heteroscedasticity. The data used in this chapter are growth rate and therefore not I(1). The results in this chapter showed that identifying the structural breaks with SDM seems to work well and can be used as an effective exploratory analysis. The main advantage of the SDM technique is that it can simultaneously test for both the linearity assumption and identify the structural breaks.

This chapter represents a first attempt to apply SDM to business and economics data. As such, it contributes to investigating the existence of nonlinearity in business cycle indicators and capturing structural breaks in these indicators. The state-dependent Model captured many of the structural breaks which were also identified by TVAR models and Bai & Perron tests. The SDM showed linearity for the Electricals and Food sectors in which the estimated parameters were fairly constant and close to the values estimated by the linear time series models. The results for the other series indicated non-linearity in the

data, with mixed evidence in terms of symmetry/asymmetry. These findings of nonlinearity were generally consistent with the models selected by Escribano & Jorda's method. The findings on the nature of business cycles were generally consistent with the literature, with existing non-linearity in most of these series (Teräsvirta and Anderson, 1992; Öcal and Osborn, 2000; Heravi, Osborn and Birchenhall, 2004; Franses and van Dijk, 2005; Hassani, Heravi and Zhigljavsky, 2009).

Suggestions for future research include: to extend the Granger Causality test and develop a general non-linear (SDM) type causality test. This test, for example, can be applied to production data, looking at causality between steel production and car production.

This page intentionally left blank

Chapter 5 Application of State Dependent Models in Testing Purchasing Power Parity

5.1 Introduction

This chapter contributes an alternative method of testing the Purchasing Power Parity condition using a general State Dependent Model. It is among the first study to check how the PPP condition changes with different levels of global uncertainty. First, a test was performed to establish if Purchasing Power Parity holds for four real exchange rates - GBP/USD, EUR/USD, JPY/USD, and BRL/USD - through testing time-varying augmented Dickey-Fuller representations of stationarity using the state dependent model. The study also tested how these real exchange rates behave with global uncertainty indices.

The structure of this paper is as follows: first, an overview of the PPP condition is provided. Then, the importance of this research is explained. The contribution of the chapter is set out after providing a literature review on testing PPP conditions. The SDM methodology in testing PPP is then explained, before the empirical results from testing PPP are presented alongside linear, STAR model fitting, nonlinearity tests and unit root against ESTAR. The rest of the chapter analyses how real exchange rates behave with different levels of global uncertainty. The findings are reported, and the chapter concludes with a discussion.

5.2 An Overview of Purchasing Power Parity

The history of purchasing power parity (PPP) can be traced back to as early as Cassel (1922). The theory was established based on the theory of Law of One Price (LOOP),

which states that in the absence of trade barriers and transportation costs, and given perfect competition in the market for goods, currencies should have the same purchasing power in obtaining the same goods when they are converted to a single common currency. Absolute Purchasing Power Parity (PPP) theory is an extension of the LOOP in the aggregate price level. Under relative PPP conditions, the percentage change in the exchange rate should be equal to the difference between the two national inflation rates. A currency with higher inflation should depreciate by the same extent as the inflation differentials between the two countries.

5.3 Real Exchange Rates

The real exchange rate is a measure of relative price of a basket of goods and services produced in a given foreign country in relation to a similar basket of goods and services produced in the domestic country. If Purchasing Power Parity holds, then the rate of change of the real exchange rate should theoretically be constant and equal to zero. In other words, the theory tells us that the real exchange rate should always be stationary, and that PPP should always hold at all times. The testing of PPP conditions may be simplified to the testing of stationarity and the mean reversion of real exchange rates.

5.4 Importance of Research on the Behaviour of Real Exchange Rates

Taylor and Taylor (2004) argued that the study of real exchange rate adjustment mechanisms is of great importance to countries with different exchange rate regimes. They explained that for fixed exchange rate regimes, it is important to set the right level of PPP equilibrium exchange rate. They also argued that countries with floating exchange rate regimes need to estimate the level and variation in their exchange rates and use it to guide their exchange rate policies. This can help policy makers to determine the extent that the real exchange rates are ‘self-equilibrating’. Javed (2019) recently argued that

understanding future exchange rates movements is important in informing export opportunities and overseas investments, and in estimating how the prices of competitive goods compare across countries. Javed (2019) also mentioned that understanding the behaviours of real exchange rates helps to determine the extent to which domestic goods and foreign goods are over/undervalued. Other benefits of a better understanding of exchange rates include measuring nominal exchange rate misalignment, setting exchange rates based on parity conditions, and facilitating comparisons of standard of living and national incomes across countries. This also has implications for corporate finance decisions determining the location of plants, capital budgeting, the determination of profitability from investments, and in informing international currency hedging decisions (Kotzé, 2017). Therefore, there are many benefits of understanding exchange rate movement/ adjustment behaviours.

5.5 Methods of Testing for Purchasing Power Parity

There are many methods of testing for Purchasing Power Parity[2], each with different merits. However, these are mathematically complicated but may not necessarily be beneficial in testing PPP conditions. In contrast, a basic Augmented Dickey-Fuller test for unit root using SDM may be simple and intuitive.

[2] Other methods of testing for PPP conditions include the variance ratio test (Cochrane, 1988), fractional integration (Diebold, Husted and Rush, 1991; Cheung and Lai, 1993), nonlinear unit root tests (Chortareas and Kapetanios, 2004), panel unit root tests (MacDonald, 1996; Oh, 1996; Huang and Yang, 2015), the Fourier quantile unit root test (Bahmani-Oskooee, Chang and Lee, 2016), cointegration analysis (Corbae and Ouliaris, 1988), the Johansen cointegration test, the Engle-Granger cointegration technique (Granger, 1986; Engle and Granger, 1987), etc.

One major traditional test for Purchasing Power Parity involves examining the presence of unit roots from the equation below:

$q_t = \rho q_{t-1} + u_t,$ $H_0 : \rho = 1(\text{unit root})$ and $H_1 : \rho < 1$ (stationary, PPP holds)

Or,

$\Delta q_t = \rho^* q_{t-1} + u_t,$ $H_0 : \rho^* = 0$ (unit root) and $H_1 : \rho^* < 0$ (stationary, PPP holds),

Where q_t represents the exchange rates, or a logarithm of the real exchange rates.

To take account of autocorrelation in residuals, an Augmented Dickey-Fuller (ADF) test can be performed, with the equation:

$$\Delta q_t = \beta_0 + \sum_{i=1}^{p} \beta_i \Delta q_{t-i} + \rho q_{t-1} + u_t$$

The lag i is chosen by minimising Akaike or Bayesian Information Criterion.

Several authors have employed models which combine ADF representation with a STAR model, as presented below (see Michael, Nobay and Peel, 1997; Chen and Wu, 2000; Baum, Barkoulas and Caglayan, 2001; Taylor, Peel and Sarno, 2001; Sarno and Taylor, 2002; Taylor, 2003, 2006).

$$\Delta q_t = \alpha + \rho q_{t-1} + \sum_{j=1}^{p-1} \phi_j \Delta q_{t-j} + (\alpha^* + \rho^* q_{t-1} + \sum_{j=1}^{p-1} \phi_j^* \Delta q_{t-j})\, \Phi(\theta; q_{t-d}; c) + \epsilon_t$$

There are mainly two different types of transition functions of Φ in the nonlinear model. The logistic representation is:

$$\Phi(\theta; q_{t-d}; c) = \frac{1}{1 + e^{-\gamma(q_{t-d}-c)}}$$

And the exponential representation is:

$$\Phi(\theta; q_{t-d}; c) = 1 - e^{-\gamma(q_{t-d}-c)^2}$$

This model is the starting point for the present method of testing PPP using the SDM model used in this paper.

5.6 Mixed findings in Testing PPP Conditions

Studies which have reported tests for purchasing power parity have produced mixed results (Su, Chang and Liu, 2012), and a rejection of the PPP condition could sometimes be found with the new methods employed. Therefore, no consensus has been reached on the stationarity of real exchange rates.

Substantial evidence shows that the STAR family of models fit and describe the behaviour of real exchange rates well. This implies non-linear mean-reversion. Under an ESTAR model, for example, when transaction costs are large, there is a non-arbitrage band in which no adjustment takes place. When the deviation from PPP is larger, this facilitates higher degrees of mean-reversion corrections. The reasons for these include non-linear international goods arbitrage due to the execution of orders only when these cover transport costs (O'Connell and Wei, 1997). Another argument is that heterogeneous agents only act to correct deviations from PPP when the deviation from PPP is larger. The third argument is that governments intervene to correct for deviations. In an LSTAR model, positive deviations from PPP adjust in a different manner from negative

deviations from PPP. However, theoretically, the ESTAR adjustment of deviations away from PPP equilibrium is much more logical.

Various studies have provided empirical evidence based on employing STAR-type models to real exchange rates. Paya and Peel (2003) studied dollar-yen real exchange rates using ESTAR with trends, and found an extensive decrease in the half-life of shocks. Yoon (2010) investigated real exchange rates for the UK, Germany, France, and Japan, and concluded that the real exchange rates for these countries could be modelled as ESTAR or Stochastic unit root (STUR) processes. Paya, Venetis and Peel (2003) employed ESTAR models to monthly real exchange rates within the European Monetary System (EMS) covering the period January 1973 to December 1998, amongst other economic variables, and found that a non-constant real equilibrium exchange rate can reduce the half-lives of shocks to below two years. Copeland and Heravi (2009) investigated the monthly real exchange rates of the USD denominated UK, German, French, and Japanese real exchange rates for January 1957 through to around 2000 by fitting a Time-varying Smooth Transition Autoregressive (TVSTAR) model, and found that TVSTAR modelled real exchange rates best, followed by LSTAR and ESTAR.

Evidence for linear stationarity was provided by Kutan and Zhou (2015). They developed a new variation of unit root tests taking nonlinearity and structural breaks into consideration in relation to the real effective exchange rates of twenty-three developed countries. They found evidence for linear adjustments to PPP level exchange rates for highly integrated economies.

However, some scholars disagree with the position that PPP empirically holds true. Dumas (1992) found a persistent deviation of real exchange rates. He argued that the probability of relative prices moving away from parity is higher than their moving towards parity. Therefore, he argued for the persistence of real exchange rates. Sercu, Uppal and Hulle (1995) reported that when shipping costs and output uncertainty are present, neither absolute nor relative PPP tends to hold (i.e., deviations from PPP are persistent). Benninga and Protopapadakis (1988) showed that because trades take time, exchange rates deviate systematically away from the LOOP value.

Therefore, as is shown here, mixed empirical evidence has emerged from testing if real exchange rates are linear or nonlinear or mean-reverting, or whether PPP holds at all. It is possible that the answer is not clear cut, i.e., that PPP may hold partially or throughout, or not hold at all. The SDM model can accommodate this. Through updating coefficients via the Kalman Filter method, the exact nature of mean-reversion can be identified, whether it is stationary, linear, non-linear, or non-existent.

5.7 Contributions

This study makes several important contributions to the literature. Firstly, most prior studies have forced ESTAR or LSTAR models when estimating the parameters of real exchange rates. These models have only two parameters, one for each regime. This is not as effective as the parameters estimated in SDM, which are updated through time, so PPP can be tested for different time periods. The use of SDM does not assume a particular (non-)linearity of the models; therefore, it provides a new approach to exploring whether the non-linear STAR models represent an accurate description of real exchange rate processes, if at all. Using SDM model fitting, it is also possible to check if a linear

autoregressive model is generally adequate for modelling real exchange rates. Secondly, the SDM also allows an examination of how real exchange rates behave under varying conditions of global uncertainty, when there has been limited research linking the two. Thirdly, the literature review section has provided evidence of prior research that indicated mixed evidence on the rejection or acceptance of a unit root in the real exchange rates. In this research, the SDM was utilised to test the mean reversion properties in different time periods and to check if the mean reversion in real exchange rates continues throughout, as well as to explore how mean reversions relate to uncertainty levels.

5.8 Modelling Real Exchange Rates with SDM

Kalman Filtering is an iterative process producing parameter updates from a system of equations through feeding in consecutive data inputs, so that the true nature of parameters can be estimated. Kalman Filtering provides a recursive and efficient computational solution, and can perform well when precise nature of the modelled system is unknown. It can work especially well in the case of data with no prior assumptions of the types of nonlinearity (Priestley, 1980). From these, an "overview" of the types of nonlinearity can be prescribed. The SDM, which incorporates extended Kalman Filtering algorithms, also contains many types of non-linear models, with linearity prescribed in special cases.

The present section first describes and utilises the SDM process to model the real exchange rate and test the PPP assumption. Then, the impact of policy uncertainty on exchange rates is examined.

A linear AR(k) model, when modified and applied to model the purchasing power parity, can be expressed in the form below:

$$\Delta q_t = \mu + \phi_1 \Delta q_{t-1} + \cdots + \phi_k \Delta q_{t-k} + \rho q_{t-1} + \epsilon_t$$

In this equation, μ, ϕ and ρ are constants and not time varying. q_t is the natural log of the real exchange rates of four currencies against the US dollar.

The state-dependent model applied to modelling exchange rates can be written in the following form:

$$\Delta q_t = \mu + \theta_1 \Delta q_{t-1} + \cdots + \theta_k \Delta q_{t-k} + \rho(q_{t-1}) q_{t-1} + \epsilon_t$$

In this model, only the ρ coefficient is now state-dependent, and can be updated as:

$$\rho(q_t) = \rho(q_{t-1}) + (q_{t-1} - q_{t-2})\gamma^{(t)}$$

Recursive equations are applied to estimate the state-dependent coefficients.

5.9 Data

The data on real exchange rates was obtained from the United States Department of Agriculture. The frequency of real exchange rates is monthly. As the website indicates, the real exchange rate is calculated by multiplying the nominal exchange rates by the ratio of price indices between the US and local currencies. The data consists of monthly real exchange rates time series for the British pound, the Euro, the Japanese yen, and the Brazilian real, starting from May 1970 and ending in July 2017. The choice of four real

exchange rates reflects a wide coverage of geographical region: Asia, Europe, North and South America. The choice of GBP/USD, EUR/USD, JPY/USD is because of the popularity of these exchange rates. The choice of BRL/USD is influenced by an initial examination of the data, where the series exhibit random walk property. Therefore, it would be quite interesting to include BRL/USD to see the results using the SDM method.

5.10 Descriptive Statistics

Figure 5-1 Plot of real exchange rates for the British pound, the Euro, the Japanese yen and the Brazilian real against the US dollar

The figure below shows four time series of real exchange rate pairs - GBP/USD, EUR/USD, JPY/USD, and BRL/USD after taking the natural log. The frequency is monthly for the period between Jan 1970 and July 2017.

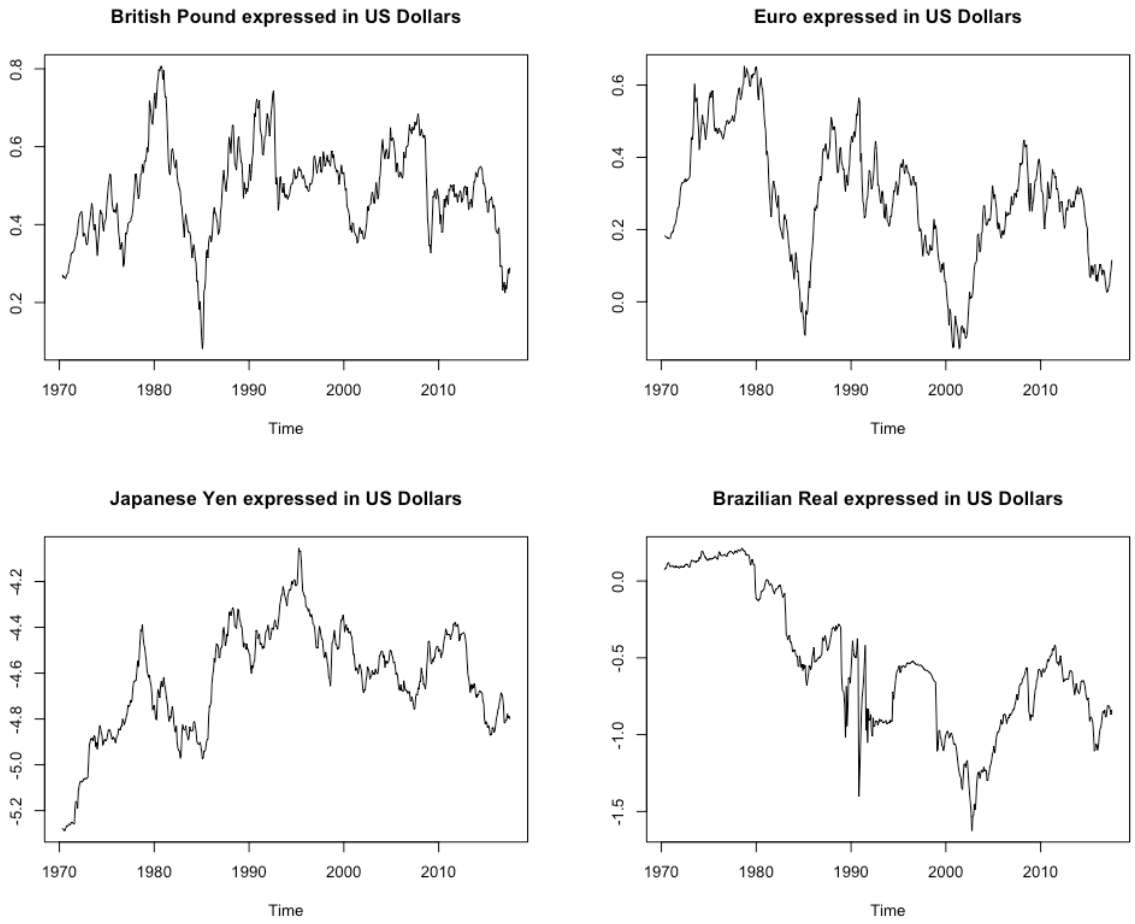

For the British pound, the Euro, and the Japanese yen, there is no noticeable trend. However, the real exchange rates for the Brazilian Real show a downward trend which is more volatile than for other currencies.

For summary statistics of the real exchange rates, see Table 5-1.

Table 5-1 Summary Statistics of Real Exchange Rates

The table below shows descriptive statistics for GBP/USD, EUR/USD, JPY/USD, and BRL/USD after taking the natural log, for the period between 1970.1 and 2017.7.

Currencies	Mean	Standard Deviation
GBP/USD	0.488	0.120
EUR/USD	0.285	0.173
JPY/USD	-4.63	0.236
BRL/USD	-0.531	0.451

5.11 Empirical Results in Testing Purchasing Power Parity

This section presents the results of the analysis from the linear AR models, the LSTAR and ESTAR models, and the state dependent models.

5.11.1 Choosing the Critical Values for the SDM unit root test

Kalman Filter produces optimal estimates of the parameters and the estimated standard errors and actual standard errors are very similar (Kim and Bang, 2018). Haggan, Heravi and Priestley (1984) also have shown that, in a Monte Carlo Simulation, the variance of the parameter is small throughout and after some initial time units it settles down to a steady state (see Haggan, Heravi and Priestley (1984), Figure 25). Therefore, for testing the significance of the parameters for the SDM, critical values from standard distributions

can be used. However, for testing the PPP, q_{t-1} may be nonstationary, and the usual Central Limit Theorem does not apply and the Dickey-Fuller t-statistic for a linear ADF representation follows a non-standard t-distribution, the sampling distribution of this test t-statistics is skewed to the left. Chen and Wu (2000), Taylor, Peel and Sarno (2001) and Sarno and Taylor (2002) also used the critical values from MacKinnon (2010). Since the SDM model is locally linear, the critical values from the Dicky-Fuller table could be used for testing the parameter ρ at each time period. Therefore, in this chapter the critical value of -2.88 /-2.87 from the Dicky-Fuller table for the sample size of 250 /500 observations is used at the 5% significance level.

5.11.2 Fitting linear models

The general equations can be represented as follows:

$$\Delta q_t = \mu + \phi_1 \Delta q_{t-1} + \rho q_{t-1}$$

Here, q_t represents the natural log of real exchange rates, and $\Delta q_t = q_t - q_{t-1}$.
Table 5-2 shows the results. For the UK and Japan, the drift represented by μ was shown to be highly significant, which indicates mean reversion. Meanwhile, for the Brazilian real, μ was not significant at 5%. The ρs for the UK, Euro, and Japanese real exchange rates were significant at 5%. Therefore, based on fitting the linear AR(1) models, the ρs for UK, Euro and Japan were mean reverting (which indicates that PPP holds for these real exchange rates in a linear fitting), but for Brazil, it was marginally insignificant at the 5% significance level. These results show that these real exchange rates might be stationary and mean-reverting. Therefore, it is possible that PPP holds for all four real exchange rate pairs through having a negative and significant ρ coefficient.

Table 5-2 Coefficient estimates for linear models for four real exchange rates

The table below shows parameter estimations for fitting an AR model using Augmented Dicky-Fuller representation $\Delta q_t = \mu + \phi_1 \Delta q_{t-1} + \rho q_{t-1}$ for the real exchange rates for GBP/USD, EUR/USD, JPY/USD, and BRL/USD. The models selected are based on minimising BIC values, and $\Delta q_t = q_t - q_{t-1}$. The table also reports p-values for the coefficient estimates. The significance level was set at 5%.

Coefficients	UK		Euro		Japan		Brazil	
	Estimate	p-value	Estimate	p-value	Estimate	p-value	Estimate	p-value
μ	0.0135	0.00113	0.00382	0.0581	-0.0596	0.00607	-0.00782	0.0684
ϕ_1	0.299	0.000	0.267	0.000	0.297	0.000	-0.0253	0.548
ρ	-0.0277	0.000825	-0.0137	0.0239	-0.013	0.00555	-0.0117	0.059

The model employed here for testing the PPP mean reversion contained the linear ADF model as special cases and also contained the ADF-STAR model previously employed by Michael, Nobay and Peel (1997), Chen and Wu (2000), Baum, Barkoulas and Caglayan (2001), Taylor, Peel and Sarno (2001), Sarno and Taylor (2002), and Taylor (2003, 2006). The model is explained in the final part of Section 5.5.

Before the results produced by the SDM algorithm were analysed, LSTAR and ESTAR models were applied to estimate the equations in the following form:

$$\Delta q_t = (\mu + \phi_1 \Delta q_{t-1} + \rho q_{t-1})\big(1 - G(q_{t-1}, \gamma, c)\big) + (\mu^* + \phi_1^* \Delta q_{t-1} + \rho^* q_{t-1}) G(q_{t-1}, \gamma, c) + \epsilon_t$$

For the ESTAR version,

$$G(q_{t-1}, \gamma, c) = \frac{1}{1 + e^{-\gamma(q_{t-1} - c)}}$$

For the LSTAR version,

$$G(q_{t-1}, \gamma, c) = 1 - e^{-\gamma(q_{t-1} - c)^2}$$

Table 5-3 Coefficient estimates after fitting an ADF-LSTAR model

The model employed for estimation used the following formula:

$\Delta q_t = \alpha + \rho q_{t-1} + \sum_{j=1}^{p-1} \phi_j \Delta q_{t-j} + (\alpha^* + \rho^* q_{t-1} + \sum_{j=1}^{p-1} \phi_j^* \Delta q_{t-j})\, \Phi(\theta; q_{t-d}; c) + \epsilon_t$, with

$\Phi(\theta; q_{t-d}; c) = \frac{1}{1-e^{-\gamma(q_{t-d}-c)}}$, taking a logistic form.

LSTAR Model	British Pound	Euro	Japan	Brazil
Gamma	215	5.96	11.2	500
	(0.0710)	(0.893)	(0.652)	(0.117)
Break at c	0.511	-0.0771	-4.23	-0.678
	(69.9)	(-0.749)	(-75.4)	(-80.2)
Regime One				
Intercept	0.0162	-0.0621	-0.0682	-0.0212
	(2.38)	(-0.641)	(-2.72)	(-0.923)
Δq_{t-1}	0.250	0.766	0.282	-0.111
	(4.58)	(0.897)	(6.87)	(-2.43)
q_{t-1}	-0.0362	-0.788	-0.0148	-0.0281
	(-2.22)	(-0.757)	(-2.75)	(-1.23)
Regime Two				
Intercept	0.0331	0.00450	-1.17	-0.00490
	(2.56)	(1.45)	(-1.66)	(-1.11)
Δq_{t-1}	0.363	0.260	0.625	0.401
	(6.17)	(6.22)	(2.91)	(4.11)
q_{t-1}	-0.0589	-0.0152	-0.280	0.00777
	(-2.73)	(-1.79)	(-1.64)	(0.726)
BIC	-7.48	-7.36	-7.24	-5.40

Table 5-4 Coefficient estimates after fitting an ADF-ESTAR model

The model employed for estimation had the formula below:

$\Delta q_t = \alpha + \rho q_{t-1} + \sum_{j=1}^{p-1} \phi_j \Delta q_{t-j} + (\alpha^* + \rho^* q_{t-1} + \sum_{j=1}^{p-1} \phi_j^* \Delta q_{t-j})\, \Phi(\theta; q_{t-d}; c) + \epsilon_t$, with

$\Phi(\theta; q_{t-d}; c) = 1 - e^{-\gamma(q_{t-d}-c)^2}$, taking an exponential form.

ESTAR Model	British Pound	Euro	Japan	Brazil
Gamma	25.0	29.6	24.9	13.9
	(4.71)	(8.65)	(9.69)	(2.90)
Break at c	0.252	0.502	-4.93	-0.317
	(13.9)	(41.4)	(-301)	(-5.18)
Regime One				
Intercept	0.0167	0.00401	-0.0595	-0.00197
	(3.12)	(1.88)	(-2.09)	(-0.390)
Δq_{t-1}	0.339	0.222	0.302	-0.0318
	(7.63)	(4.55)	(6.94)	(-0.726)
q_{t-1}	-0.0335	-0.0158	-0.0130	-0.00952
	(-3.29)	(-2.07)	(-2.07)	(-1.49)
Regime Two				
Intercept	-0.00538	0.0171	-1.07	-0.0147
	(-0.123)	(0.357)	(-1.35)	(-0.185)
Δq_{t-1}	-0.00828	0.535	0.264	0.173
	(-0.0375)	(3.10)	(1.90)	(0.708)
q_{t-1}	0.0294	-0.0381	-0.220	0.0530
	(0.179)	(-0.393)	(-1.36)	(0.231)
BIC	-7.44	-7.31	-7.19	-5.36

Table 5-3 and Table 5-4 report the coefficient estimates for the LSTAR and ESTAR models and their respective t-statistics for each coefficient. The BIC values are reported at the bottom of each table. From Table 5-3 and Table 5-4, it is evident that based on minimising BIC values, the BIC values for both models were very close for the same currency pairs. In general, LSTAR dominates ESTAR, judging by the marginally lower BIC values for LSTAR for all four currency pairs.

When LSTAR was fitted, except for the Euro real exchange rate, all other breakpoints c were significant. When ESTAR was fitted, the speeds of transition were highly significant for all four currency pairs, and the breakpoints c for all four currency pairs were significant too.

Generally, the rule to decide if PPP holds is to check the significance of ρ. A statistically significant negative ρ parameter implies mean reversion and that PPP holds, while an insignificant ρ indicates that the time series process follows a random walk and PPP does not hold. As mentioned in the previous sections, critical values used for testing ρ for this study is taken as -2.88 at 5% significance level.

When LSTAR was fitted for the four exchange rate pairs, the t-statistics for the coefficient for q_{t-1}, indicated random walk in both regimes for all four currencies. The ESTAR fitting for the Pound and Euro showed potential ESTAR, while for Yen and Brazilian Real, both regimes were shown as random walk.

5.11.3 Test of linearity against STAR for the four real exchange rate pairs

Before implementing the SDM model on the four real exchange rate pairs, STAR-type nonlinearity was tested using Escribano and Jordá's (1997) method. As shown in Table 5-5, all four real exchange rates were linear, possibly indicating that neither LSTAR nor ESTAR were appropriate to model the real exchange rates. The SDM model was then used to check for the mean reversion properties and (non)linear properties of the real exchange rates.

Table 5-5 Test of nonlinearity

This table shows the results of a test proposed by Escribano and Jordá (1997), used here for two reasons. It first compares the relative strength in rejecting the null hypotheses of $H_{0E}: \beta_2 = \beta_4 = 0$ and $H_{0L}: \beta_1 = \beta_3 = 0$. If the odd power has the minimum p-value and is statistically significant, an LSTAR is more appropriate against linear alternatives. Otherwise, an ESTAR is more appropriate if it is statistically significant against linear alternatives. Secondly, if neither H_{0E} nor H_{0L} are significant, a linear model is more appropriate to model the time series. The delay was set to lag one of the dependent variables, because for all four real exchange rate pairs, BIC selected the AR(1) model.

Real Exchange Rate Pairs	H_E (p-values)	H_L (p-values)	Result
GBP/USD	0.363	0.278	Linear
EUR/USD	0.311	0.281	Linear
JPY/USD	0.444	0.443	Linear
BRL/USD	0.344	0.189	Linear

5.11.4 Fitting the state dependent models

5.11.4.1 Analysing the real exchange rate of the British Pound

Visual inspection of the plot of real exchange rate for GBP/USD showed no trend. So, stationarity and linearity were possibilities. The Augmented Dickey Fuller test was significant at 10% level, rejecting the null hypothesis of a unit root. It is worthy of note that there were abnormally large fluctuations of the real exchange rate in the late 1970s and 1980s. The possibility of the existence of different regimes could be tested using the State Dependent Model. This study was interested in testing the presence of stationarity

(mean-reversion) through examining and interpreting coefficient ρ using the State-Dependent Model.

Figure 5-2 Plot of $\boldsymbol{\rho}$ against the transition variable

In this graph, $\boldsymbol{\rho}$ is plotted against the transition variable for the GBP/USD real exchange rates. The transition variable is lag 1 of q_t.

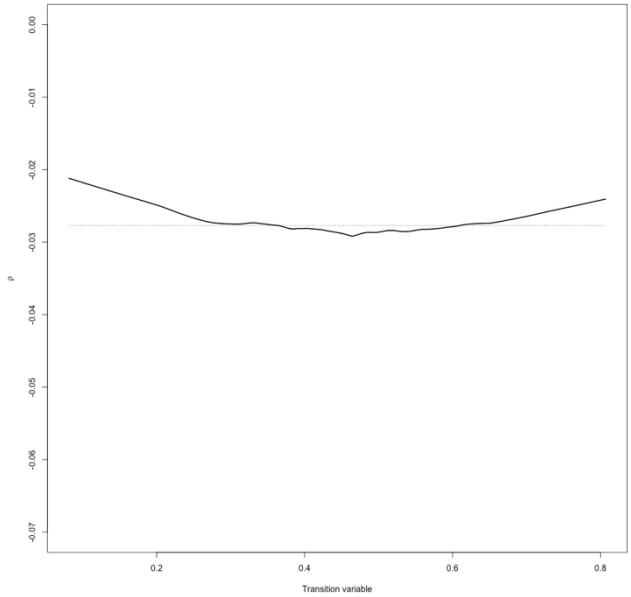

Figure 5-3 Plot of ρ against time with upper 95% Confidence Interval

In the figure below, $\boldsymbol{\rho}$ is estimated by SDM and plotted against time. A 95% one-sided confidence interval has been plotted. This is calculated as $\hat{\rho}_t + t_{5\%,ADF}.SE_t(parameter)$.

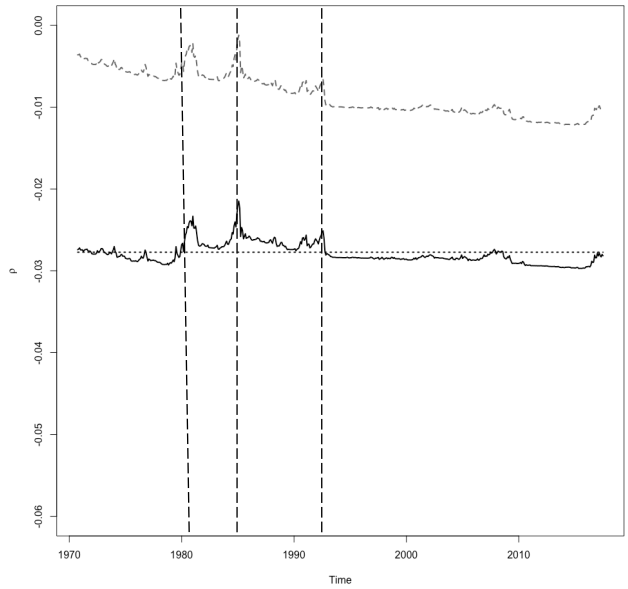

The straight dotted line shows the linear estimate by fitting a linear model to all data. The SDM has done a reasonably good job. Figure 5-2 indicates that the speed of adjustment as shown by ρ followed a symmetric pattern, indicating that a linear or ESTAR model may be appropriate. However, the range of variation for the adjustment parameter was small and close to the linear estimate of -0.025. The SDM time varying estimates for ρ as shown in Figure 5-3 captured significant structural breaks at around 1980, 1985, 1992, and 2014. The plot of the 95% confidence interval of ρ against time indicates that ρ became more negative (increasingly mean-reverting) as time passed. The confidence interval for ρ shows that despite the two strong shocks near 1980 and 1985, 100% of the time the GBP/USD was mean-reverting, and the mean reversion became stronger over time. This finding is consistent with the linearly estimated coefficient of q_{t-1}.

5.11.4.2 Analysing the real exchange rate of the Euro

Visual examination of the time plot of the EUR/USD real exchange rates indicates a slight downward trend. The unit root test of this time series rejected the unit root at 5%, but not 1%. However, before the SDM algorithm was implemented, the possibility of linearity and stationarity was not ruled out.

Figure 5-4 Plot of $\boldsymbol{\rho}$ against the transition variable

In this graph, $\boldsymbol{\rho}$ is plotted against the transition variable for the EUR/USD real exchange rates. The transition variable is lag 1 of q_t.

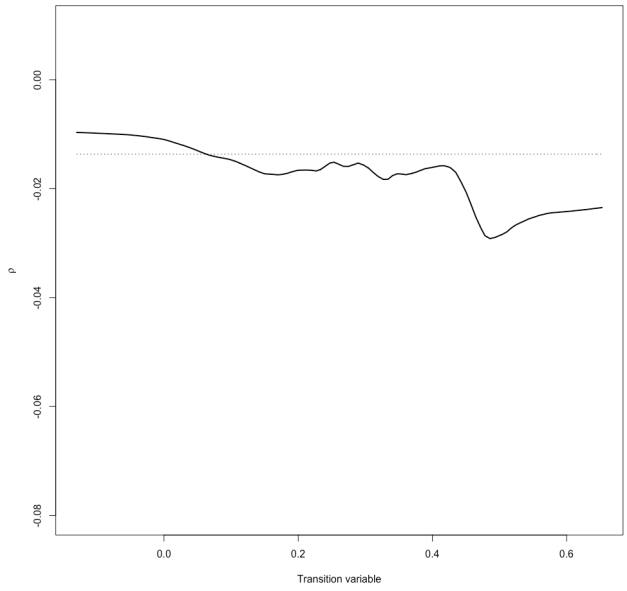

Figure 5-5 Plot of ρ against time with upper 95% Confidence Interval

In the figure below, the $\boldsymbol{\rho}$ estimated by SDM is plotted against time. A 95% one-sided confidence interval has been plotted This is calculated as $\hat{\rho}_t + t_{5\%,ADF}..SE_t(parameter)$.

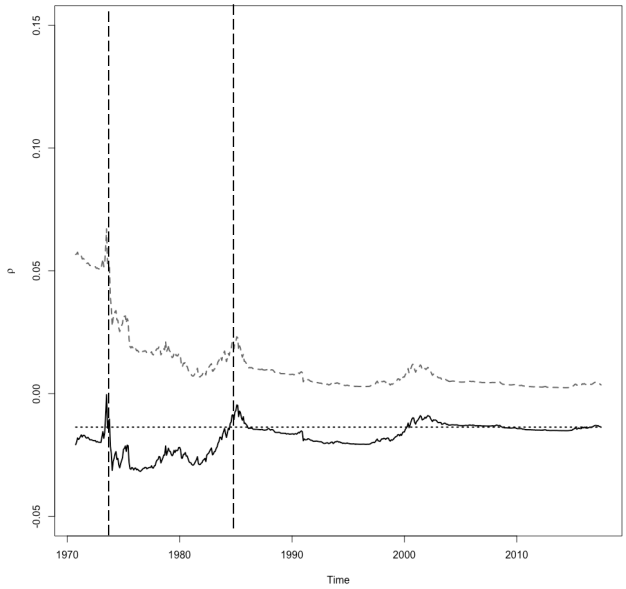

The general shape of ρ when plotted against q_{t-1} in Figure 5-4 shows that they are approximately constant. The parameter ρ has a constant shape at around -0.020, implying a constant speed of adjustment. In Figure 5-5, the SDM algorithm has done a good job, as the parameters fluctuate around their respective linear estimates. The SDM captured the structural break at around 1974 and 1985. The structural break observed around q_{t-1} = 0.48 ($e^{q_{t-1}} = 1.62$) is close to the break point c identified by ESTAR at 0.502 ($e^{q_{t-1}} = 1.65$).

In the linear AR(1) model fitting, ρ is significant. The SDM shows that ρs were never significant. Figure 5-5 shows that ρ exhibits random walk all the time.

5.11.4.3 Analysing the real exchange rate of the Japanese Yen

The plot of the Japanese yen real exchange rates generally shows a gentle decreasing trend, and after the mid-1970s, the real exchange rate stays relatively constant. The mean real exchange rate is 0.00978 JPY/USD. The Augmented Dickey-Fuller test indicates that the series is highly stationary at 1%. Therefore, the possibility of linearity and stationarity is not excluded in the time series. Coefficient ρ is constant, with a very flat value of around -0.0120, implying that the degree of adjustment is constant for different values of the exchange rate.

Figure 5-6 Plot of $\boldsymbol{\rho}$ against the transition variable

In this graph, $\boldsymbol{\rho}$ is plotted against the transition variable for the JPY/USD real exchange rates. The transition variable is lag 1 of q_t.

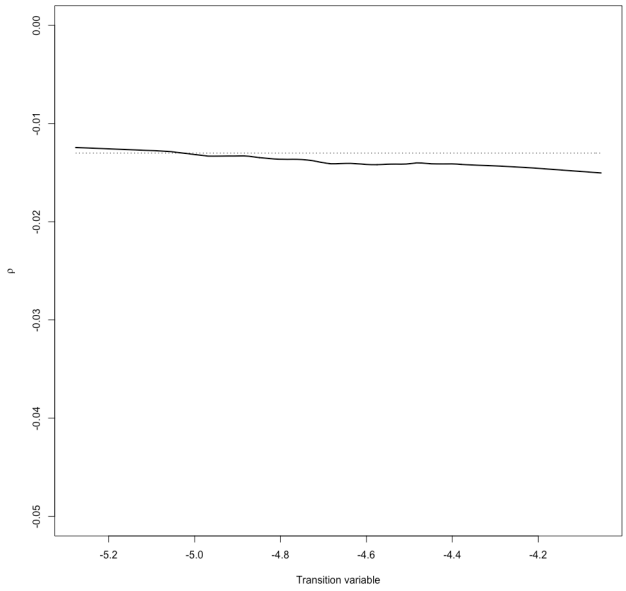

Figure 5-7 Plot of $\boldsymbol{\rho}$ against time with upper 95% Confidence Interval

In the figure below, $\boldsymbol{\rho}$ is estimated by SDM and plotted against time. A 95% one-sided confidence interval has been plotted. This is calculated as $\hat{\rho}_t + t_{5\%,ADF}.SE_t(parameter)$.

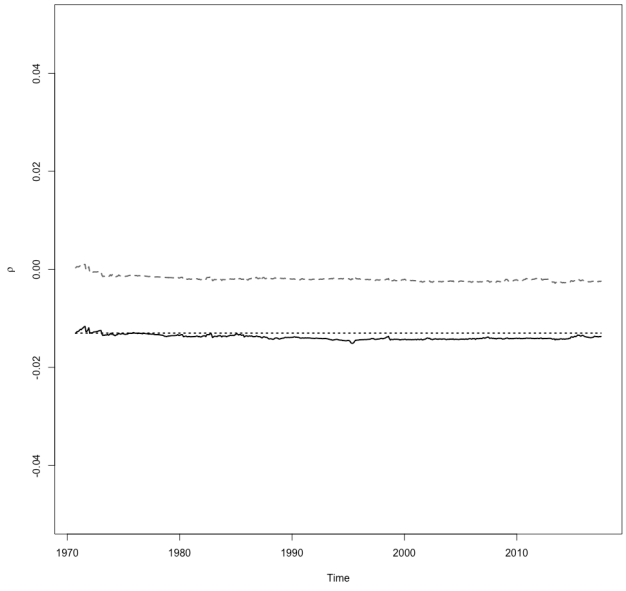

From the plots of ρ generated from the SDM algorithm in Figure 5-7, there seem to be no noticeable structural breaks.

The SDM has done a reasonably good job, as the SDM estimates of ρ evidently fluctuates mildly around their respective linear estimates. The 95% one-sided confidence interval for ρ was significantly different from zero all the time, and that the real exchange rate was 97.69% mean reverting throughout the period. As the linear model shows ρ as also significant, the SDM result was consistent with this. The process was initially random walk during the 1970s, and increasingly mean reverting as time passes. There seems to be little evidence of structural breaks present in Figure 5-7.

5.11.4.4 Analysing the real exchange rate for the Brazilian Real

Figure 5-8 Plot of ρ against the transition variable

In this graph, $\boldsymbol{\rho}$ is plotted against the transition variable for the BRL/USD real exchange rates. The transition variable is lag 1 of q_t.

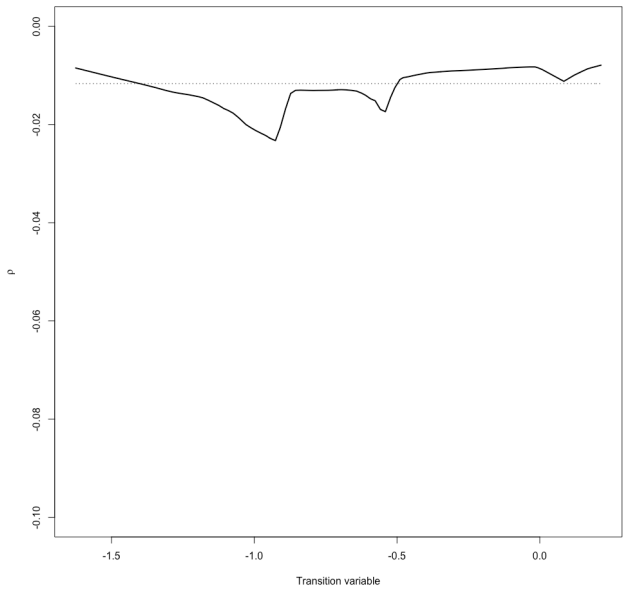

Figure 5-9 Plot of ρ against time with upper 95% Confidence Interval

In the figure below, the $\boldsymbol{\rho}$ estimated by SDM is plotted against time. A 95% one-sided confidence interval has been plotted. This is calculated as $\hat{\rho}_t + t_{5\%,ADF} SE_t(parameter)$.

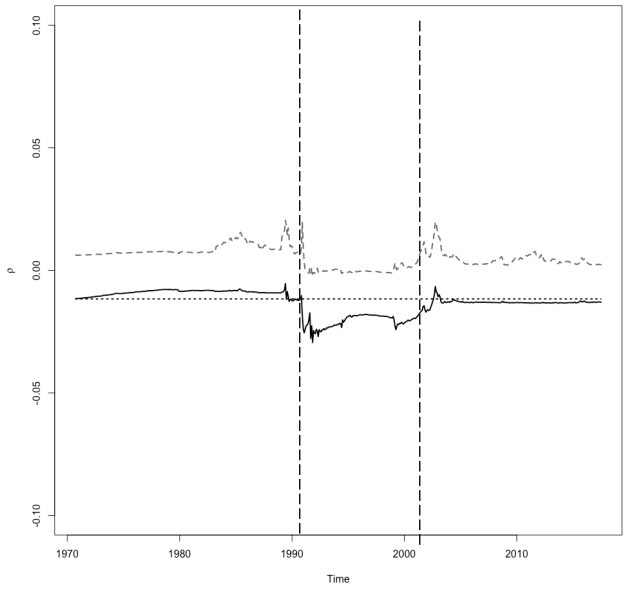

A decrease in trend in plot of BRL/USD real exchange rates can be seen. Two structural breaks can be observed in the time plot, near 1991 and 2002. There is suspected non-linearity in the series. The SDM was applied to reveal the results. The shape of ρ indicates some degree of LSTAR shape. However, the range of ρ was small. The break at around q_{t-1}= -0.60 ($e^{q_t-1} = 0.549$) was in a similar place to threshold c when LSTAR was fitted, having been identified at -0.678 ($e^{q_{t-1}} = 0.508$).

As seen in Figure 5-9, ρ fluctuated around the linear AR(1) estimate. Therefore, the SDM has done a good job. The ρ estimates were close to the LSTAR estimates of ρs in both regimes. The LSTAR estimates for ρs for the two regimes were -0.02 and 0.01 respectively.

The estimated ρs produced by SDM were 13.88% of the time statistically significant and mean reverting. While between 1990 and 2000 the SDM estimated ρs were significant and mean reverting, at other times they seemed to behave in a random walk process (as they were statistically insignificant).

Table 5-6 Mean reverting behaviour, testing random walk against ESTAR and linear ADF test result

Note: The following table reports proportion of time the four real exchange rate pairs show mean reversion, together with p-values of unit root test against ESTAR (Hu and Chen, 2016), and p-values of linear Augmented Dickey-Fuller test estimation

Currency	% of time mean reverting (SDM)	p-value unit root against ESTAR	p-value of ρ in linear ADF
GBP/USD	100.00%	0.00	0.000825
EUR/USD	0.00%	0.00	0.0239
JPY/USD	97.69%	0.00	0.00555
BRL/USD	13.88%	5.68%	0.059

Table 5-6 tabulates linear Augmented Dickey-Fuller test, nonlinear unit root test against STAR and percentage of times the four real exchange rates mean-reverting.

5.11.5 Analysis of findings

Overall, the Pound and Yen show mean reversion at all times, and both generally exhibit tendencies to behave as mean-reverting ESTAR models. The overall results for GBP/USD real exchange rates are also consistent with the unit root test results from Bec, Ben Salem and Carrasco (2010), and mean reversion was supported in Nikolaou (2008). For JPY/USD, Christopoulos and León-Ledesma (2010) rejected unit root against linear stationarity at 10% significance level, which is consistent with this SDM result. For the Euro, the SDM shows random walk all the time, but linear and nonlinear unit root tests rejected random walk. Additional evidence suggests that the Euro behaves in a manner supportive of an ESTAR model (Schnatz, 2006), in which the mean reversion of Euro was also supported in Nikolaou (2008). For BRL, we see that 13.88% of the time the real exchange rate mean reverts, and the unit root tests marginally rejecting the unit root at

5% significance level. The overall result of random walk for BRL/USD is consistent with the stochastic unit root test result by Bleaney, Leybourne and Mizen (1999).

5.12 Impact of Policy Uncertainty on Real Exchange Rates

5.12.1 Policy uncertainty

Growing attention has been paid to the quantification of policy uncertainties since the 2008 global financial crisis. Uncertainty was claimed by the Federal Open Market Committee minutes repeatedly and by Stock and Watson (2012) to have significant contributions to the financial crisis (Barrero, Bloom and Wright, 2017). Therefore, there is a high demand for research related to uncertainty.

Baker, Bloom and Davis (2015) developed an economic policy uncertainty (EPU) index for the United States and eleven other countries from newspaper coverage frequency based on a process of human reading of 12,000 newspaper articles, and reported that for the United States, the EPU index spiked during periods of tight presidential elections, outbreaks of war, terrorist attacks, the bankruptcy of major banks, policy disputes, etc. Similar uncertainty indices have also been designed by Arbatli *et al.* (2017) using a similar approach to policy uncertainties for Japan. Baker *et al.* (2019) addressed uncertainty in the equity market. Other quantification methods of policy uncertainty have included implied stock market volatility (Baker, Bloom and Davis, 2015), text analysis (Hassan *et al.*, 2016), survey-based measures, multivariate GARCH models, time-varying uncertainty related to fiscal policy derived from the New Keynesian model, etc.

High policy uncertainty tends to be followed by negative consequences. Baker, Bloom and Davis (2015) found that it resulted in reduced investment and employment in sectors

which are sensitive to policy change – for example, the defence, healthcare, finance, and infrastructure construction sectors. These authors argued that in a highly uncertain environment, many firms choose to defer hiring and investment in order to avoid making costly decisions. Baker, Bloom and Davis (2015) also found that uncertainty about fiscal and monetary policy contributed to steep economic deterioration in 2008/09 and a slow recovery afterwards. Using vector autoregressive (VAR) models, these authors found that the increase in EPU in 2005/06 to 2011/12 was followed by about 6% in gross investment, 1.2% in industrial production output and a 0.35% decrease in employment. An increase in EPU also results in greater stock price volatility, reduced output, and worsening macroeconomic performance (Arbatli *et al.*, 2017). Other concerns in relation to rising uncertainty are an increase in the cost of capital in terms of risk premium for firms, and a strong negative effect on financial constraints (Bloom, 2014, 2015; Gilchrist, Sim and Zakrajsek, 2014). While economic uncertainty can be minimised via a strong and credible policy framework, good policies can also have positive effects on macroeconomic performance, and reduce policy uncertainty (Arbatli *et al.*, 2017). There is evidence that economies tend to rebound after spikes of policy uncertainty dissipate (Fernández-Villaverde *et al.*, 2015).

As policy action (and inaction) have economic consequences; therefore, it is important to study policy uncertainty and to use research evidence to inform policy actions to yield a positive effect on the economy.

Arghyrou, Gregoriou and Pourpourides (2009) found that exchange rate uncertainty causes significant deviations from the condition of Purchasing Power Parity. They tested this hypothesis and found similar results for the G7 countries. They argued that the

uncertainty of the foreign exchange market may cause real exchange rates to drift apart and seem to run against the notion of PPP mean reversion. Guerron-Quintana (2011) found that technology and uncertainty make real exchange rates more volatile.

The research analysing the impact of EPU on exchange rate volatility has found that it mostly amplifies exchange rate movements. Chen, Du and Hu (2020) recently found that EPU has significant asymmetric and heterogeneous effects on the volatility of Chinese exchange rates. Bartsch (2019) found that the impact of EPU on exchange rate volatility on dollar-pound exchange rates can have a one-month lag. However, no studies have linked policy uncertainty with the mean reversion properties of exchange rates.

Since accurately predicting the consequences of economic uncertainty on the foreign exchange market is likely to be beneficial to interested parties, it is worthwhile studying the mean-reversion properties of real exchange rates during different instances of policy uncertainty. This study therefore applied the SDM model to check how the behaviour of real exchange rates varies with different levels of economic uncertainty. This makes full use of the key advantage of the SDM model: that it does not pre-assume the behaviour of real exchange rate movements, and simply lets the data reveal its behaviour.

5.12.2 SDM model with uncertainty

This section describes the results when the state dependent model was applied, incorporating the policy uncertainty index. The SDM model used was extended as:

$$\Delta q_t = \mu + \theta_1 \Delta q_{t-1} + \cdots + \theta_k \Delta q_{t-k} + \rho(\boldsymbol{u_{t-1}}) q_{t-1}.$$

Where global uncertainty indices were applied into the SDM algorithm, in this case, the ρ coefficient was updated according to the changes in global uncertainty indices u_t.:

$$\rho(u_t) = \rho(\boldsymbol{u_{t-1}}) + (\boldsymbol{u_{t-1}} - \boldsymbol{u_{t-2}})\gamma^{(t)}.$$

$$\mu_u(\boldsymbol{q_t}) = \mu_u(\boldsymbol{q_{t-1}})$$

$$\theta_u(\boldsymbol{q_t}) = \theta_u(\boldsymbol{q_{t-1}})$$

5.12.3 Data

To match the availability of uncertainty indices, the data for this section of analysis was the same but shortened version of the real exchange rates for GBP/USD, EUR/USD, JPY/USD, and BRL/USD. As the world is interconnected, the global economic policy index was used as the policy uncertainty index. The chosen uncertainty indices were global economic policy indices. The frequency of real exchange rates and uncertainty indices were monthly, ranging between January 1997 and July 2017. This choice of sample period reflected the data availability.

5.12.4 Descriptive statistics

Figure 5-10 provides a time plot of the global uncertainty indices. It shows that from the start of the series to around 2009, there was almost a constant low level of uncertainty index. However, afterwards, the index fluctuated more widely while exhibiting a rising trend. The highest level of the uncertainty index was 308, with an average level of 109.

Figure 5-10 Time plot of global policy uncertainty index

The figure below shows a time series plot of the global policy uncertainty index, from 1997.2 to 2017.7. The choice of dates reflected the data availability.

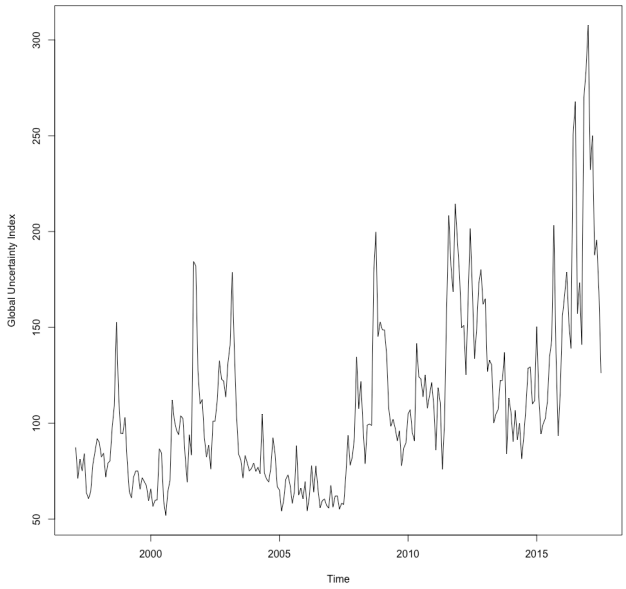

Events that corresponded to spikes in the index are reported in Figure 5-11. It can be seen that spikes of global economic policy uncertainty took place during a war, financial crises and political events. The occurrence of uncertain events becomes more frequent, and as can be see from the graph, uncertainty increased significantly during this period.

Figure 5-11 Global economic policy uncertainty index, January 1997 to May 2017[3]

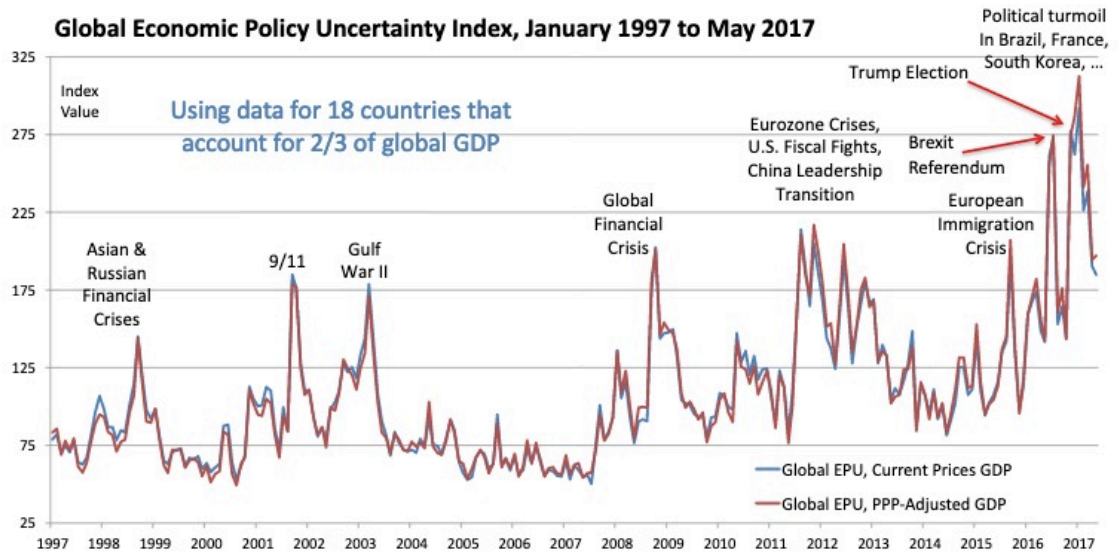

[3] Adapted from the policy uncertainty website: http://www.policyuncertainty.com/global_monthly.html

5.12.5 Empirical results incorporating the uncertainty index

5.12.5.1 Uncertainty indices and real exchange rates for the British Pound

Figure 5-12 Plot of ρ against uncertainty indices

This figure shows a plot of $\boldsymbol{\rho}$ against the uncertainty indices for the British pound real exchange rates.

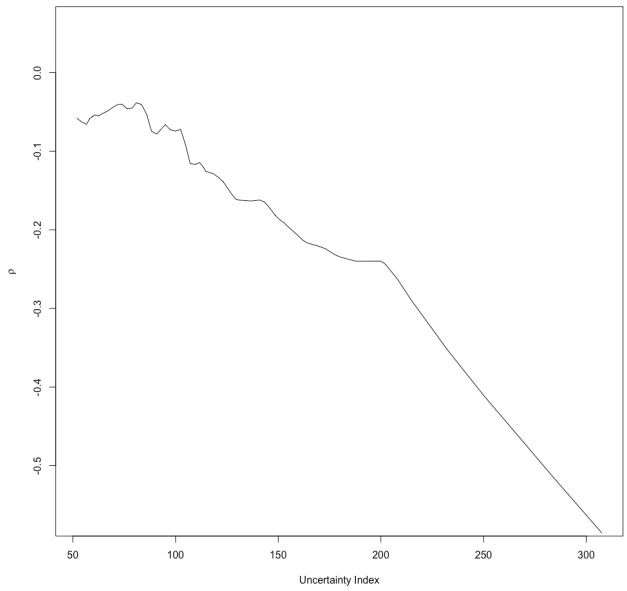

Figure 5-13 Plot of ρ against time

This figure below shows a plot of $\boldsymbol{\rho}$ against time for the British pound real exchange rates with upper 95% confidence intervals after incorporating the uncertainty indices.

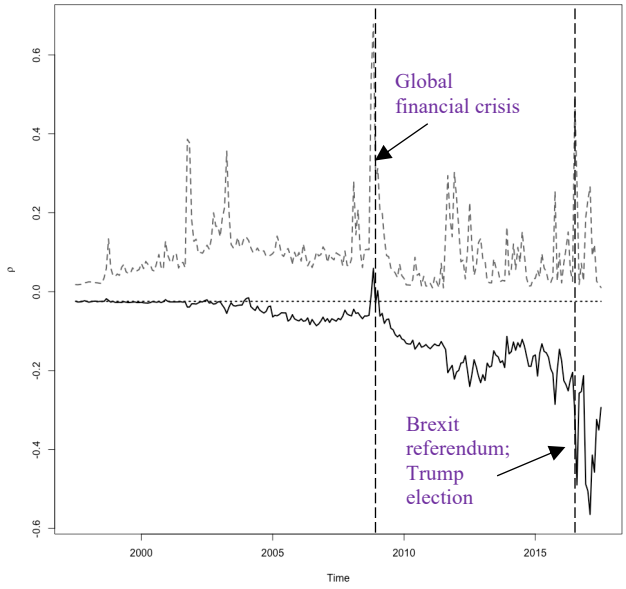

After model fitting using the SDM algorithm and updating the coefficients according to changes in the uncertainty indices, the SDM was plotted to estimate coefficients against the transition variable, the first lag of uncertainty index, u_{t-1}, against time.

It can be observed from Figure 5-12 that with a higher uncertainty index, ρ was more mean reverting. This probably suggests that during periods of high uncertainty, the real exchange rates tended to revert back to their equilibrium levels at a faster rate. The degree of mean reversion started to increase significantly with a rising uncertainty index. From Figure 5-13, it is clear that before 2010, the ρs were never significant and were following a random walk. A mean reversion took place especially after 2010 when uncertainty indices were higher. This corresponds with the finding that the higher the uncertainty indices, the higher the degree of mean reversion.

5.12.5.2 Uncertainty indices and real exchange rates for the Euro

Figure 5-14 Plot of ρ against the uncertainty indices

This figure shows a plot of $\boldsymbol{\rho}$ against the uncertainty indices for the Euro real exchange rates.

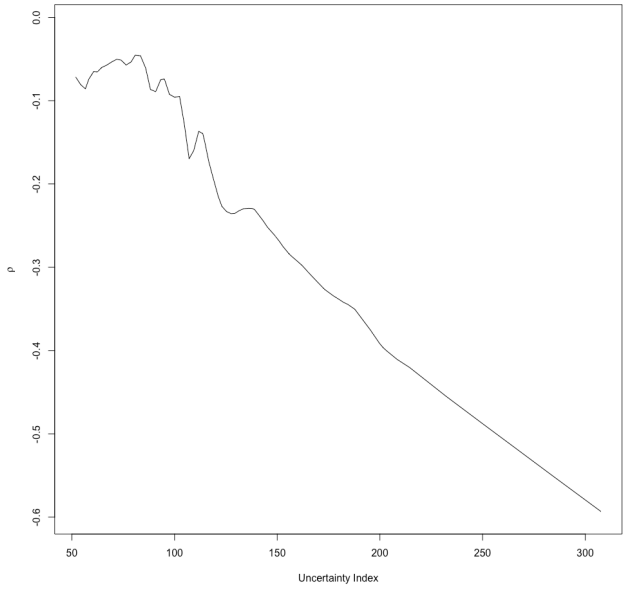

Figure 5-15 Plot of ρ against time

This figure below shows a plot of $\boldsymbol{\rho}$ against time for the Euro real exchange rates with upper 95% confidence intervals after incorporating the uncertainty indices.

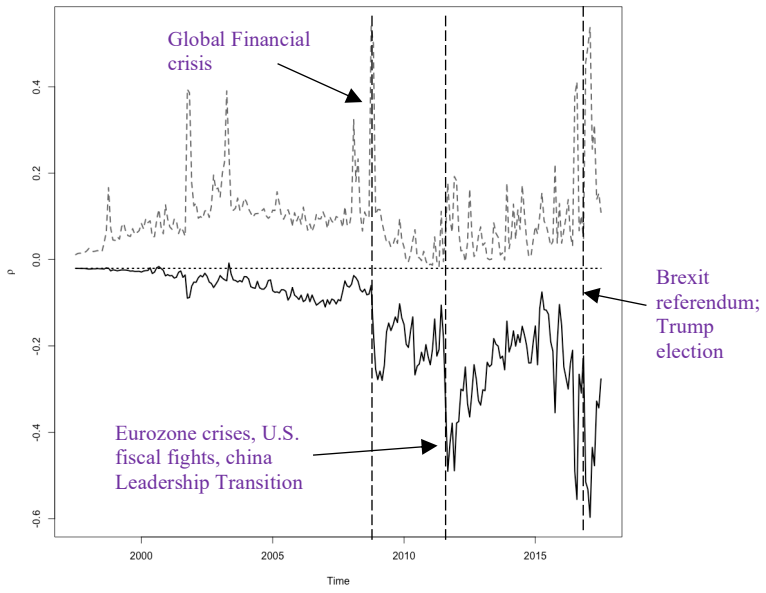

As Figure 5-14 shows, the mean reversion increased with higher uncertainty indices. There was an increasing degree of mean reversion after 2009. The uncertainty indices were also significantly higher after 2009. Therefore, the degree of mean reversion correlated positively with the uncertainty indices.

5.12.5.3 Uncertainty indices and real exchange rates for the Japanese Yen

Figure 5-16 Plot of ρ against uncertainty indices

This figure shows a plot of ρ against the uncertainty indices for the Japanese Yen real exchange rates.

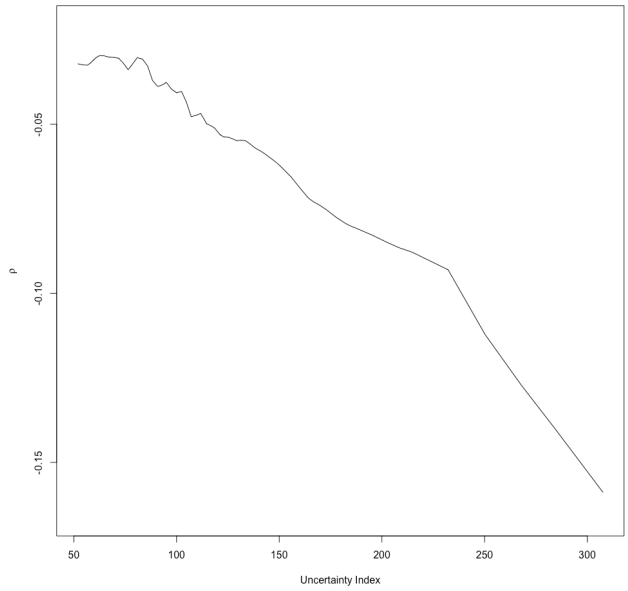

Figure 5-17 Plot of ρ against time

This figure below shows a plot of $\boldsymbol{\rho}$ against time for the Japanese Yen real exchange rates with upper 95% confidence intervals after incorporating the uncertainty indices.

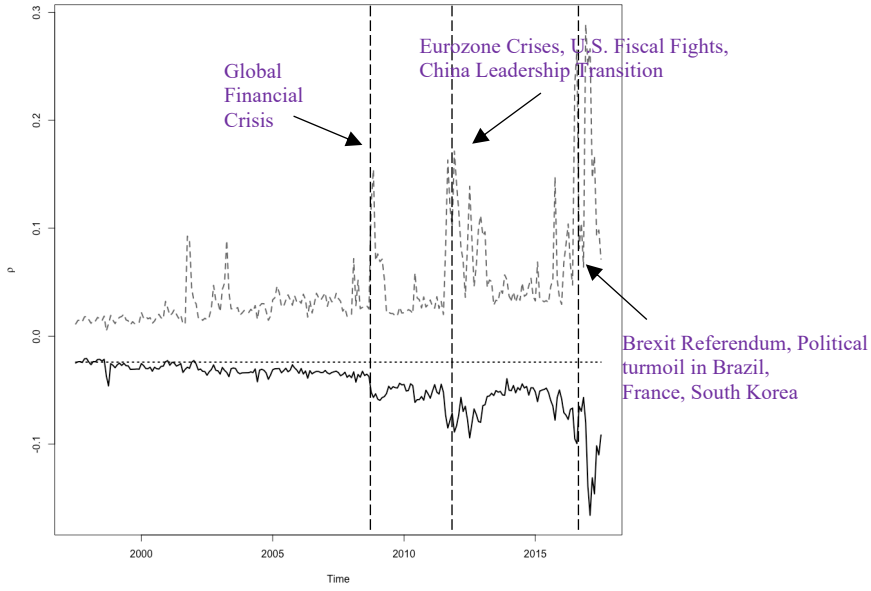

The same results were observed when the mean-reversion behaviour was analysed with the uncertainty index as an exogenous variable. A higher level of uncertainty corresponded to a rising level of mean-reversion. Figure 5-17 shows that the real exchange rates started to mean revert in a stronger manner after 2009 in general. However, ρ ranged from -0.05 to 0.15, which is quite small. This shows the stability of the Japanese Yen, and confirms that the Yen is less affected by global uncertainty.

5.12.5.4 Uncertainty indices and real exchange rates for the Brazilian Real

Figure 5-18 Plot of ρ against uncertainty indices

This figure shows a plot of $\boldsymbol{\rho}$ against the uncertainty indices for the Brazilian Real real exchange rates.

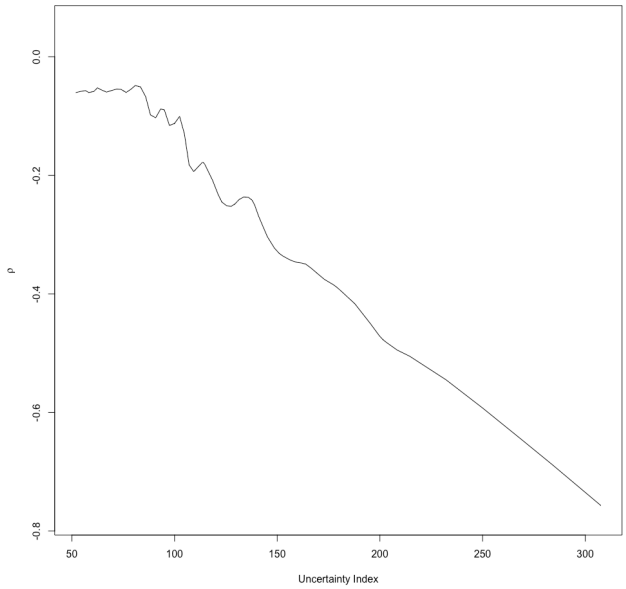

Figure 5-19 Plot of ρ against time

This figure below shows a plot of $\boldsymbol{\rho}$ against time for the Brazilian Real real exchange rates with upper 95% confidence intervals after incorporating the uncertainty indices.

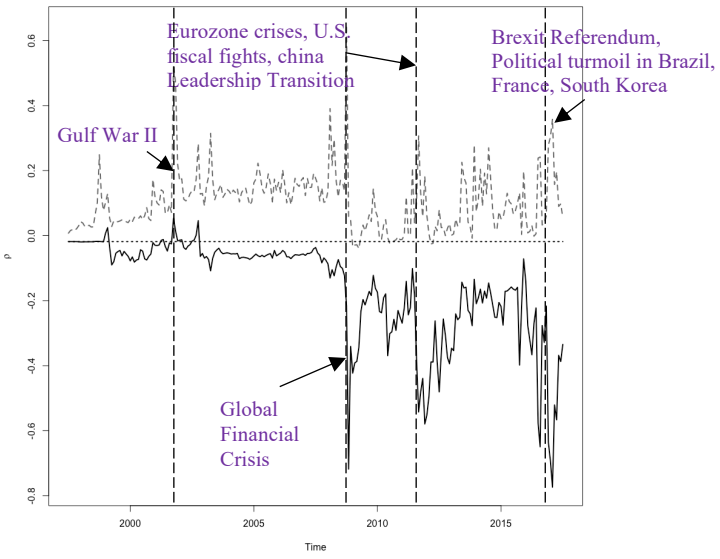

Regarding the BRL/USD real exchange rates with uncertainty indices, it appears that the higher the uncertainty index, the stronger the mean reversion. The mean reversion started to become stronger and more significant after 2009.

5.12.6 Mean reversion and policy uncertainty

The results in the previous subsection show strongly that the mean reversion of real exchange rates increases with rising uncertainty indices. In general, three recent events strongly affected the mean reversion properties of the four currency pairs - Global financial crisis, Eurozone crisis and Brexit referendum. It is also seen that mean reversion is increasingly stronger through time. This implies that for the four real exchange rates during low uncertainty periods, the real exchange rates behave like a random walk process. When the uncertain events become more frequent, the real exchange rates become increasingly mean reverting, in a nonlinear manner. Another interesting finding of the mean reversion properties of real exchange rates is that uncertainty always led to initial shocks in real exchange rates before a strong mean reversion reaction. Over the longer term, real exchange rates mean reverted more strongly.

The finding in this section is consistent with the PPP theory. In normal situations and during the periods of low uncertainty, and in an efficient market there is low volatility in the market and real exchange rates behave like a random walk model. However, during the periods of high uncertainty, the real exchange rates become more volatile and further away from the equilibrium. There will be more people entering the market to profit from higher deviations caused by higher uncertainty. High volumes of sell / buy to gain profit during the uncertain times, and possible government intervention will cause faster adjustment to exchange rates, and thus mean reverting behaviour.

5.12.7 Impact of long run uncertainty on real exchange rates

Barrero, Bloom and Wright (2017) claimed that through measuring the implied volatility from options of 30 days duration, short term uncertainty can be measured; long-term uncertainty can be measured from options with a duration of 10 years. While oil price volatility drives short-run uncertainty, economic policy uncertainty is an important factor for long-run uncertainty. They also argued that in terms of sensitivity, R&D and investments were more significantly and negatively impacted by high policy uncertainty, followed by hiring (Barrero, Bloom and Wright, 2017), in a Peking order. As recently global uncertainty has reached an all-time high, it is worrying to see that the short and long-term outlook of the global economy is still gloomy, as it affects R&D, investment and unemployment negatively. Combined with the Coronavirus outbreak, we will have to wait some time before noticing reduction in policy uncertainty. In terms of real exchange rates, there will be stronger mean reversion with higher global uncertainty. This self-adjustment mechanism shows that real exchange rates will always revert to the PPP level more strongly when experiencing a higher level of global policy uncertainty.

5.13 Findings and Conclusions

This chapter has contributed to testing the Purchasing Power Parity hypothesis using the State-Dependent Model and as such, is among the first to have explored the behaviour of real exchange rates in terms of whether Purchasing Power Parity holds continuously through different levels of global uncertainty. When ρ was updated as a function of the past exchange rate, q_{t-1}, the results indicated both Pound and Yen behave in a mean reverting ESTAR model. This finding is confirmed by Bec, Ben Salem and Carrasco (2010), Nikolaou (2008). For JPY/USD, the SDM result is also consistent with Christopoulos and León-Ledesma (2010). For EUR/USD, the SDM has found a different result from other methods employed in this chapter. Therefore, on the whole, it behaves

in a manner supportive to an ESTAR model (Schnatz, 2006), and mean-reverting consistent with Nikolaou (2008). For BRL, we see consistent results at 10% significance level, and the results are supported by that of Bleaney, Leybourne and Mizen (1999). This implies for GBP/USD and JPY/USD, PPP held throughout. Apart from modelling for EUR/USD, the SDM performed well when modelling nonlinearity and mean reversion behaviours of the other real exchange rates. It is clear that GBP/USD and JPY/USD currencies make appropriate self-adjustments, while for BRL/USD it is a random walk model. In the second part of the chapter, the results indicated a strong positive association between rising uncertainty indices and the degree of mean reversion, increasing degree of mean reversion over time, and shocks in real exchange rates during uncertain events. Subsection 5.12.6 explains the reason for this behaviour. The real exchange rate seemed to be able to self-adjust when spikes in the uncertainty index occurred. The mean reversion behaviour of the real exchange rates started generally after 2009/2010, and the degree of mean reversion increased over time. Overall, it can be said that PPP holds increasingly with increased global uncertainty. This research therefore suggest that governments may not need to take immediate steps to intervene in the currency market during a high uncertainty environment, as the results in this study suggested that the market will self-adjust. The results in this study also provide some evidence that the behaviour of real exchange rates are different for different countries, and an extended analysis of the behaviour of the exchange rates for more countries based on different regions and political systems would be beneficial.

This page intentionally left blank

Chapter 6 Forecasting Industrial Production and Japanese Tourist Arrivals Using the State Dependent Models

6.1 Introduction

This chapter contributes to assessing the forecasting performance of a general class of non-linear models called “State Dependent Models” (SDM), which were developed by Priestley (1980), on two sets of real data. It also extends the SDM forecasting methodology using non-parametric LOWESS smoothing methods. Three different forecasting methods of state dependent models - the traditional recursive method, and two other forecasting methods involving a smoothed and an unsmoothed coefficient grid search method - were considered and employed to forecast industrial production indices for the UK and tourism demand in Japan. The forecast performances were then compared with ARIMA, the Error Trend Seasonality (ETS) model, and neural network autoregressive models. The results indicate that SDM models can forecast at least as well as the other three models, and that improvements in forecasting are more pronounced in long-run forecasting.

In this chapter, a brief description of these methods is given at first. The empirical sections which follow include two separate applications. Section 6.2 reports the forecasting results for eight industrial production series of seasonally unadjusted industrial production indices for the United Kingdom. Section 6.3 reports the results for tourism arrivals data in Japan.

6.2 Forecasting Industrial Production Data

6.2.1 Introduction

Priestley (1980) developed a general class of non-linear models called "State Dependent Models", or SDM. The main advantage of the SDM model is that it allows for a general form of non-linearity without imposing any specific functional form, and includes ARIMA and non-linear models as special cases. Embedded in the SDM is the Kalman Filtering algorithm, which enables the calculation of exact finite sample forecasts and an exact Gaussian likelihood function. A limited study of the application of SDM models, both on real and simulated data, was given in Haggan, Heravi and Priestley (1984). Very few studies have evaluated the forecasting accuracy of the State Dependent Models.

Cartwright and Newbold (1982) applied the SDM models to forecast oil discoveries and found that when a broader class of models (such as the SDM models) are used in forecasting, substantial gains can be achieved in forecast accuracy, compared to linear ARMA models. Heravi (1985) applied the SDM to short term prediction and compared the forecasting performance of the SDM and Box-Jenkins approach against simulated series. He demonstrated that short term SDM forecasting performance is comparable with linear and other non-linear models using Canadian lynx data and sunspot data. Cartwright (1985a) compared the SDM's forecasting performance against bilinear and standard linear models and found a significant improvement in the forecasting performance of this broader class of time series models relative to ARMA models.

Industrial production is one of the most important types of time series data for policy makers and economists. Industrial production indices are PRODCOM statistics that are used to address several questions. They are important as they are commonly used as

business cycle indicators measuring outputs (Bianchi *et al*., 2010). Industrial production and its components have become increasingly important globally since the creation of the European Monetary Union as they show the productivity of different industries in different countries, and also show trends in total industrial productions and GDP. The monetary policies of each of the EMU countries are based on forecasts of future output and prices. Therefore, there is a need for reliable forecasting models for industrial production indices.

A number of studies have forecast industrial production data. For example, using seasonally unadjusted industrial production data for eight sectors, Osborn *et al*. (1999) tested for seasonal unit roots and found that when out of sample forecasts are considered, the annual difference is superior. Heravi *et al*. (2004) compared linear models against neural network methods in forecasting 24 series measuring annual change in monthly seasonally unadjusted industrial productions for France, Germany, and the United Kingdom, and found that linear forecasting models' forecasts were better for horizons of up to a year, while Neural network forecasts were better at predicting directions of change.

Hassani *et al*. (2009) compared the forecast accuracy of SSA, Holt-Winters, and ARIMA models, and found that although all three models produce a similar level of forecast accuracy in the short term, the SSA significantly outperforms the other two forecasting models at longer horizons. Hassani, Heravi and Zhigljavsky (2013) showed that the SSA performed well in extracting the harmonics and trend components at the same time in eight industrial production series for the United Kingdom, and that SSA can also perform well when structural breaks exist in the series. These authors showed that univariate SSA forecasts were better than those of the ARIMA model. The Multivariate SSA they employed also outperformed the VAR model in predicting the industrial production indices in terms of direction of change.

Hassani, Heravi, Brown and Ayoubkhani (2013) also employed the nonparametric singular spectrum analysis (SSA) model and computed their forecasts for the periods before, during, and after recession for eight of the most important UK economic indicators. They compared SSA forecasts against the benchmark ARIMA and Holt-Winters models, and found that the SSA produced the best forecasts of the three models. as it was able to produce eight times better than the ARIMA and Holt-Winters methods for all series. They also reported that SSA was able to produce better forecasts in terms of direction of changes.

The global financial crisis of 2008 had significant ramifications. It undoubtedly resulted in stagnation or decline in production in many European countries. Therefore, evaluating forecasting accuracy performance in the presence of structural breaks is important. This paper shows strong improvements in forecasting performance relative to other forecasting models, such as ARIMA, ETS, and Neural Networks, when three different forecasting methods for state dependent models are implemented. The improvement is more pronounced with long term time forecasting.

The structure of this section is as follows. In the following sub-section, a brief description of the three forecasting procedures for the SDM are given. The data used in the study and the results of the study are then presented, before the findings are discussed in Section 6.4.

6.2.2 State dependent forecasting procedures

This section proposes three different SDM forecasting methods, which are outlined in the following sub-sections.

6.2.2.1 The classical recursive forecasting method

Similar to other forecasting methods, the forecasting performance of the SDM depends on fitting the appropriate SDM scheme. Given observations on $\{X_{(t)}\}$ up to time t and using the SDM model with the state vector as $\boldsymbol{x_{t-1}} = (1, -X_{t-1}, \dots, -X_{t-k})$, one step ahead forecasts, $\hat{X}_{t+1}$ can be computed by:

$$\hat{X}_{t+1} = \hat{\mu}^{(t)} - \hat{\phi}_1^{(t)} X_t - \cdots - \hat{\phi}_k^{(t)} X_{t-k+1} = H_{t+1}\hat{\theta}_{t+1} \qquad (6.1)$$

Where $\hat{\theta}_{t+1} = F_t\hat{\theta}_t$ and $H_{t+1} = (1, -X_t, \dots, -X_{t-k+1}, 0, 0, \dots, 0)$,

$$\boldsymbol{F_{t+1}^*} = \begin{pmatrix} & \boldsymbol{\Delta x_t'} & 0 & 0 \\ I_{k+1} & 0 & \ddots & 0 \\ & 0 & 0 & \boldsymbol{\Delta x_t'} \\ 0 & & \mathrm{I}_{k(k+1)} & \end{pmatrix}$$

In essence, using (6.1), the parameters $\hat{\mu}$, $\hat{\phi}_1 \dots$, $\hat{\phi}_k$ and the gradients $\alpha^{(t)}$, $\gamma_1^{(t)}, \dots, \gamma_k^{(t)}$ are updated as follows:

$$\mu^{(t)} = \mu^{(t-1)} + \Delta x'_t \gamma^{(t)} \qquad \phi_u^{(t)} = \phi_u^{(t-1)} + \Delta x'_t \gamma^{(t)}$$

$$\alpha^{(t+1)} = \alpha^{(t)} \qquad \gamma^{(t+1)} = \gamma^{(t)}$$

Similarly, two-step ahead forecast can be obtained from:

$$\hat{X}_{t+2} = H_{t+2}.\hat{\theta}_{t+2}$$

Where $\hat{\theta}_{t+2} = F_{t+1}\hat{\theta}_{t+1}$, $H_{t+2} = \{1, -\hat{X}_{t+1}, -X_t, \dots, -X_{t-k+2}, 0, 0, \dots, 0\}$

Therefore, the gradient parameters remain the same as the last available estimated gradients, i.e.: $\alpha^{(t+2)} = \alpha^{(t+1)} = \alpha^{(t)}$, $\gamma^{(t+2)} = \gamma^{(t+1)} = \gamma^{(t)}$.

Similarly, the h-step ahead forecast can also be computed recursively as:

$$\hat{X}_{t+h} = H_{t+h}.\hat{\theta}_{t+h} \qquad (6.2)$$

And, the gradient parameters for this case remain the same as the values in time t, i.e., they are equal to $\alpha^{(t)}$ and $\gamma_u^{(t)}$ for the h-steps ahead forecast.

6.2.2.2 Estimating the parameters, evaluated with the most recent forecasts

As has been seen, between time t and $t+h$, the coefficients of $\hat{\mu}$, $\hat{\phi}_1 \ldots$, $\hat{\phi}_k$ are strictly linear functions of the state vector, as the gradients remain unchanged. However, for long term forecasting, assuming strict linearity in the parameters is not desirable, so in this case it may be better to estimate the parameters from the surfaces fitted up to time t, but evaluated with the most recent forecast values. Therefore, if the parameter surfaces fitted up to time t are denoted by $\hat{\mu}^{(t)}(\boldsymbol{x_{t-1}})$, $\hat{\theta}_u^{(t)}(\boldsymbol{x_{t-1}})$, then the h-step ahead forecast can be similarly obtained from (6.2) with the parameter estimated as:

$$\hat{\mu} = \mu^{(t)}(\hat{\boldsymbol{x}}_{\boldsymbol{t-1+j}}), \qquad j = 1,2 \ldots, h$$

$$\hat{\phi}_u = \phi_u^{(t)}(\hat{\boldsymbol{x}}_{\boldsymbol{t-1+j}}), \qquad j = 1,2 \ldots, h$$

Using this method, the forecasts are no longer based on parameters constrained to be linear functions of the state vector, $\boldsymbol{x_t}$.

6.2.2.3 Estimating the parameters from the smoothed surfaces

The smoothed version of SDM is very similar to the unsmoothed version of SDM, except that grid searching is performed for smoothed coefficients. A LOWESS smoothing method (Cleveland, 1979; Cleveland *et al.*, 1981) was performed and the estimates of the parameters were extracted from the smoothed surface.

6.2.3 Data

The data were collected from the Datastream platform. The motivation for choosing these eight sectors was the same as in the literature - they are major industries in the United Kingdom. Several studies have forecast industrial production using the same eight sectors (see Osborn *et al*., 1999; Heravi *et al*., 2004; Hassani *et al*., 2009; Hassani, Heravi and Zhigljavsky, 2013). This study used the same categorisation. The sectors are food products, chemicals, basic metals, fabricated metal, machinery, electrical and electronic, vehicles, and gas. These reflect a diverse range of key industries. In all cases, the sample period was from January 1992 to December 2017. To make the series stationary, annual differencing of logged series was used, which refers to annual percentage growth/decline in production.

Figure 6-1 provides a graphical representation of the original series for the eight sectors as used in this study. Some sectors, such as basic metal, and electrical and electronic, experienced a substantial decline in production over this period, while there was no noticeable trend for machinery and fabricated metals. Food products, Chemical, Vehicles, and Gas had similar characteristics, as all had upward trends. Further, all eight series had obvious structural breaks in 2008/2009 due to the global financial and banking crises.

Table 6-1 shows the summary statistics for each of the annual difference series. The most noticeable differences across the industries were for vehicles, a sector which showed an annual average growth of 1.89%, an average decline of 2.36% for electrical & electronics, and an average decline of 1.92% for basic metals in the UK over the period. Seasonal R^2 were also computed to check the degree of seasonality in the series. The study found that all the series have strong seasonality, and Food had the least explained seasonal variation.

Figure 6-1 Plot of eight UK industrial production sectors

In the following figure, time plots of the eight sectors are provided for UK Industrial Production Indices.

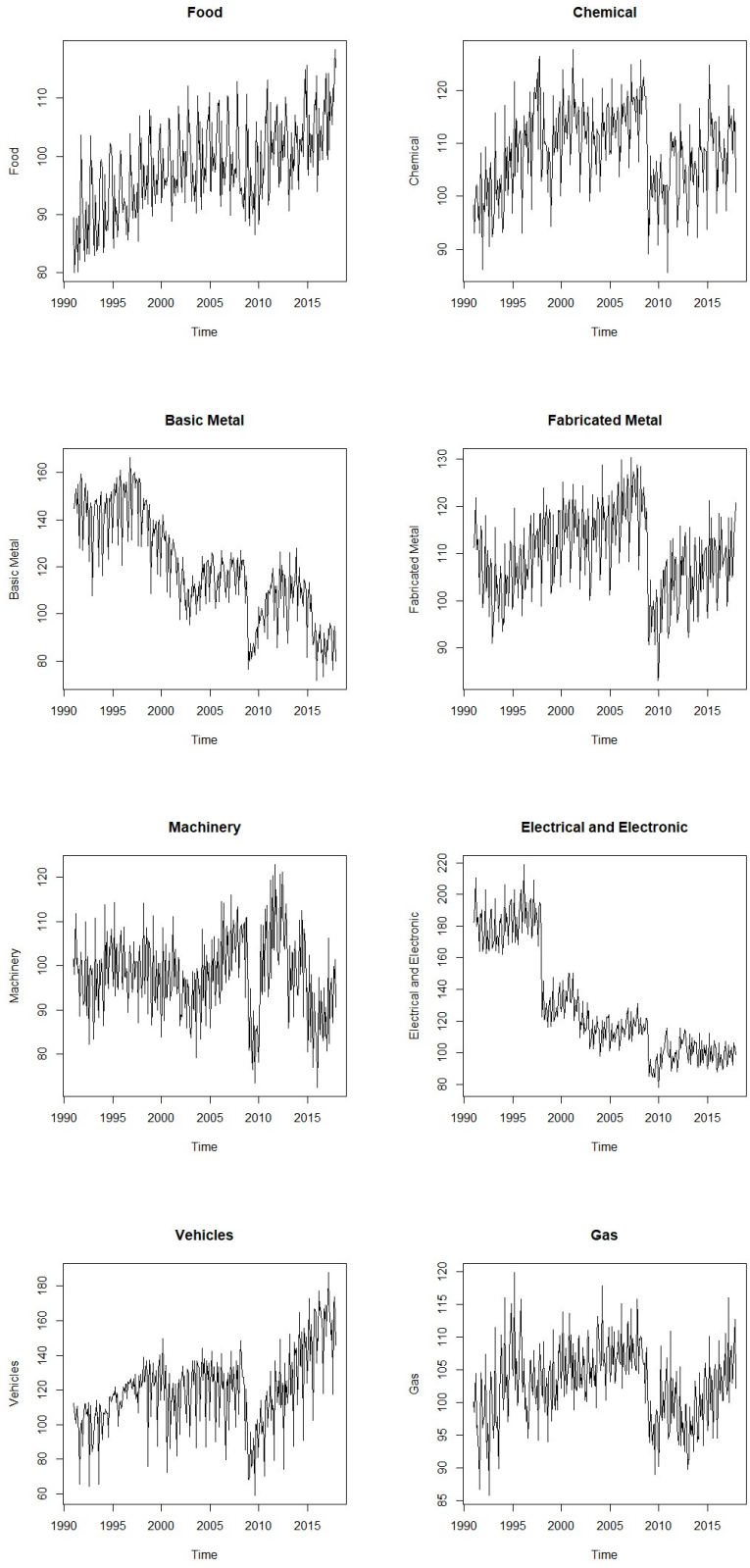

Table 6-1 Descriptive statistics for the eight series

The following table provides summary statistics of the eight industrial production indices after taking natural logs of 12-months differencing. Seasonal R^2 was computed to check the extent to which seasonal variations were explained by the models. This was done by running a regression of the dependent variable against 11 seasonal dummy variables.

Series	Mean	Standard Deviation	Seasonal R^2
Food Products	0.82	3.84	0.5882
Chemical	0.49	5.50	0.7847
Basic Metal	-1.92	9.78	0.7868
Fabricated Metal	-0.02	5.83	0.8149
Machinery	-0.28	8.87	0.7280
Electrical & Electronic	-2.36	10.7	0.7897
Vehicles	1.89	13.0	0.7686
Gas	0.338	4.08	0.6624

Table 6-2 Correlation matrix for eight UK industrial production sectors

The table below presents the Pearson (upper diagonal) and Spearman rank (lower diagonal) correlation matrix for all eight industrial production sectors for the UK.

	Food	Chemical	Basic Metal	Fabricated Metal	Machinery	Electricals	Vehicle	Gas
Food	1.000	0.191	0.127	0.299	0.503	0.030	0.203	0.548
Chemical	0.223	1.000	0.578	0.476	0.355	0.504	0.454	0.510
Basic Metal	0.121	0.400	1.000	0.568	0.601	0.494	0.557	0.407
Fabricated Metal	0.285	0.235	0.368	1.000	0.640	0.435	0.558	0.597
Machinery	0.489	0.267	0.479	0.467	1.000	0.410	0.416	0.626
Electricals	0.042	0.280	0.397	0.348	0.377	1.000	0.292	0.357
Vehicle	0.167	0.146	0.297	0.278	0.220	0.055	1.000	0.499
Gas	0.538	0.364	0.237	0.397	0.546	0.288	0.313	1.000

The table shows that the correlation between every pair of annual percentage growth series has positive signs. The correlation coefficients range from 0.030 to 0.640. In other words, the sectors generally grow and decline together in the same direction.

6.2.4 Analysis of the forecasting results

Turning now to consider the main interest of the study, the evaluation of forecasting performance, the optimised ***auto.arima, ets, nnetar*** functions in the ***forecast*** package in R (Hyndman and Khandakar (2008)) were employed to produce forecasts for ARIMA, Error Trend Seasonality, and Neural Network models. Post-sample forecast root mean square error (RMSE) was used here to measure performance. Annual percentage growth/decline were forecasted using different models. The performance of one-, three-, six- and twelve-

months ahead forecasts were also computed, compared, and reported. In order to examine the forecast accuracy between models, the data window was split into training and out-of-sample validation data. The initial in-sample window spanned from January 1992 to December 2009, with post-sample validation up to December 2017. This set the out-of-sample window as 96 for one-step ahead forecasts, 94 for three-steps ahead forecasts, 91 for six-steps ahead forecasts, and 85 twelve-steps ahead out-of-sample forecasts. To compare forecast accuracy between models, the Relative Root Mean Squared Error (RRMSE) was calculated for each forecasting model, given by:

$$RRMSE = \frac{RMSE\ of\ a\ model}{RMSE\ of\ ARIMA}$$

With ARIMA as the benchmark. Therefore, if the RRMSE was below 1.00, then there was an improvement in forecasting performance relative to the ARIMA models. If the RRMSE was above one, then the model had produced poorer forecasts compared to the ARIMA models. The smaller the RRMSE, the more superior the model was compared to the forecast performance of the ARIMA model. The overall scores for the number of times each model outperformed the ARIMA benchmarks in terms of post sample RMSE were also recorded.

Table 6-3 RRMSE for one-month ahead forecasts relative to ARIMA forecasts

Each column in the table below represents a one-step ahead forecast RRMSE of models, taking the ARIMA forecasts as the benchmark model. Modified Diebold-Mariano tests were carried out to test for equality of errors against the errors from an ARIMA model. Average RRMSE is reported, recording the number of times a model beat the ARIMA forecasts out of eight. * and ** represent 10% and 5% significance levels.

Variable	1-month ahead				
	ETS	NNetar	SDM Ordinary	SDM Unsmoothed	SDM Smoothed
Food Products	1.15	0.82**	0.96	0.96	0.96
Chemicals	0.98	1.14	0.97	1.08	1.06
Basic metals	1.02	1.08	1.06	1.06	1.06
Fabricated metal	0.99	0.95	0.98*	0.97	0.97*
Machinery	0.99	1.02	1.09	1.10	1.09
Electrical and Electronic	1.04	1.09	1.00	1.01	1.00
Vehicles	0.99	1.05	0.93*	0.95	0.95
Gas	1.02	0.92	0.97	0.98	0.98
Summary					
Average RRMSE	1.02	1.01	0.99	1.01	1.01
Score	4	3	5	4	4

Table 6-4 RRMSE for three-months ahead forecasts relative to ARIMA forecasts

Each column in the table below represents a three-step ahead forecast RRMSE of models, taking the ARIMA forecasts as the benchmark model. Modified Diebold-Mariano tests were carried out to test for equality of errors against the errors from an ARIMA model. Average RRMSE is reported, recording the number of times a model beat the ARIMA forecasts out of eight. * and ** represent 10% and 5% significance levels.

Variable	3-months ahead				
	ETS	NNetar	SDM Ordinary	SDM Unsmoothed	SDM Smoothed
Food Products	1.22	0.93	1.01	1.01	1.00
Chemicals	1.11	1.22	0.99	0.99	0.98
Basic metals	1.06	1.30	1.03	1.14	1.13
Fabricated metal	1.06	1.02	0.95*	0.94	0.92
Machinery	1.03	1.19	1.08	1.05	1.05
Electrical and Electronic	1.08	1.04	0.97	0.98	0.97
Vehicles	0.92	0.99	0.80**	0.77**	0.78**
Gas	0.99	0.90	0.93	0.93	0.92
Summary					
Average RRMSE	1.06	1.07	0.97	0.97	0.97
Score	2	3	5	5	5

Table 6-5 RRMSE for six-months ahead forecasts relative to ARIMA forecasts

Each column in the table below represents a six-step ahead forecast RRMSE of models, taking the ARIMA forecasts as the benchmark model. Modified Diebold-Mariano tests were carried out to test for equality of errors against the errors from an ARIMA model. Average RRMSE was reported, recording the number of times a model beat the ARIMA forecasts out of eight. * and ** represent 10% and 5% significance levels.

Variable	6-months ahead				
	ETS	NNetar	SDM Ordinary	SDM Unsmoothed	SDM Smoothed
Food Products	1.16	0.84**	0.97	0.95**	0.95**
Chemicals	1.23	1.28	1.03	0.95	0.98
Basic metals	1.14	1.41	1.02	1.14	1.11
Fabricated metal	1.12	1.11	0.93	0.91	0.88
Machinery	1.13	1.20	1.04	0.94	0.97
Electrical and Electronic	1.16	1.01	0.95	0.91	0.94
Vehicles	0.86*	1.40	0.65**	0.68**	0.68**
Gas	0.99	0.92	0.90	0.88	0.88
Summary					
Average RRMSE	1.10	1.15	0.94	0.92	0.92
Score	2	2	5	7	7

Table 6-6 RRMSE of twelve-months ahead forecasts relative to ARIMA forecasts

Each column in the table below represents a twelve-step ahead forecast RRMSE of models, taking the ARIMA forecasts as the benchmark model. Modified Diebold-Mariano tests were carried out to test for equality of errors against the errors from an ARIMA model. Average RRMSE is reported, recording the number of times a model beat the ARIMA forecasts out of eight. * and ** represent 10% and 5% significance levels.

Variable	12-months ahead				
	ETS	NNetar	SDM Ordinary	SDM Unsmoothed	SDM Smoothed
Food Products	1.22	0.93	0.97	0.91*	0.92*
Chemicals	1.33	0.90*	0.99	0.92	0.93
Basic metals	1.31	1.45	0.99	1.01	1.00
Fabricated metal	1.18	1.14	0.84	0.78	0.76
Machinery	1.76	1.33	1.06	0.91	0.90
Electrical and Electronic	1.43	1.58	0.94	0.83*	0.89
Vehicles	0.99	2.17	0.66**	0.64**	0.64**
Gas	1.13	0.95	0.77*	0.74	0.73*
Summary					
Average RRMSE	1.29	1.31	0.90	0.84	0.85
Score	1	3	7	7	7

Table 6-3 through to Table 6-6 present the post-sample results. They show that the three versions of the SDM model performed reasonably well for one-, three-, six- and twelve-months ahead forecasts. While the average performance of the three SDM methods for forecasting one month ahead, as reflected by the average RRMSEs, were roughly the same as the average for the ARIMA, ETS, and Neural network models, the superiority of the SDM forecasts revealed itself as the time horizon increased. Compared with the benchmark model (ARIMA), there was an approximate 3% reduction in RMSE by SDM for the three months ahead forecasts, an approximate 7% reduction for six months ahead, forecasts, and the improvement became about 14% for the twelve months ahead forecasts. The improvements of the SDM forecasting approaches over the other two methods were much more pronounced, with up to around 71% reduction in RMSE for 12-

steps ahead forecasts over the Neural network and 50% reduction in RMSE for the twelve months ahead forecasts compared to ETS.

There was not much difference in forecasting performance between the two procedures proposed in Section 6.2.2 except that for the 6- and 12-steps ahead forecasting, the two new methods seemed to perform substantially better than the SDM. The smoothed and unsmoothed SDM forecasting procedures outperformed the ARIMA, ETS and Neural network in the majority of cases. The high performance of the SDM models was particularly pronounced over the long run, in that the longer the forecast horizon, the higher the score by which the SDM models beat the ARIMA. For example, both the smoothed and unsmoothed SDM forecasting methods outperformed the benchmark ARIMA models seven times out of eight for the six- and twelve- months ahead forecasts. In comparing the three SDM forecasting methods, while the three methods produced similar results in short term forecasting, the results indicated the superiority of the two proposed forecasting methods for longer horizons over the classical recursive SDM forecasting approach.

The ETS and Neural Network (NNetar) models performed very poorly compared to the ARIMA and SDM models in terms of forecasting performance. Across all the time horizons, the scores were less than or equal to four. The ETS and NNetar models performed better in the short-run, and the NNetar scores at different horizons were at least equally as good as the ETS models.

6.3 Forecasting Tourist Arrivals for Japan

In this section, inbound Japanese tourist arrivals are the units of analysis. This research aimed to employ different models such as the three variants of state-dependent models and compare them with the forecast performance of the automatic ARIMA, automatic ETS, and artificial neural network models. The objective of doing so was to establish if the SDM models were better at forecasting disaggregated tourist arrivals to Japan.

6.3.1 Introduction

6.3.1.1 The need for tourism demand forecasting

Tourism demand forecasting has attracted attention from academics seeking to improve forecasting methodologies as a way of boosting forecasting tourist arrivals to various regions (Hassani *et al*., 2015). It has also been a hot topic among politicians, as tourist arrivals generate large revenues for governments. The revenue generated from tourism can create employment and be deployed to stimulate the economy and build infrastructure, among other things (Álvarez-Díaz and Rosselló-Nadal, 2010).

Accurate tourist demand forecasting is important for several reasons. Firstly, tourism-related products and services are perishable in nature. Their consumption cannot be delayed to future dates (Archer, 1987). Inaccurate predictions of trends, directions, and numbers in terms of tourist demand can therefore bring huge financial costs to businesses. Traditionally, the tourism sector is vulnerable to strong seasonality (Hassani *et al.*, 2015). Good forecasts therefore help different users of information to anticipate tourist inflows and outflows, enabling them to develop better strategies to prepare for and deal with the strong seasonal patterns. Good forecasts also facilitate a good allocation of revenue, direct supplier activities in the sector, and help policy makers to estimate the

sector's profitability (Armstrong, 1972; Álvarez-Díaz and Rosselló-Nadal, 2010). Furthermore, tourism forecasts can inform government decisions on whether or not to intervene and deploy funds during downturns.

6.3.1.2 Japanese tourism

The Japanese tourism industry had not received much attention from the government until recently. The country's tourism industry has been adversely affected by prolonged deflation and recession since 1991, the global credit crunch, the US subprime crisis, and the European debt crisis in 2007. After these crises, inbound tourist arrivals bounced back quickly and began to receive more attention from the Japanese government.

Since then, the Japanese government has acknowledged the high importance of its tourism industry to its retail sector (The Japan Times, 2015), and treated the tourism industry as the main driver of its economy (The Japan Times, 2014). Japanese people are hopeful that tourism will thrive, prosper, and boost their economy, thus spreading its benefits to rural development (The Japan Times, 2018). As was mentioned above, reliable tourism forecasts can facilitate planning, budgeting, economic development, and wealth creation. This research contributes to the evidence-base of tourism demand forecasting research.

6.3.2 Methodological literature review

In tourism demand forecasting, there is currently no universally superior model in forecasting which is applicable in all situations (Hassani *et al.*, 2015). Forecasting performance depends on data frequencies, origin-destination pairs, and length of data (Witt and Song, 2000; Li, Song and Witt, 2005), which means that further empirical

research is needed in this field to help to better understand and improve upon forecasting accuracy.

Econometric forecasting methods such as Error-correction models (ECM), vector autoregressive (VAR) models, and time-varying parameters (TVP) have all produced good forecasts (Song, Witt and Jensen, 2003; Li *et al.*, 2006; Song and Li, 2008; Vanegas, 2013; Gunter and Önder, 2015, 2016). Other econometric methods include models such as the Autoregressive Distributed Lag Model (ADLM), Almost Ideal Demand System (AIDS), structural equation models (SEM), and panel data analysis (Song and Li, 2008; Huang, Zhang and Ding, 2017).

The focus of the present research was mainly on employing time series methods and machine learning models. Time series methods (e.g. seasonal ARIMA) are claimed to perform well in predicting high-frequency data, and such data are easy to collect (Song and Li, 2008), generally from a single source. Artificial intelligence models such as Artificial Neural Network models can cope with nonlinearity and non-stationarity even when there is no specific distributions or incomplete data (Song and Li, 2008). Therefore, the neural network model was included as one of the forecasting models for comparison.

6.3.2.1 Autoregressive Integrated Moving Average Family of Models

Cho (2001) compared univariate ARIMA, modified ARIMA, and exponential smoothing in forecasting Hong Kong tourism demand, and found that the ARIMA models provided the best forecast performance. Goh & Law (2002) reported the superb forecast performance of the multivariate ARIMA (MARIMA) model. They observed that SARIMA beat eight other models, and that the univariate ARIMA model beat the average

performance of all other models. Chen *et al*. (2009) compared Seasonal ARIMA (SARIMA) against Holt-Winters and Grey forecasting models for Taiwanese tourist arrivals and found SARIMA to be the best in terms of mean absolute percentage errors.

6.3.2.2 Exponential Smoothing (ETS) methods

Exponential smoothing (ETS) methods have performed well in numerous forecasting competitions (Bergmeir, Hyndman and Benítez, 2016). Therefore, they have also been used frequently as benchmark statistical models, and much research using them has been conducted since 2000 (Song and Li, 2008).

The simple ETS method works well for data without strong trends and seasonality. Holt's ETS has performed well for time series with a strong linear trend (Tideswell, Mules and Faulkner, 2001), and gradually changing behaviours (Yaffee & McGee, 2000). The Holt Winters ETS predicts the smoothed versions of level, trend, and seasonality of data, and produces forecasts based on these components (Lim and McAleer, 2001). Additive ETS works well for linear data, while multiplicative ETS fits better for data with exponentially growing trends.

Athanasopoulos *et al*. (2011) found that the exponential smoothing and ARIMA methods consistently outperformed seasonal Naïve methods for monthly and quarterly data, and that exponential smoothing methods outperformed seasonal Naïve methods in forecasting for the first three quarters. Athanasopoulos and de Silva (2012) forecast tourist arrivals for Australia and New Zealand, and found that a multivariate exponential smoothing model, that incorporated exponential smoothing with multivariate stochastic models,

performed better than univariate alternatives. Other studies that have shown better forecasts than exponential smoothing have included Witt *et al*. (1992) and Law (2000).

6.3.2.3 Artificial Neural Network

The Artificial Neural Network (ANN) class of models is a heuristic (Toshinori, 1998) form of model, in which the learning process resembles that of neurons in the human brain (Song and Li, 2008). ANN does not require a time series to follow any particular probability distributions, while it can produce good forecasts. It can handle missing and noisy data, non-linear functions, and arbitrary function mapping (Cho, 2003; Song and Li, 2008; Claveria and Torra, 2014). It can also produce better forecasts in continuously changing and dynamic situations (Vellido, Lisboa and Vaughan, 1999), and can forecast much better than static regressions (Burger *et al*., 2001). A potential limitation of the ANN is that the hidden layer is unobservable and operates like a "black-box" (Small and Wong, 2002). There is no universal rule in selecting inputs to the models.

In tourism demand forecasting, there is numerous evidence that ANN produce good forecasts. Yao *et al*. (2018) developed a structural neural network model to forecast tourism demand for the United States from twelve markets, and found that the Neural Network model outperformed other benchmarks for short and long horizons. Álarez-Díaz & Rosselló-Nadal (2010) forecast British tourist arrivals to the Balearic Islands through adding a meteorological explanatory variable, and found that ANN produced the best forecasts compared to the ARIMA model, a transfer function model, and an autoregressive ANN model. Burger *et al.*(2001) forecast US outbound tourist arrivals to Durban and South Africa, and also found ANN to be the best model compared to exponential smoothing and the ARIMA model. Chen and Wang (2007) found that ANN

beat the multiple regression, exponential smoothing methods, and the moving average method. Cho (2003) similarly reported that ANN was the best performing model compared to exponential smoothing models and ARIMA for inbound tourist arrivals to Hong Kong from six countries. Kon and Turner (2005) compared ANN against the Holt-Winters model and other models for Singaporean tourist demand data, and reported ANN as the best performing model. Heravi, Osborn and Birchenhall (2004) found ANN forecasts best at predicting the direction of change among a selected number of statistical models. Other empirical evidence that has supported the ANN models include studies by Law (2000), Law and Au (1999), and Pattie and Snyder (1996).

However, Claveria and Torra (2014) compared forecasting performance for tourist data among ARIMA, self-exciting threshold autoregression, and the ANN, and found that the ANN performed significantly worse for France, the United Kingdom, Belgium and the Netherlands, Italy, Switzerland, etc. for shorter horizons when the root mean squared forecast error (RMSFE) measure was used. On the other hand, Teräsvirta, van Dijk and Medeiros (2005) claimed that Neural Network AR models did not offer a substantial gain compared to linear autoregressive models.

6.3.2.4 Singular Spectrum Analysis

Hassani *et al*. (2015) employed Singular Spectrum Analysis to forecast monthly tourist arrivals into the United States for a period between 1996 and 2012, and compared forecasting performance together with ARIMA, exponential smoothing, and neural networks, and found that the SSA performed best in forecasting performance. Silva *et al*. (2017) introduced a multivariate Singular Spectrum analysis and applied different variations of SSA models to European tourism demand forecasting for ten European nations. They found that in the univariate forecasting, SSA-Recurrent performed better

than SSA-Vector across all countries, regardless of short- or long-term horizons. Moreover, they found that in the multivariate forecasting, Horizontal MSSA-Vector performed better than Horizontal MSSA-Recurrent. They concluded that automated multivariate SSA beat its univariate counterparts with RMSE and Direction of Change criteria. Silva *et al*. (2019) forecast European tourism demand using the original SSA and SSA denoised neural network, and found that denoising greatly improved the forecasts.

6.3.2.5 Ensemble Empirical Mode Decomposition

Empirical mode decomposition (EMD) is an adaptive data driven method which separates non-stationary signals from non-linear systems in different oscillations (Colominas, Schlotthauer and Torres, 2014). One of the advantages of Ensemble EMD is that it makes use of the statistical properties of white noise, and cancels itself out after being used (Wu and Huang, 2009). Yahya, Samsudin and Shabri (2017) employed a hybrid model comprising empirical mode decomposition (EMD) and Group Method of Data Handling (GMDH) to data on tourist arrivals from China, Thailand and India to Malaysia from 2000 to 2016, and reported that the hybrid model produced better forecasts than two benchmark models. Wei and Chen (2012) employed a hybrid of EMD-Back Propagation Neural Networks to predict short term metro passenger flow. They found that the hybrid model worked well.

6.3.3 Data

It is unusual to find forecasting research for disaggregated tourist arrivals to a single destination, as few organisations provide readily accessible data on disaggregated tourist arrivals. Thanks are therefore due to the Japan Tourist Board Research & Consulting Co. website for making such disaggregated data available. This study attempted to forecast continent-specific time series - Asian, European, and North American. For each

continent, tourist arrivals for tourism and business and other purposes were explored. This study also forecast the Grand Total. The data ranged from January 1996 to December 2018. The data were split into test and validation data. Using a similar approach to Heravi, Osborn and Birchenhall (2004), Hassani, Heravi and Zhigljavsky (2009), and Hassani *et al.* (2013), the present study left 96, 94, 91, and 85 data out-of-sample for 1-, 3-, 6-, 12-steps ahead forecasts. Using data in the form of annual percentage growth, to make the series stationary, the training data window was set at 168 data points (14 years) and 96 data points (8 years) as validation data. Therefore, data from January 1997 to December 2010 were used as an initial window, then the window was expanded by 1 data point at a time to produce 1-, 3-, 6-, and 12-steps ahead forecasts recursively until the end of the validation (out-of-sample) period.

6.3.4 Descriptive statistics

Figure 6-2 Plot of tourist arrivals for different purposes

In the following figure, time plots of the inbound tourist arrivals for tourism, business, and other purposes for Asia, Europe, North America, and a Grand Total are shown.

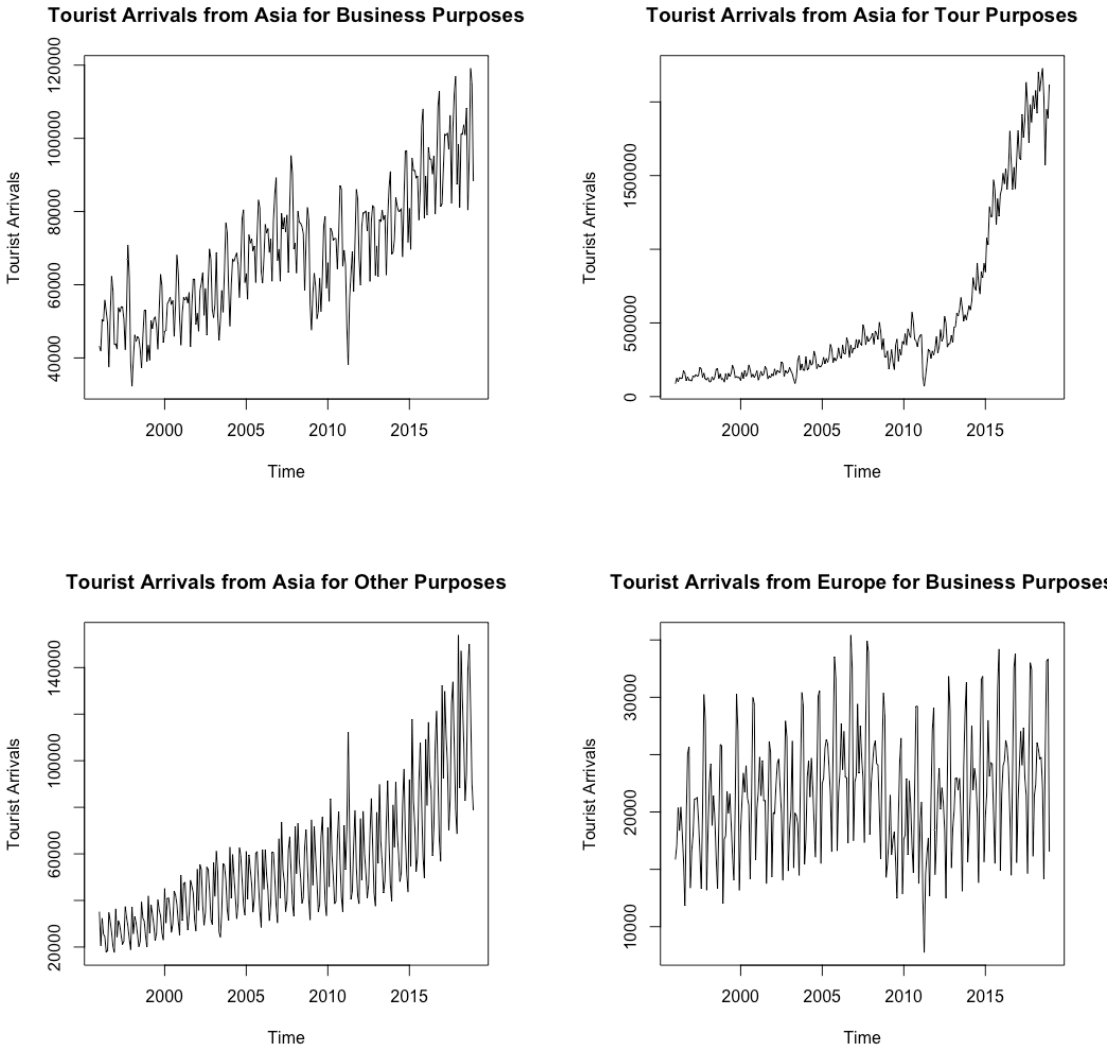

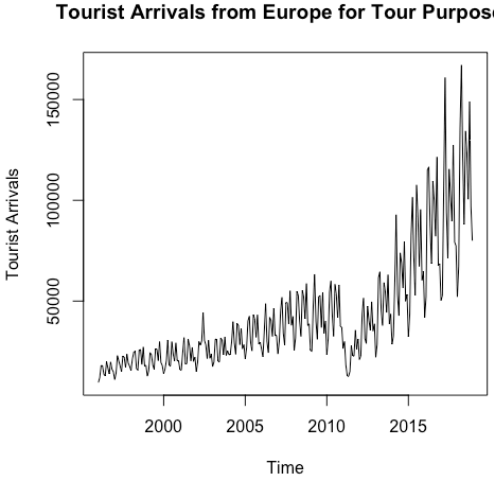
Tourist Arrivals from Europe for Tour Purposes
Tourist Arrivals
50000
100000
150000
2000
2005
2010
2015
Time

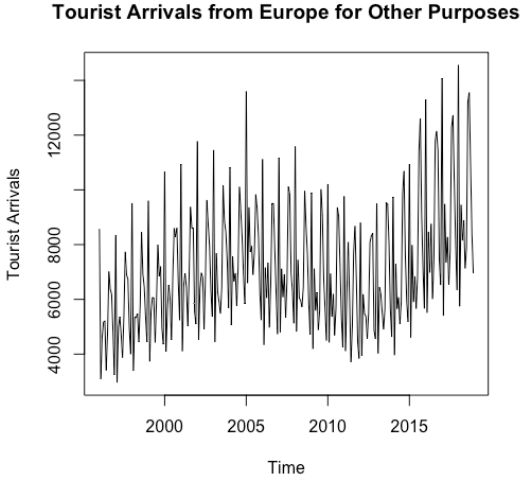
Tourist Arrivals from Europe for Other Purposes
Tourist Arrivals
4000
6000
8000
12000
2000
2005
2010
2015
Time

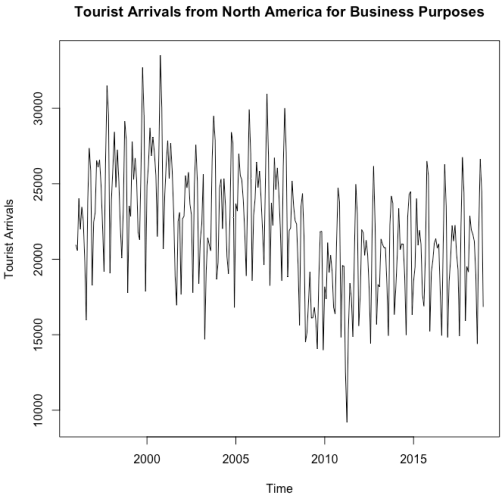
Tourist Arrivals from North America for Business Purposes
Tourist Arrivals
10000
15000
20000
25000
30000
2000
2005
2010
2015
Time

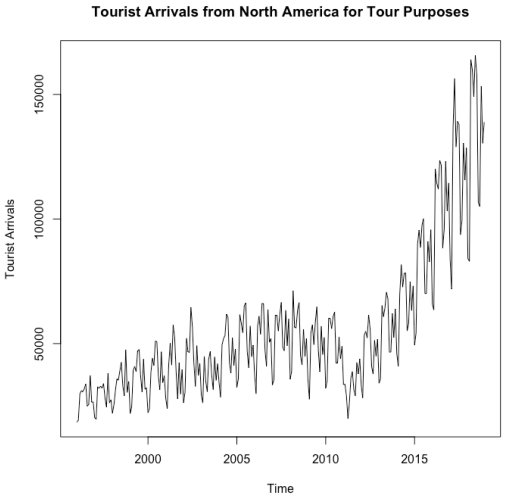
Tourist Arrivals from North America for Tour Purposes
Tourist Arrivals
50000
100000
150000
2000
2005
2010
2015
Time

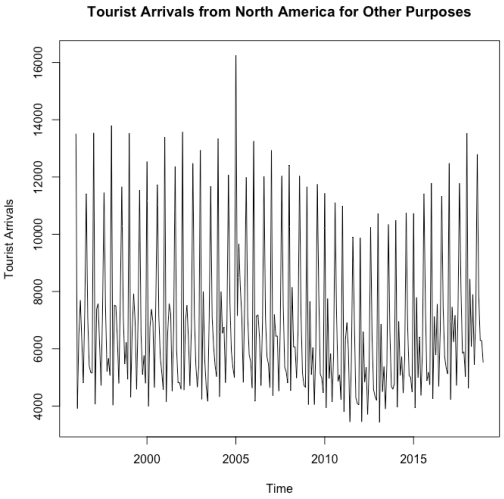
Tourist Arrivals from North America for Other Purposes
Tourist Arrivals
4000
6000
8000
10000
12000
14000
16000
2000
2005
2010
2015
Time

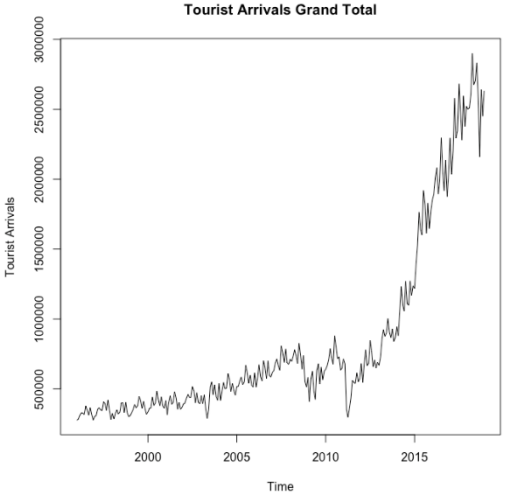
Tourist Arrivals Grand Total
Tourist Arrivals
500000
1000000
1500000
2000000
2500000
3000000
2000
2005
2010
2015
Time

Almost all Asian tourist arrivals for tourism purposes showed an increasing trend. Dominant seasonality was also evident in all series, except tourism from Asia.

Table 6-7 Summary statistics of yearly logarithmic growth of tourist arrivals

The following table provides summary statistics of the ten tourist arrival series after taking natural logs of 12-months differencing. Seasonal R^2 was computed to check the extent to which seasonal variations were explained by the models. This was done by running a regression of the dependent variable against 11 seasonal dummy variables.

Category	Mean	Standard deviation	Seasonal R^2
Asia Tourist	12.72	32.69	0.4791
Asia Business	3.158	14.07	0.7317
Asia Others	6.893	10.40	0.9237
North America Tourist	7.054	19.55	0.8546
North America Business	-0.277	14.30	0.8114
North America Others	0.439	10.31	0.9601
Europe Tourist	8.760	26.56	0.8108
Europe Business	1.201	14.92	0.8964
Europe Others	0.497	39.460	0.9463
Grand Total	9.534	20.857	0.577

The seasonal R^2 in the table was computed by regressing log first differences as the dependent variable, against eleven seasonal dummies. The Seasonal R^2 reported in Table 6-7 showed that for all series, the values ranged from 47.9% to as high as 94.6%. In terms of annual growth rates, tourism evidently increased far more than business purposes and others, and the Asian tourist component had the highest growth. The European Others component had the highest standard deviation amongst all regions, followed by Asian tourism and the Grand Total.

Table 6-8 Correlation matrix for different components of tourist arrivals

In the table below, the Pearson (upper diagonal) and Spearman rank (lower diagonal) correlation matrix are presented for all ten tourist arrivals time series for Japan.

	Asia Tourist	Asia Business	Asia Others	North America Tourist	North America Business	North America Others	Europe Tourist	Europe Business	Europe Others	Grand Total
Asia Tourist	1	0.657	-0.114	0.812	0.635	0.136	0.759	0.674	-0.003	0.976
Asia Business	0.362	1	-0.006	0.494	0.776	0.055	0.448	0.785	0.01	0.679
Asia Others	0.107	0.248	1	-0.068	-0.113	0.446	-0.13	-0.122	0.038	0.006
North America Tourist	0.608	0.132	0.235	1	0.544	0.243	0.861	0.591	-0.006	0.84
North America Business	0.311	0.632	0.119	0.113	1	0.143	0.483	0.894	-0.006	0.638
North America Others	0.25	0.091	0.353	0.423	0.149	1	0.123	0.1	0.026	0.219
Europe Tourist	0.613	0.093	0.152	0.714	0.17	0.304	1	0.584	0.005	0.786
Europe Business	0.31	0.628	0.183	0.133	0.806	0.158	0.211	1	0.006	0.682
Europe Others	0.004	0.026	0.012	-0.015	-0.002	0.003	0.035	0.025	1	0.006
Grand Total	0.966	0.421	0.236	0.687	0.342	0.313	0.669	0.350	0.010	1

Table 6-8 shows the Pearson (upper diagonal) and Spearman's rank (lower diagonal) correlation matrix for the different components of annual growth of tourist arrivals. From the signs in the correlation matrix, it appears that most of the series were positively correlated with one another. The negative correlations were generally weak. The Asian Tourist component was highly correlated (ρ = 0.976) with the Grand Total. Therefore,

most of the growth rates of the Grand Total came from the growth in the Asian tourist component.

6.3.5 Forecasting results

Table 6-9 to Table 6-12 present the forecasting results. Again, the ARIMA method was taken as the benchmark. The data were divided into test and validation data. Using the data in the form of annual growth, to make the series stationary, the forecasting performance was tested, setting the training window as 168 data points (14 years) and 96 data points (8 years) as validation data. Therefore, data for after December 2010 were used as validation data. Using a similar approach to Heravi, Osborn and Birchenhall (2004), Hassani, Heravi and Zhigljavsky (2009), and Hassani *et al*. (2013), this study left 96, 94, 91, and 85 data out-of-sample for 1-, 3-, 6-, 12-steps ahead forecasts.

Table 6-9 RRMSE of one-month ahead tourist arrival forecasts relative to ARIMA forecasts

Each column in the table below presents a one-step ahead forecast RRMSE of models, taking ARIMA forecasts as the benchmark model. Modified Diebold-Mariano tests were carried out to test for equality of errors against the errors from an ARIMA model. Average RRMSE is reported, scoring the number of times a model beat the ARIMA forecasts out of ten. * and ** represent 10% and 5% significance levels.

Variable	1-month ahead				
	ETS	NNetar	SDM Ordinary	SDM Unsmoothed	SDM Smoothed
Asia					
Business	1.073	0.87	0.984**	0.976**	0.967**
Tourism	1.063	1.396	0.995	1.014	1.004
Others	1.002	1.078	0.999	1.004	1.002
Europe					
Business	1.041	1.068	0.975*	0.972**	0.978**
Tourism	1.092	1.166	1.003	1.146	1.03
Others	1.219	0.310**	1.04	1.018	0.941
North America					
Business	1.125	0.976	0.971**	0.976**	0.969**
Tourism	1.041	1.468	0.972*	0.965*	0.963
Others	0.959*	0.963	0.944	1.018	1.02
Grand Total	1.046	1.197	0.983*	0.992	0.983*
Summary					
Average RRMSE	1.066	1.049	0.987	1.008	0.986
Score	1	4	8	5	6

Table 6-10 RRMSE of three-months ahead tourist arrival forecasts relative to ARIMA forecasts

Each column in the table below presents a three-step ahead forecast RRMSE of models, taking ARIMA forecasts as the benchmark model. Modified Diebold-Mariano tests were carried out to test for equality of errors against the errors from an ARIMA model. Average RRMSE is reported, scoring the number of times a model beat the ARIMA forecasts out of ten. * and ** represent 10% and 5% significance levels.

Variable	3-months ahead				
	ETS	NNetar	SDM Ordinary	SDM Unsmoothed	SDM Smoothed
Asia					
Business	1.184	0.914	0.976	0.958	0.954*
Tourism	1.106	2.179	0.961*	0.961	0.958
Others	1.018	1.067	0.989	0.974	0.961**
Europe					
Business	1.138	1.406	0.957	0.930*	0.936
Tourism	1.037	1.2	0.925**	0.903*	0.916*
Others	0.973	0.323**	0.99	0.975	0.931
North America					
Business	1.252	0.964	0.972	0.955	0.956
Tourism	1.023	2.686	0.908**	0.913**	0.913**
Others	0.938*	0.991	1.025	1.037	1.034
Grand Total	1.07	1.211	0.966*	0.966	0.953*
Summary					
Average RRMSE	1.074	1.294	0.967	0.957	0.951
Score	2	4	9	9	9

Table 6-11 RRMSE of six-months ahead forecast arrival forecasts relative to ARIMA forecasts

Each column in the table below presents a six-step ahead forecast RRMSE of models, taking ARIMA forecasts as the benchmark model. Modified Diebold-Mariano tests were carried out to test for equality of errors against the errors from an ARIMA model. Average RRMSE is reported, scoring the number of times a model beat the ARIMA forecasts out of ten. * and ** represent 10% and 5% significance levels.

Variable	6-months ahead				
	ETS	NNetar	SDM Ordinary	SDM Unsmoothed	SDM Smoothed
Asia					
Business	1.375	0.802	0.918	0.901*	0.898*
Tourism	1.264	2.561	0.862*	0.846*	0.846*
Others	0.993	1.106	0.979**	0.976*	0.920**
Europe					
Business	1.173	1.439	0.836	0.807	0.805
Tourism	1.056	1.154	0.761*	0.715*	0.713*
Others	1.001	0.287**	0.989	0.983*	1.007
North America					
Business	1.494	0.986	0.995*	0.978*	0.969*
Tourism	1.077	2.651	0.737**	0.710**	0.715**
Others	1	1.004	1.015	1.024	1.029
Grand Total	1.19	1.821	0.867**	0.862*	0.83
Summary					
Average RRMSE	1.162	1.381	0.896	0.88	0.873
Score	1	3	9	9	8

Table 6-12 RRMSE of twelve-months ahead tourist arrival forecasts relative to ARIMA forecasts

Each column in the table below presents a twelve-step ahead forecast RRMSE of models, taking ARIMA forecasts as the benchmark model. Modified Diebold-Mariano tests were carried out to test for equality of errors against the errors from an ARIMA model. Average RRMSE is reported, scoring the number of times a model beat the ARIMA forecasts out of ten. * and ** represent 10% and 5% significance levels.

Variable	12-months ahead				
	ETS	NNetar	SDM Ordinary	SDM Unsmoothed	SDM Smoothed
Asia					
Business	1.602	0.89	0.862	0.862*	0.861*
Tourism	1.572	3.239	0.785*	0.743*	0.750*
Others	1.015	1.029	0.930**	0.934**	0.962**
Europe					
Business	1.148	1.518	0.689	0.649	0.649
Tourism	1.192	1.253	0.575*	0.544	0.528*
Others	0.997	0.240**	0.982**	0.988	0.959**
North America					
Business	1.859	0.978	0.988*	0.971	0.966*
Tourism	1.079	2.465	0.503**	0.460**	0.461**
Others	1.106	1.264	1.031	1.000*	0.998*
Grand Total	1.409	2.341	0.728**	0.728**	0.675**
Summary					
Average RRMSE	1.298	1.522	0.807	0.788	0.781
Score	1	3	9	9	10

Modified Diebold-Mariano tests were conducted to compare forecasting errors between ETS, ANN, and three types of SDM against the forecasting errors of the benchmark ARIMA models. For the one step ahead forecasts, only in one instance did the ETS achieve a statistically significantly lower forecasting error than the ARIMA models, and for the Neural Network AR models, there was only one instance of statistically significant forecasting error measure, for the European others sector. These results show that for all ten sectors, the ETS and Neural Network AR models did not manage to outperform the ARIMA models. Except for the one-step ahead forecast, the three types of SDM models almost always outperformed the ARIMA models. For the one-step ahead forecast, it should be noted that the average RRMSE of all three SDM models and ETS and NN were very similar, against the benchmark of the ARIMA models.

Regarding the three steps ahead forecasts, there were 12 significant cases for the SDMs either at the 10% or 5% level. In terms of RMSE, the average RRMSE of ETS and Neural Network AR were worse than those of the three SDM models. The average reduction in RMSE for the three SDM models was around 4.17%, while the ETS had a 7.4% increase in RMSE, and ANN had an increase of 29.4% in RMSE compared to the ARIMA models. In terms of score, all three SDM models achieved 9/10 compared to the ARIMA models, while the ETS and Neural Network AR models only outperformed ARIMA twice and four times out of 10, respectively.

Turning to the six steps ahead forecasts, the ETS and Neural Network did not produce good forecasts. The average RRMSE of ETS was 16.2% more than that of the ARIMA, and the RMSE of the Neural Network was 38.1% more than that of the ARIMA models. The three types of SDMs produced a 11.7% lower RSME on average compared to the

ARIMA models. The number of significant forecasts by these three variants of SDM increased to 20. The statistically significant forecast errors came from all sectors except for the North American Others sector. The superiority of the new SDM models was about 2% over the traditional SDM models. The traditional SDM and unsmoothed SDM forecasts achieved scores of 9/10, and smoothed SDM forecasts achieved a score of 8/10.

For the twelve-steps ahead forecasts, the superiority of the three SDM models was clear. The average RRMSE of ETS was 29.8%, and the RRMSE of the Neural Network was 52.2% more than the ARIMA's. On the other hand, the reduction in RMSE compared to the ARIMA models of three variants of SDM ranged from 19.3% to 22.9%, with 22 significant cases at 1% or 5% compared to the ARIMA models. Surprisingly, for the European Business sector the RRMSE was around 66%, but insignificant. The scores for the three SDM models were 9, 9, and 10 out of 10 cases, respectively. It was also encouraging to note that the three variants of SDM were able to reduce forecast errors by as much as 54% compared with the ARIMA RMSEs. These results are consistent with the forecasting results for industrial production data, where the superiority of SDM models mainly came from the long-term forecasts (12 steps ahead forecasts).

When all three SDM forecasting models were compared, the SDM Lowess smoothed forecasts achieved the lowest average RRMSEs compared to the other two SDM variants for 1, 3, 6, and 12 steps ahead forecasts. Further, the unsmoothed SDM forecasts, method 2, produced better average RRMSEs than classical SDM for 3, 6, and 12 steps ahead forecasts. The findings show that both smoothed and unsmoothed forecasts can improve forecast errors compared to traditional SDM models in the long-term horizon. However,

the improvement achieved by these methods over the traditional recursive SDM method in terms of RRMSE was not substantial.

The study also sought to understand why the SDM forecasts are able to achieve such superior forecasting results compared to other three models. As in the simulation chapter, the intercept term μ can capture the dynamics of the movements in simulated data. The SDM was applied using AR(k) models on the industrial production data and the tourist arrivals data, and for all series, the time plot of μ was remarkably similar to the shape of the dependent variable (annual differenced data) and could capture sudden changes in the mean (see Appendix B). Since all these time series have successfully been modelled in-sample by SDM, this may explain why the SDM may perform out-of-sample forecasting.

6.3.6 Examples of nonlinearity and structural breaks

In the simulation chapter, we found that the SDM can capture mean shifts and structural breaks well. In This section presents the nonlinearity and breaks for two time series arrival data. As can be seen from Figure 6-3, the SDM has managed to capture nonlinearity well, and is consistent with the nonlinear ESTAR model. The SDM has also captured structural breaks for these two sectors well, around 2001and 2009. These show that the Japanese inbound tourist arrivals were significantly affected by the 9.11 terrorist attack and the aftermath of the global financial crisis, demonstrated by the structural breaks in the parameters. This also shows that the SDM parameters adjust well with breaks and capture nonlinearity as well.

Figure 6-3 Nonlinear forms and Structural Breaks for Japanese inbound tourist arrivals

The following four diagrams show nonlinear forms and structural breaks captured by the slope coefficient of the SDM model for Japanese tourist arrivals from European for tourist purposes (top two), and from North America for tourist purposes (bottom two).

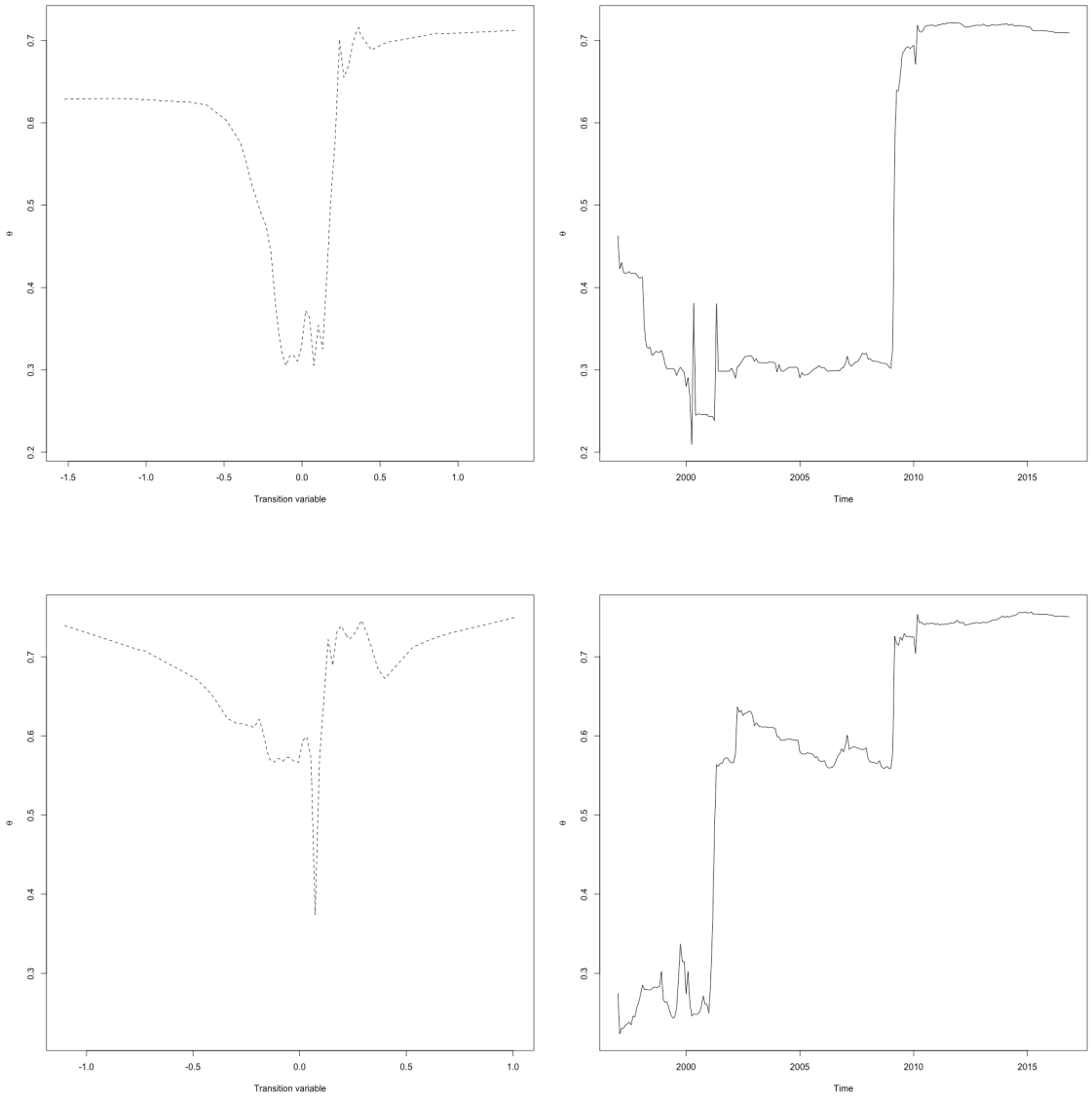

6.4 Concluding remarks

This chapter has contributed to assessing the forecasting performance of SDM using two different sets of real data. The study first attempted to extend the SDM methodology through combining it with non-parametric LOWESS smoothing methods. Three forecasting approaches were considered for the general non-linear State Dependent Models. The three SDM forecasting methods along with three other models: ARIMA, ETS, and Neural Network, were used to forecast seasonally unadjusted data on industrial production for the UK, and a Grand Total of inbound Japanese tourist arrivals and its components. The results indicated the superiority of the SDM models compared to the ARIMA benchmarks for forecasting at longer time horizons. The unsmoothed and smoothed versions of the SDMs produced similar results and generally performed better than the traditional SDM forecasting model in long-term forecasting. As the SDM can sometimes reduce forecast errors by about 50%, it is a promising method in forecasting.

This page intentionally left blank

Chapter 7 Conclusions

This thesis has focused on investigating the modelling, testing, and forecasting capabilities of the State-Dependent Model using both simulated and real data. The following paragraphs provide a summary and a general discussion. In the concluding chapter, an overview of the thesis and contributions are being laid out. The strengths, weaknesses, role of the SDM in modelling and forecasting and comparison between different models are discussed. This chapter ends with discussing the Policy implications, and with suggestions of further extensions to the SDM model.

7.1 An Overview about This Study and Contributions

This research makes several contributions to the nonlinear modelling and forecasting literature. Firstly, the theory of the SDM model was examined in details through a Monte Carlo Simulation study. Secondly, the SDM model was applied on the UK industrial production data and compared with the linear and nonlinear models. Thirdly, the SDM was extended to a case of multivariate SDM in order to test the theory of Purchasing Power Parity. Fourthly, this study proposed two new forecasting methods using the SDM algorithm and examined the forecasting performance of these two methods with the traditional recursive SDM forecasting, classical time series forecasting and a machine learning methods at short and long horizons. Finally, the thesis employed this novel method and applied it on two sets of real data, in order to forecast the UK industrial production and Japanese tourism demand.

Chapter 1 aims to provide a general introduction of the background of the linear and nonlinear time series model, which sets the theme of the state-dependent model. In this chapter, the importance of nonlinear modelling and forecasting was explained. The

chapter presented specific nonlinear models which closely linked to the State-Dependent Model (SDM), and comparisons between these models and SDM were evaluated.

In chapter 2, many of the nonlinear models which included in the SDM algorithm were presented. The methodology of the AR-SDM recursive algorithm was explained. Attempts to explain the role of SDM as a preliminary analysis in time series modelling and forecasting before fitting individual linear or nonlinear models were presented. thus SDM can be used to solve the difficulty faced by practitioners in deciding which model they should fit (Franses and Dijk, 2000) while preserving the good properties of the nonlinear models.

In the first empirical chapter, the State-Dependent Models were empirically fitted with on data generated from different linear and nonlinear models. As to the author's knowledge, only limited simulation study was done such as Haggan, Heravi and Priestley (1984), Heravi (1985) to test the theory of SDM. This study fills the gap and has carried out an extensive simulation study from various linear and nonlinear modes. The simulation study includes STAR models which are important in modelling financial and economic data. The SDM has also been implemented on linear models with shift in the level, to see if they can capture the time-varying shifts in the mean. Results show that the SDM algorithm can correctly identify the true nonlinear form and shift in the mean of the simulated data. This shows the excellent ability of the SDM in model fitting. In Chapter 6 we further found that the SDM can capture much of the characteristic of a time series. rs. More importantly, it can capture shifts in the mean, and also show different degrees of structural breaks. Overall, the results from the simulation study showed that SDM method

can be used in practice as an exploratory analysis to identify the correct linearity / nonlinearity in the real data.

The second application of the SDM was in modelling nonlinearity in the business cycle indicators. This study found that most of the industrial production data exhibited some form of nonlinearity, with a few exceptions. The SDM results are , in general, in line with the previous literature in this field which has argued that business cycles are nonlinear. However, regarding the question if business cycle is symmetric or asymmetric, the present study showed mixed results. In general, except Food and Electricals sectors, all other sectors exhibit strong nonlinearity. The date of the structural breaks pointed out by the SDM models occurs at terrorist attacks, wars, and financial crises.

In Chapter 4, the SDM model then extended and was applied in a multivariate sense to test the theory of Purchasing Power Parity. The theory of SDM was extended to develop a multivariate SDM model and the coefficients updated as a function of an exogenous variable such as a global uncertainty index. The results were compared with different linear and nonlinear methods such as Bai & Perron structural break tests, linearity tests, and unit root tests against ESTAR alternatives. It was found that mean reversions for GBP/USD, JPY/USD are happening all the time, while for GBP/USD, JPY/USD and EUR/USD there is evidence supporting ESTAR characteristics. These real exchange rates also became more mean reverting with higher levels of global uncertainty, and uncertainty cause an instantaneous shock in real exchange rates before mean reversions occur. Reasons for increasing mean reversion in higher uncertainty were probably due to transactions costs, heterogeneous beliefs in trading and government intervention. This provides some evidence that real exchange rates should behave as self-correcting mean-

reverting mechanisms. The results indicated high volatility in real exchange rates during high uncertainty. Trading opportunities, therefore, exist during uncertain events.

In the last empirical Chapter, the forecasting performance of the SDM model was assessed. Two new extensions of the SDM model were proposed, then the three variants of SDM forecasting algorithm were applied to forecast industrial production indices and inbound Japanese tourist arrivals. The results were compared with classical ARIMA, ETS, and the machine learning Neural Network Autoregressive models. The three SDM forecasting methods were demonstrated to perform at least as well as the three other models in short horizons, with increasingly superior forecasts at longer horizons. In fact, the two new developed grid-searching methods provided more accurate forecasts than the traditional recursive SDM. To the best of my knowledge, this is one of the first study that attempted to evaluate the forecasting performance of the SDM method in short- and long-term horizons for Economics and Business data.

This thesis has clearly demonstrated that SDM to be a viable and reliable tool in model-fitting, identification of structural breaks, and forecasting in the contexts of business, economics, and financial data. The last section of this concluding chapter will explain some of the possible extensions to the SDM model in finance, business and economics.

7.2 Strengths and role of The State-Dependent Model

The SDM is a general model, which can give us an overview of the (non)linear forms in a time series process. It contains the functional forms of many of the nonlinear models such as the exponential time series, threshold autoregressive, non-linear threshold autoregressive, logistic smooth transition autoregressive (LSTAR), exponential smooth transition autoregressive (ESTAR), bilinear models as special cases. SDM is flexible and

require no prior presumptions about the nonlinear form. The SDM can handle multiple structural breaks, multiple regimes and show relative magnitudes of structural breaks as demonstrated in Chapter 4 in this thesis. The algorithm behind it – the extended Kalman Filtering provides optimal parameter estimates, requires little computer time and storage and has a good model fitting ability, as demonstrated in the simulated study section of the thesis. In Chapter 6, the results indicated that superiority of the three different versions of SDM over other methods in forecasting long horizons.

Lumsdaine and Papell (1997) claimed that allowing for only one structural break may not be the best characterisation of macroeconomic time series. Therefore, STAR, TVAR, linear and nonlinear TAR models and many other nonlinear models suffer from this problem. As discussed in Chapter 4, robust structural break tests such as in Harvey, Leybourne and Taylor (2009), Sobreira and Nunes (2016) require the number of breaks, m, or break fractions to be known (Sobreira and Nunes, 2016). Most of these models suffer from nonmonotonic power functions when the number of breaks is large or with serially correlated errors (Kejriwal and Perron, 2010). The SDM does not need to assume the presence of structural breaks. There is no a priori assumptions that need to be made in this model. The relative magnitudes between the structural breaks can be assessed using SDM.

Deciding on a nonlinear form for data is a complicated process. Through implementing the SDM, we can answer the question of which nonlinear model is the best model to fit, or if a linear model is equally satisfactory, without committing to an individual model.

The empirical evidence in chapter 6 indicated the superiority in forecasting accuracy of SDM over other classical forecasting and machine learning methods. Therefore, in

forecasting financial, business and economic time series data, we do not need to fit a specific model, and SDM can be employed directly as a reliable forecasting method.

7.3 Potential Issues and Limitations of the SDM Approach

SDM model is general and used as a preliminary analysis to estimate the functional form of parameters before any model fitting. If the nonlinear surface gives a strong indication of the specific form of (non)linearity, we will fit that family of the model with efficient parameter estimation procedures (Priestley, 1980). This is a minor limitation of SDM.

The model fitting and forecasting performance of SDM requires to set a smoothing parameter. Based on experimenting with different values of the smoothing parameters, this should ideally be between 0.0001 to 0.01. Too large a value of alpha will make estimated values of coefficients explode, and too small value will make it difficult to detect nonlinearity (Haggan, Heravi and Priestley, 1984). However, as long as the value of the smoothing parameter is selected between 0.0001 and 0.01, the results do not differ significantly.

Graphical interpretations are needed in deciding which specific models should be chosen to model time series processes. There may be cases that the nonlinear functional form estimated by SDM is not a clear-cut decision and making it difficult to decide which model is more appropriate to fit.

To identify significant structural breaks is judgemental, as SDM has no formal test to determine the time of the breaks. This is a limitation of exploratory data analysis. However, the structural breaks identified by the SDM, in general, were in agreement with the structural breaks identified by STAR models, TVAR models and Bai & Perron

structural break tests. Therefore, the interpretation of structural breaks from a time plot of the SDM coefficient can be judged together with application of other models.

Machine learning and nonparametric methods such as Neural networks and Singular Spectrum Analysis have the advantage that can be applied directly on nonstationary and seasonal data. SDM, similar to other classical time series methods, should be applied on stationary and seasonally adjusted data. Therefore, we need to remove seasonality and work with annual change rather than the level of time series. After removing the seasonality, forecasts of growths /declines will be computed instead of the level in the time series. However, this does not create any problem and without loss of information we can rebuild the original seasonally unadjusted forecasts.

7.4 Policy Implications

Business cycle forecasting is an important area of research and has attracted a great deal of interest in the world. Modelling production data for different sectors help to find the lead/lag relations between different industries. Industries can organise and adjust their production strategies better. Forecasting productions for different industrial sectors also helps the government, policy and decision-makers in the UK. The business cycle modelling chapter has offered evidence that industrial productions for different sectors are dynamic and nonlinear. Therefore, to obtain more accurate forecasts, practitioners should try the nonlinear forecasting methods.

The results of testing mean reversion properties of PPP, offers fresh insights to the governments. For example, the results in Chapter 4 indicated mean reversion of real exchange rates for Pound, Yen and Euro, while a random walk behaviour for the

Brazilian Real. In further analysis of the relationship between mean reversion against uncertainty indices, we found evidence of a faster adjustment and mean-reversion associated with high uncertainty. The timing of the structural break estimated by the SDM shows shocks took place during high uncertainty.

Forecasting Japanese tourism study will help business and tourism policymakers to develop better and more informed tourism marketing strategies. This would benefit the businesses, local community, and eventually the Japanese economy, especially after the Covid-19 pandemic, based on the data available. The results in Chapter 6 showed that the SDM can forecast better than many of the alternative time series forecasting models. Thus SDM is a promising forecasting technique , especially for long horizons, and helps the professional forecasters, academics and the government in computing more accurate forecast. Based on the forecasting results for UK industrial productions, the UK government can make sound and effective economic policies to maintain the desired level of productions. Finally, at an aggregated and disaggregated level based on the purpose of travel, forecasts for Japanese tourism demand were provided in this Chapter, and this can be useful for stakeholders for the creation of better tailored policies for Japanese tourism.

7.5 Future Research & Further Extensions to SDM

The State Dependent Model can be extended theoretically as follows:

1. In this study, a constant smoothing parameter was used for all time periods. However, a time varying smoothing parameter may be used so that outliers can be dealt more effectively.

2. Adopt a time-varying σ_ϵ^2 and update it together with the SDM algorithm. This method adds a heteroscedastic variance into the model.

3. Extend the graphical presentation of the parameters from line graphs into surfaces with higher dimensions.
4. Include a grid search algorithm to find the best value of the smoothing coefficient, based on minimising the forecast errors. This can provide optimal forecasts at different horizons.
5. Assess the SDM forecasting performance by comparing it with more nonlinear models such as STAR modes.
6. Extend the Granger causality test into a general SDM causality test.
7. SDM can also be implemented in a Vector Autoregressive (VAR) model as a further extension.

In addition, in terms of further applications in the area of finance and economics, the SDM can be used in the Capital Asset Pricing Model to estimate the specific behaviour of the risk loading beta. Interest rate parity conditions can also be tested through the SDM algorithm. Kostakis et al. (2015) have recently developed a model that allow for highly persistent regressors for long horizon forecatsing. It is interestig to compare the long term forecatsing of the SDM with this model. Furthermore, highly persistent regressors can be included into the SDM model as a further extension and assess its forecasting performance.

In the end, I hope this research sparks more interest by academics and practitioners to consider applying and developing the State Dependent Models further, especially in the area of Economics, Finance and Business.

This page intentionally left blank

Appendix

Appendix A

Appendix Table A.1 Definition of the eight sectors of industrial production for the United Kingdom, France, and Germany

Gas	Electricity, gas, steam, and air conditioning supply
Chemical	Manufacture of chemicals and chemical productions
Fabricated metal	Manufacture of fabricated metal products, excluding machinery & equipment
Motor vehicles	Manufacture of motor vehicles, trailers, and semi-trailers
Food	Manufacture of food products
Basic metals	Manufacture of basic metals
Electrical & electronic	Manufacture of electrical equipment
Machinery	Manufacture of machinery and equipment

Appendix B

The following 36 pairs of diagrams show the SDM estimated μ against time, and time plot of annual differenced series for the data used in **Chapter 6**:

- Industrial production: “Food”, “Chemical”, “Basic Metal”, “Fabricated Metal”, “Machinery”, “Electricals”, “Vehicles”, “Gas”.
- Japanese tourist arrivals: “Asia Tourist”, “Asia Business”, “Asia Others”, “Europe Tourist”, “Europe Business”, “Europe Others”, “North America Tourist”, “North America Business”, “North America Others”, and the “Grand Total”.

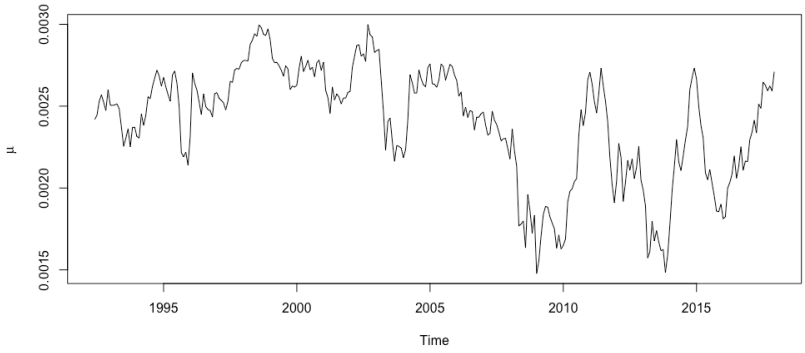

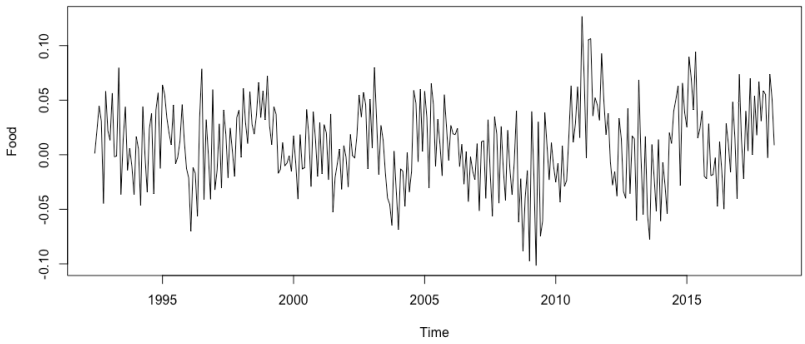

Food

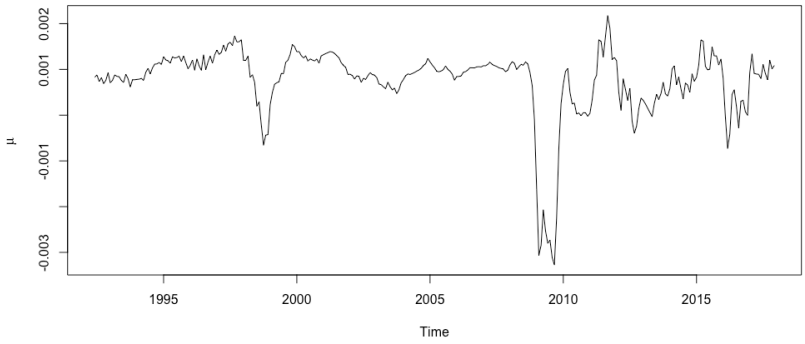

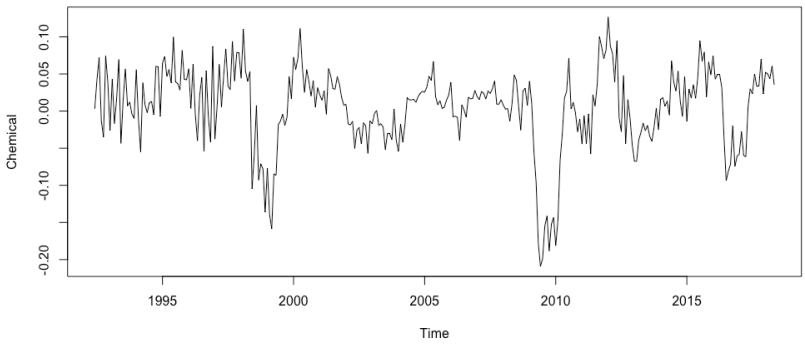

Chemical

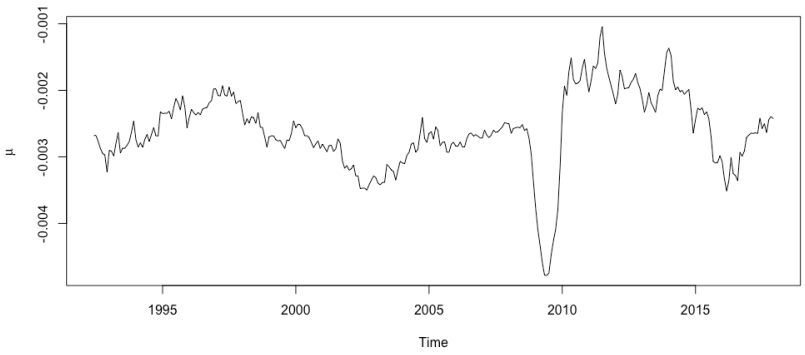

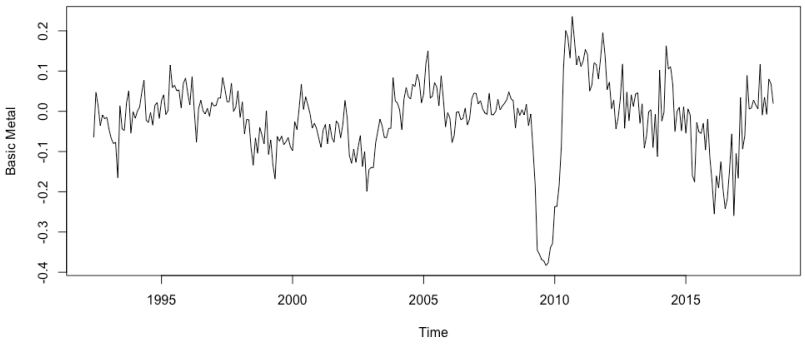

Basic Metal

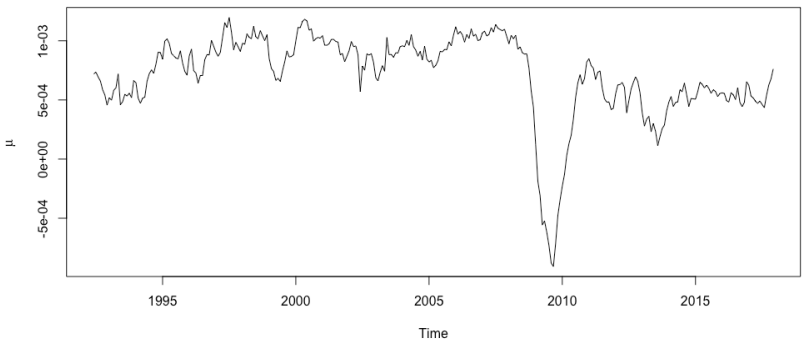

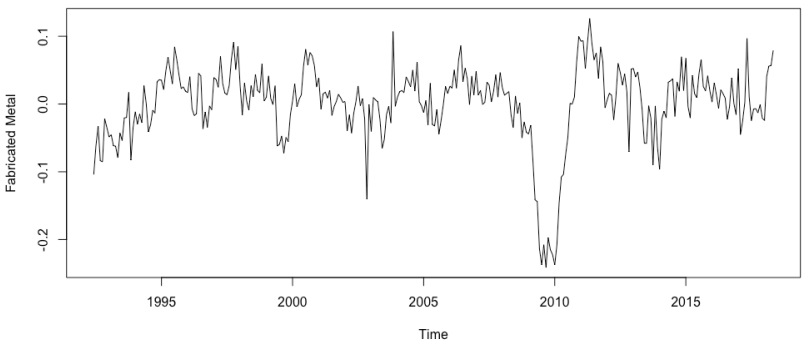

Fabricated Metal

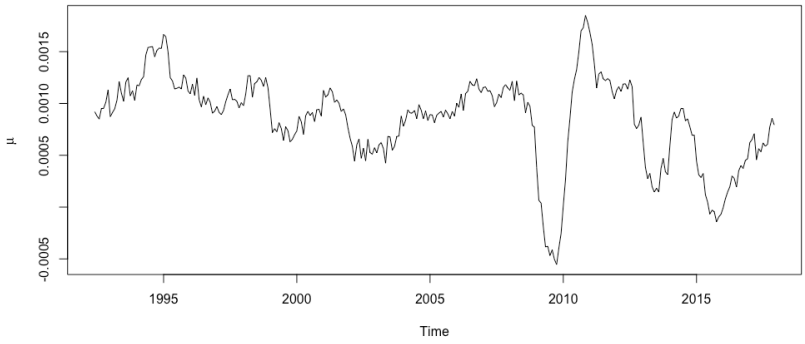

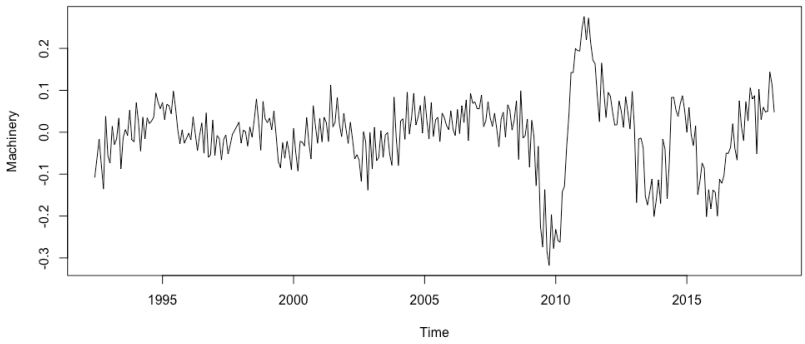

Machinery

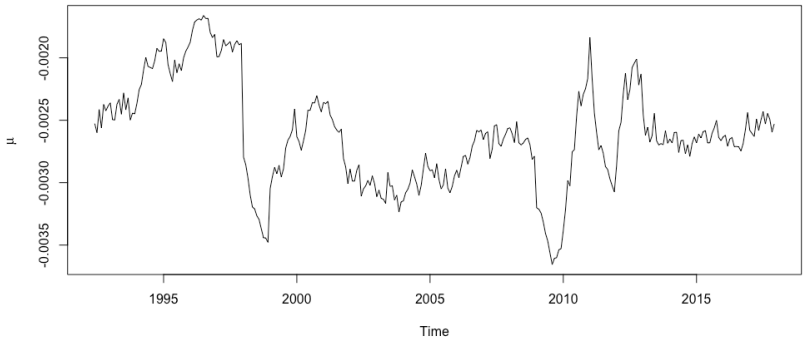

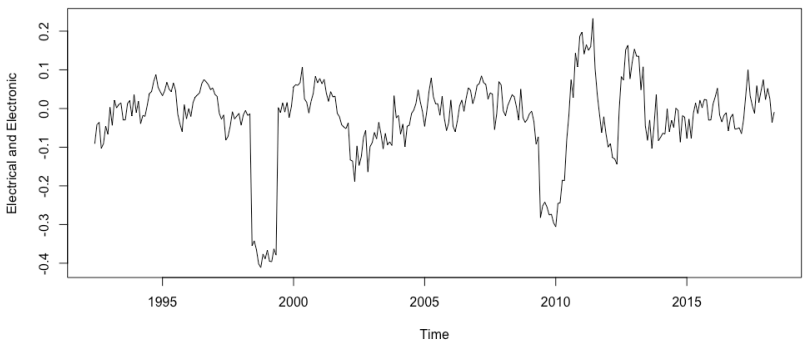

Electricals

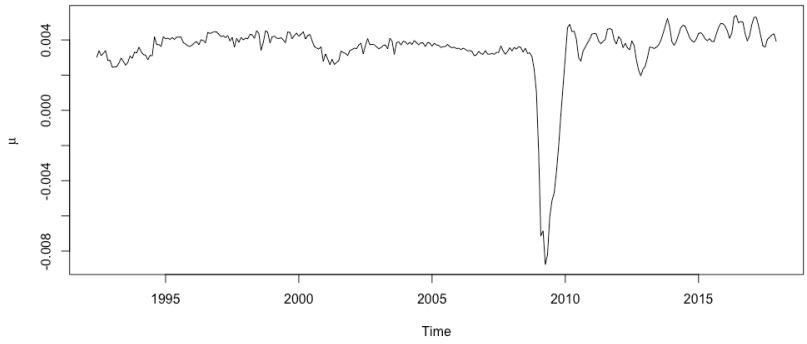

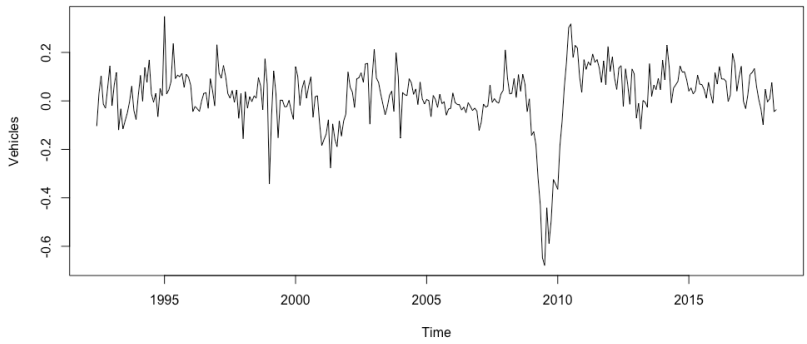

Vehicles

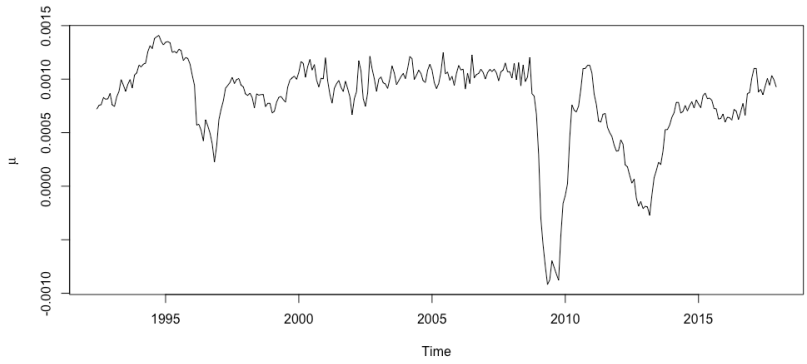

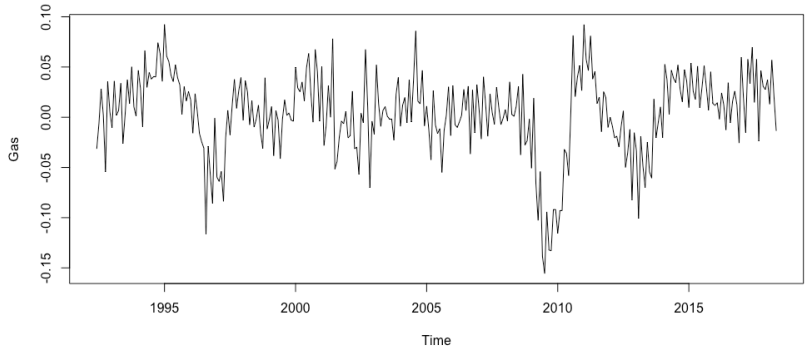

Gas

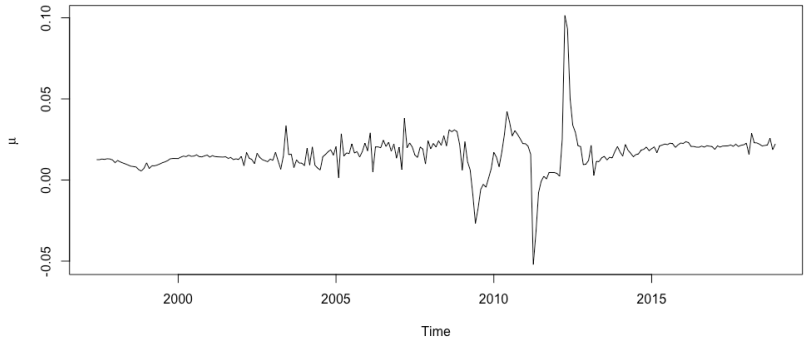

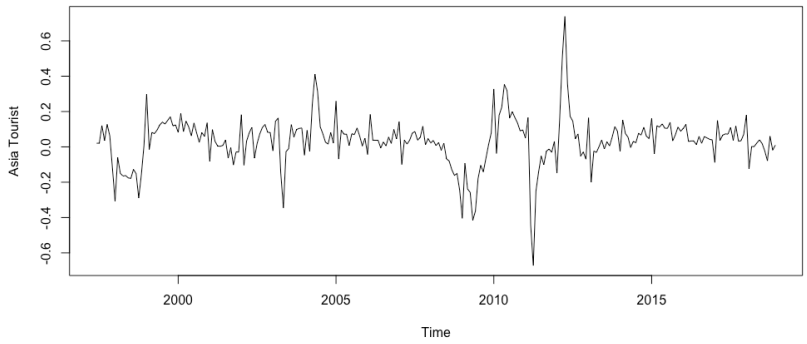

Asia Tourist

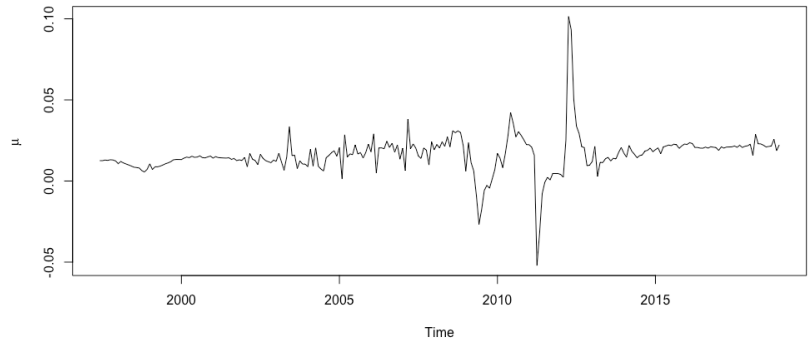

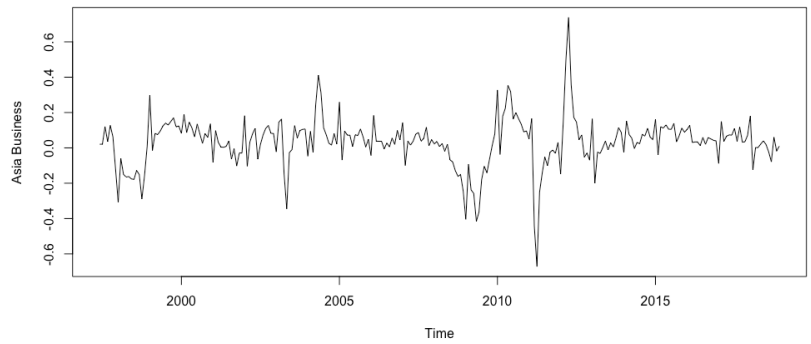

Asia Business

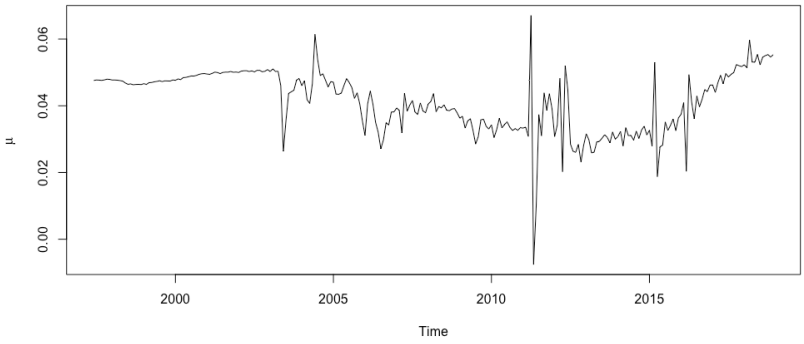

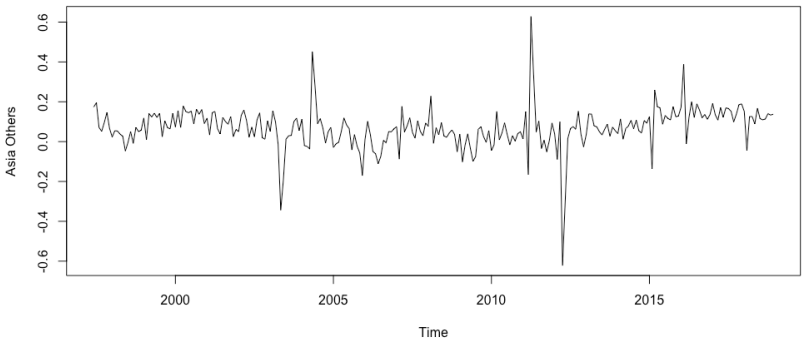

Asia Others

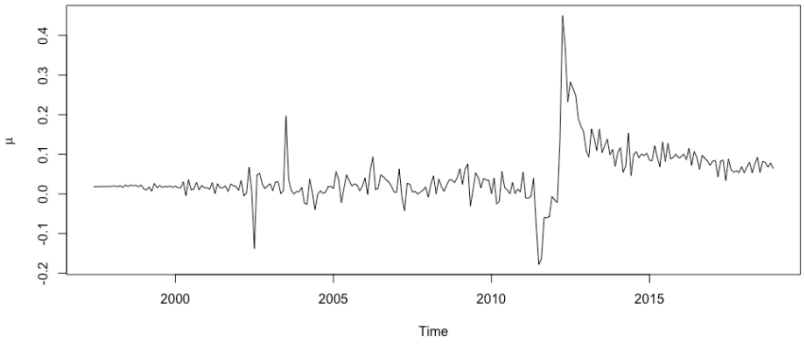

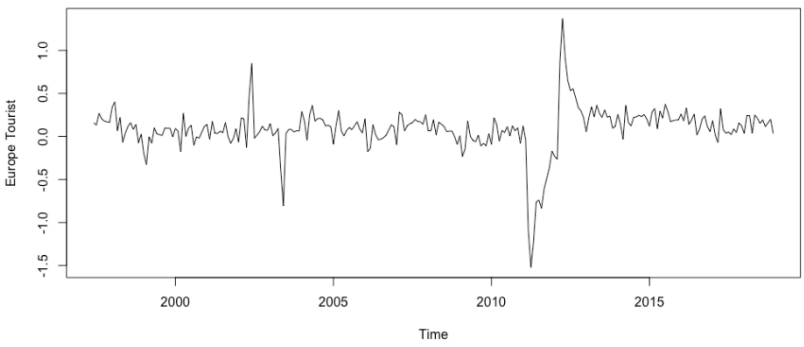

Europe Tourist

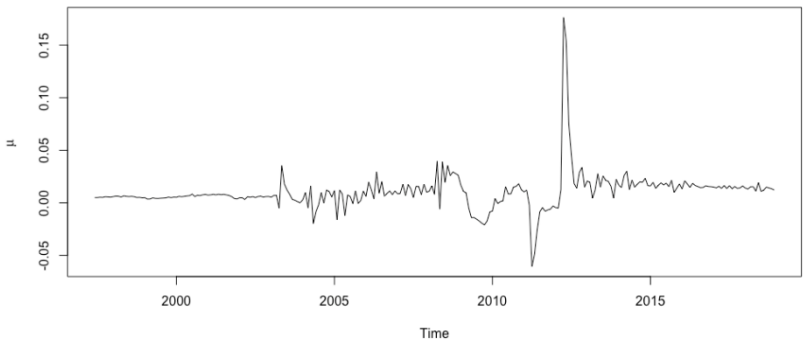

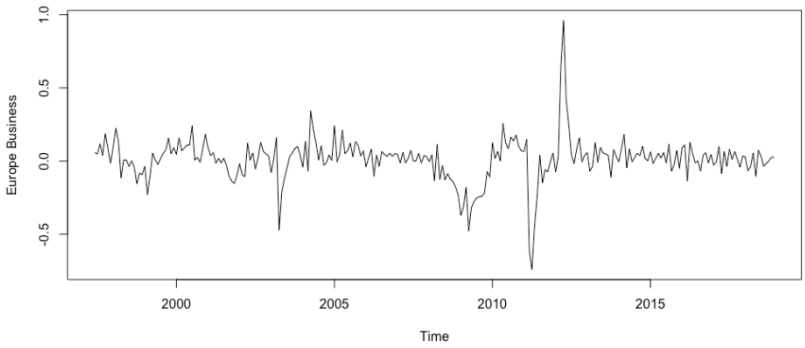

Europe Business

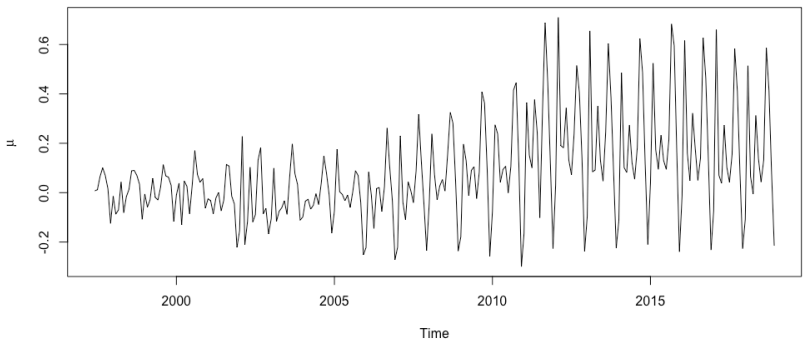

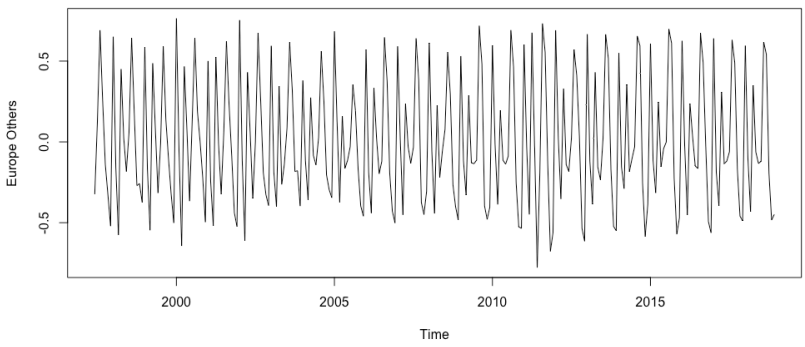

Europe Others

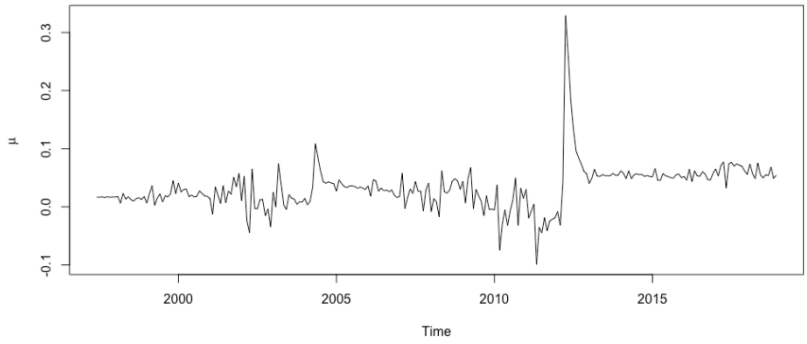

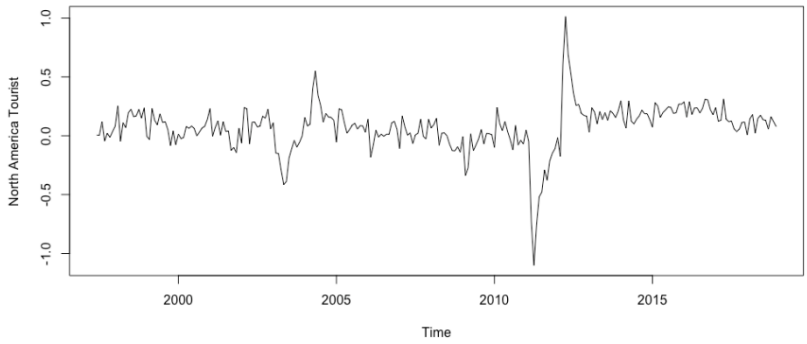

North America Tourist

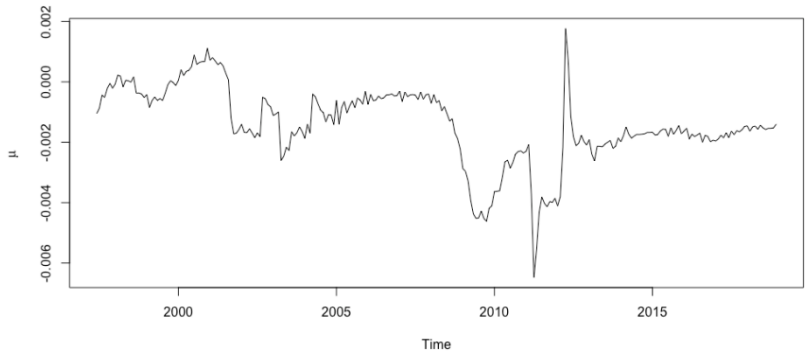

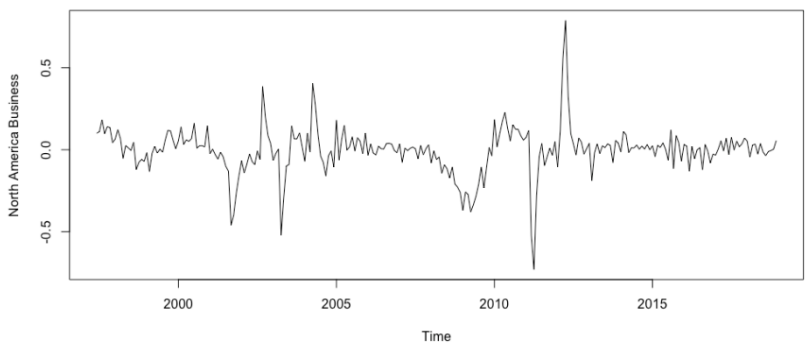

North America Business

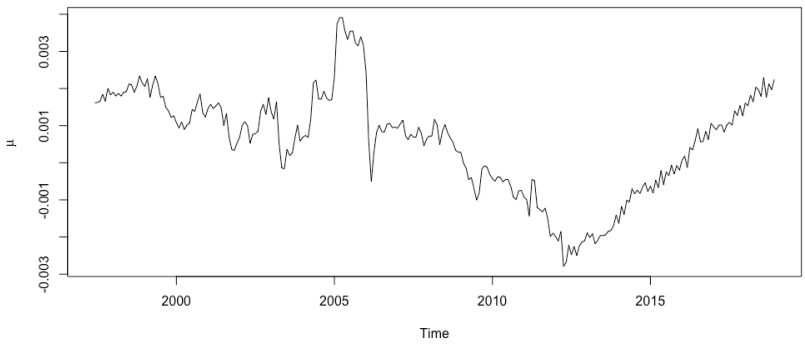

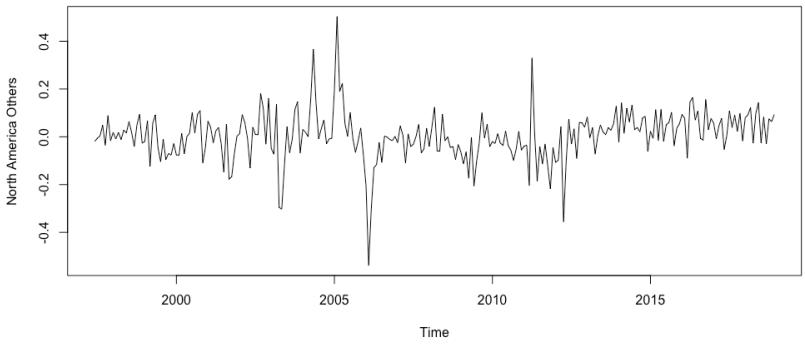

North America Others

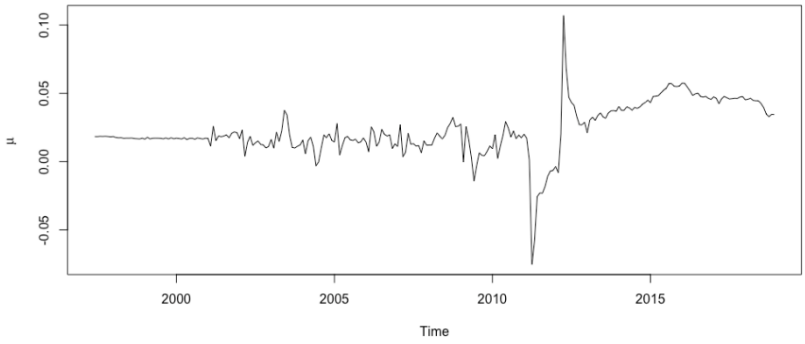

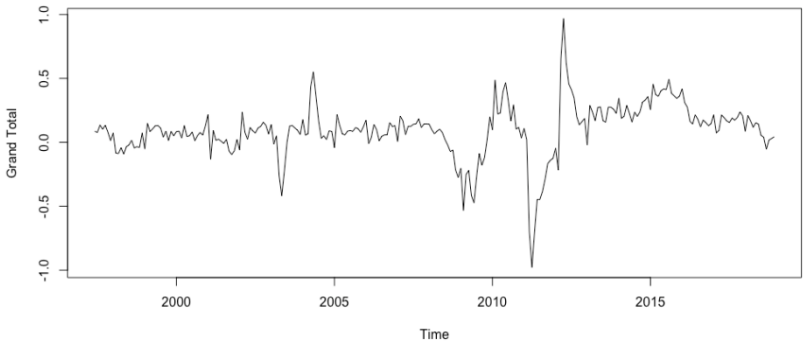

Grand Total

Bibliography

Álvarez-Díaz, M. and Rosselló-Nadal, J. (2010) 'Forecasting British tourist arrivals in the Balearic Islands using meteorological variables', *Tourism Economics*, 16(1), pp. 153–168. doi: 10.5367/000000010790872079.

Ang, A. and Bekaert, G. (2007) 'Stock Return Predictability : Is it There ?', *Oxford Journals, Oxford University Press*, 20(3), pp. 651–707.

Arbatli, E. C. *et al.* (2017) 'Policy uncertainty in Japan', *SSRN Electronic Journal*. doi: 10.2139/ssrn.2972891.

Archer, B. H. (1987) 'Demand forecasting and estimation', in *Travel, tourism and hospitality research*. New York: Wiley, pp. 77–85.

Arghyrou, M., Gregoriou, A. and Pourpourides, P. M. (2009a) 'A New Solution to the Purchasing Power Parity Puzzles: Risk-Aversion, Exchange Rate Uncertainty and the Law of One Price', *SSRN*. doi: 10.2139/ssrn.1341850.

Arghyrou, M., Gregoriou, A. and Pourpourides, P. M. (2009b) 'Exchange rate uncertainty and deviations from purchasing power parity: evidence from the G7 area'.

Armstrong, C. W. G. (1972) 'International tourism: coming or going, the methodological problems of forecasting', *Futures*, 4(2), pp. 115–125.

Artis, M. J., Kontolemis, Z. G. and Osborn, D. R. (1997) 'Business cycles for G7 and European countries', *The Journal of Business*, 70(2), pp. 249–279. doi: 10.1086/209717.

Athanasopoulos, G. *et al.* (2011) 'The tourism forecasting competition', *International Journal of Forecasting*, 27, pp. 822–844. doi: 10.1016/j.ijforecast.2010.04.009.

Athanasopoulos, G. and de Silva, A. (2012) 'Multivariate Exponential Smoothing for Forecasting Tourist Arrivals', *Journal of Travel Research*, 51(5), pp. 640–652. doi: 10.1177/0047287511434115.

Bahmani-Oskooee, M., Chang, T. and Lee, K. C. (2016) 'Purchasing power parity in emerging markets: A panel stationary test with both sharp and smooth breaks', *Economic Systems*, 40(3), pp. 453–460. doi: 10.1016/j.ecosys.2015.12.002.

Bai, J. and Perron, P. (2003) ‘Computation and analysis of multiple structural change models’, *Journal of Applied Econometrics*, 18(1), pp. 1–22. doi: 10.1002/jae.659.

Baker, S. R. *et al.* (2019) ‘Policy news and stock market volatility’, *University of Chicage, Becker Friedman Institute for Economics Working Paper*.

Baker, S. R., Bloom, N. and Davis, S. J. (2015) ‘Measuring economic policy uncertainty’, *NBER Working Paper Series*. doi: 10.1007/s13398-014-0173-7.2.

Barrero, J. M., Bloom, N. and Wright, I. (2017) ‘Short and long run uncertainty’, *NBER Working Paper Series*. Available at: http://www.nber.org/papers/w23676.

Bartsch, Z. (2019) ‘Economic policy uncertainty and dollar-pound exchange rate return volatility’, *Journal of International Money and Finance*, 98. doi: 10.1016/j.jimonfin.2019.102067.

Baum, C. F., Barkoulas, J. T. and Caglayan, M. (2001) ‘Nonlinear adjustment to purchasing power parity in the post-Bretton Woods era’, *Journal of International Money and Finance*, 20(3), pp. 379–399. doi: 10.1016/S0261-5606(00)00043-7.

Bec, F., Ben Salem, M. and Carrasco, M. (2010) ‘Detecting Mean Reversion in Real Exchange Rates from a Multiple Regime STAR Model’, *Annals of Economics and Statistics*, (99/100), p. 395. doi: 10.2307/41219172.

Becker, R., Chambers, J. and Wilks, A. R. (1988) *The New S Language*. Wadsworth & Brookes/Cole.

Benninga, S. and Protopapadakis, A. (1988) ‘The equilibrium pricing of exchange rates and assets when trade takes time’, *Journal of International Money and Finance*, 7(2), pp. 129–149. doi: 10.1016/0261-5606(88)90012-5.

Bergmeir, C., Hyndman, R. J. and Benítez, J. M. (2016) ‘Bagging exponential smoothing methods using STL decomposition and Box-Cox transformation’, *International Journal of Forecasting*, 32, pp. 303–312. doi: 10.1016/j.ijforecast.2015.07.002.

Bleaney, M. F., Leybourne, S. J. and Mizen, P. (1999) ‘Mean reversion of

real exchange rates in high-Inflation countries', 65(4), pp. 839–854.
Bloom, N. (2014) 'Fluctuations in uncertainty', *Journal of Economic Perspectives*, 28(2). doi: 10.1257/jep.28.2.153.

Bloom, N. (2015) 'Does policy uncertainty matter?', in *Stanford University & NBER Conference*.

Boudoukh, J., Richardson, M. and Whitelaw, R. (2005) 'The myth of long-horizon predictabiilty', *NBER Working Paper Series*.

Bradley, M. D. and Jansen, D. W. (2004) 'Forecasting with a nonlinear dynamic model of stock returns and industrial production', *International Journal of Forecasting*, 20(2), pp. 321–342. doi: 10.1016/j.ijforecast.2003.09.007.

Brockett, R. W. (1976) 'Volterra series and geometric control theory', *Automatica*, 12(2), pp. 167–176. doi: 10.1016/0005-1098(76)90080-7.

Brooks, C. (1996) 'Testing for non-linearity in daily sterling exchange rates', *Applied Financial Economics*, 6(4), pp. 307–317. doi: 10.1080/096031096334105.

Burger, C. J. S. . *et al.* (2001) 'A practitioners guide to time-series methods for tourism demand forecasting — a case study of Durban, South Africa', *Tourism Management*, 22(4), pp. 403–409. doi: 10.1016/S0261-5177(00)00068-6.

Cao, C. Q. and Tsay, R. S. (1992) 'Nonlinear time-series analysis of stock volatilities', *Journal of Applied Econometrics*, 7(S1), pp. S165–S185. doi: 10.1002/jae.3950070512.

Cartwright, P. A. (1985a) 'Forecasting time series: a comparative analysis of alternative classes of time series models', *Journal of Time Series Analysis*, 6(4), pp. 203–211.

Cartwright, P. A. (1985b) 'Using state dependent models for prediction of time series with missing observations', *Time Series Analysis: Theory and Practice 7*, pp. 157–167.

Cartwright, P. A. and Newbold, P. (1982) *A time series approach to the prediction of oil discoveries*. University of Illinois at Urbana-Champaign.
Cassel, G. (1922) *Money and Foreign Exchange After 1914*. London: Constable.

Chen, C. F., Chang, Y. H. and Chang, Y. W. (2009) 'Seasonal ARIMA forecasting of inbound air travel arrivals to Taiwan', *Transportmetrica*, 5(2), pp. 125–140. doi: 10.1080/18128600802591210.

Chen, K. Y. and Wang, C. H. (2007) 'Support vector regression with genetic algorithms in forecasting tourism demand', *Tourism Management*, 28, pp. 215–226. doi: 10.1016/j.tourman.2005.12.018.

Chen, L., Du, Z. and Hu, Z. (2020) 'Impact of economic policy uncertainty on exchange rate volatility of China', *Finance Research Letters*, 32. doi: 10.1016/j.frl.2019.08.014.

Chen, R. and Tsay, R. S. (1993) 'Functional-coefficient autoregressive models', *Journal of the American Statistical Association*, 88(421), pp. 298–308. doi: 10.2307/2290725.

Chen, S. L. and Wu, J. L. (2000) 'A re-examination of purchasing power parity in Japan and Taiwan', *Journal of Macroeconomics*, 22(2), pp. 271–284. doi: 10.1016/S0164-0704(00)00132-4.

Cheung, Y. and Lai, K. (1993) 'A fractional cointegration analysis of purchasing power parity', *Journal of Business & Economic Statistics*. doi: 10.1080/07350015.1993.10509936.

Cho, V. (2001) 'Tourism forecasting and its relationship with leading economic indicators', *Journal of Hospitality and Tourism Research*, 25(4), pp. 399–420.

Cho, V. (2003) 'A comparison of three different approaches to tourist arrival forecasting', *Tourism Management*, 24(3), pp. 323–330. doi: 10.1016/S0261-5177(02)00068-7.

Chortareas, G. and Kapetanios, G. (2004) 'The Yen real exchange rate may be stationary after all: evidence from non-linear unit-root tests', *Oxford Bulletin of Economics and Statistics*, 66(1), pp. 113–131. doi: 10.1046/j.0305-9049.2003.00080.x.

Christopoulos, D. K. and León-Ledesma, M. A. (2010) 'Smooth breaks and non-linear mean reversion: Post-Bretton Woods real exchange rates', *Journal of International Money and Finance*, 29(6), pp. 1076–1093. doi: 10.1016/j.jimonfin.2010.02.003.

Claveria, O. and Torra, S. (2014) 'Forecasting tourism demand to Catalonia:

Neural networks vs. time series models', *Economic Modelling*, 36, pp. 220–228. doi: 10.1016/j.econmod.2013.09.024.

Cleveland, W. S. (1979) 'Robust locally weighted regression and smoothing scatterplots', *Journal of the American Statistical Association*, 74(368), pp. 829–836. doi: 10.1080/01621459.1979.10481038.

Cleveland, W. S. *et al.* (1981) 'Lowess: A program for smoothing scatterplots by robust locally weighted regression', *The American Statistician*, 35, p. 54. doi: 10.1080/00031305.1981.10479306_3.

Cochrane, J. H. (1988) 'How big is the random walk in GNP?', *Journal of Political Economy*, 96(5), pp. 893–920. doi: 10.1086/261569.

Colominas, M. A., Schlotthauer, G. and Torres, M. E. (2014) 'Improved complete ensemble EMD: A suitable tool for biomedical signal processing', *Biomedical Signal Processing and Control*, 14, pp. 19–29. doi: 10.1016/j.bspc.2014.06.009.

Copeland, L. and Heravi, S. (2009) 'Structural breaks in the real exchange rate adjustment mechanism', *Applied Financial Economics*, 19(2), pp. 121–134. doi: 10.1080/09603100701765216.

Corbae, D. and Ouliaris, S. (1988) 'Cointegration and tests of Purchasing Power Parity', *The Review of Economics and Statistics*, 70(3), pp. 508–511. doi: 10.2307/1926790.

Crato, N. and de Lima, J. F. (1994) 'Long-memory and non-linearity: a time series analysis of stock returns and volatilities', *Managerial Finance*, 20(2), pp. 49–67.

Delong, J. B. and Summers, L. H. (1986) 'Are business cycles asymmetric', in Gordon, R. J. (ed.) *The American Business Cycle: Continuity and Change*. Chicago University Press.

Diebold, F. X., Husted, S. and Rush, M. (1991) 'Real exchange rates under the gold standard', *Journal of Political Economy*, 99(6), pp. 1252–1271. doi: 10.1086/261799.

Dijk, D. van, Teräsvirta, T. and Franses, P. H. (2000) 'Smooth transition autoregressive models - a survey of recent developments', *Econometric Institute Research Report EI2000-23/A*, 4938(September), p. 56. doi: 10.1081/ETC-120008723.

Dixon, H., Easaw, J. and Heravi, S. (2019) 'Forecasting inflation gap persistence: Do financial sector professionals differ from nonfinancial sector ones?', *International Journal of Finance & Economics*, pp. 1–14.

Drogobetskii, S. (2005) 'Singular spectrum analysis of price movement in Forex (part 2)', *Stocks & Commodities*, 23, pp. 44–48.

Drogobetskii, S. and Smolynsky, V. (2008) 'Forecasting singular spectrum analysis', *Stocks & Commodities*, 26, pp. 38–40.

Dumas, B. (1992) 'Dynamic equilibrium and the real exchange rate in a spatially separated world', *Review of Financial Studies*, 5(2), pp. 153–180. doi: 10.1093/rfs/5.2.153.

Easaw, J., Heravi, S. and Dixon, H. D. (2015) 'Professionals' forecast of the inflation gap and its persistence', *Cardiff Economics Working Papers E2015/13*.

Engle, R. F. and Granger, C. W. J. (1987) 'Cointegration and error correction: representation, estimation, and testing', *Econometrica*, 55, pp. 251–276.

Escribano, A. and Jordá, O. (1997) *Improved testing and specification of smooth transition regression models*, *University of California Working Paper Series*. doi: 10.1017/CBO9781107415324.004.

España, M. and Landau, I. D. (1978) 'Reduced order bilinear models for distillation columns', *Automatica*, 14(4), pp. 345–355. doi: 10.1016/0005-1098(78)90034-1.

Fernández-Villaverde, J. *et al.* (2015) 'Fiscal volatility shocks and economic activity', *American Economic Review*, 105(11), pp. 3352–3384. doi: 10.1257/aer.20121236.

Franses, P. H. and Dijk, D. van. (2000) *Nonlinear time series models in empirical finance*. Cambridge University Press.

Franses, P. H. and van Dijk, D. (2005) 'The forecasting performance of various models for seasonality and nonlinearity for quarterly industrial production', *International Journal of Forecasting*, 21(1), pp. 87–102. doi: 10.1016/j.ijforecast.2004.05.005.

Gabr, M. and Rao, S. (1981) 'The estimation and prediction of subset

bilinear time series models with applications', *Journal of Time Series Analysis*, 2, pp. 155–171.

Ghoshray, A. (2019) 'Do international primary commodity prices exhibit asymmetric adjustment?', *Journal of Commodity Markets*. doi: 10.1016/j.jcomm.2018.08.002.

Gilchrist, S., Sim, J. and Zakrajsek, E. (2014) 'Uncertainty, financial frictions, and investment dynamics', *SSRN Electronic Journal*. doi: 10.2139/ssrn.2503636.

Goh, C. and Law, R. (2002) 'Modeling and forecasting tourism demand for arrivals with stochastic nonstationary seasonality and intervention', *Tourism Management*, 23, pp. 499–510. doi: 10.1016/S0261-5177(02)00009-2.

Granger, C. and Anderson, A. (1978) *An Introduction to Bilinear Time Series Models*. Göttingen: Vandenhoeck and Ruprecht.

Granger, C. W. J. (1986) 'Developments in the study of cointegrated economic variables', *Oxford Bulletin of Economics and Statistics*, 48(3), pp. 213–228. doi: 10.1111/j.1468-0084.1986.mp48003002.x.

Granger, C. W. J. and Teräsvirta, T. (1993) *Modelling nonlinear economic relationships*. Oxford University Press.

Guerron-Quintana, P. (2011) 'Do uncertainty and technology drive exchange rates?', *SSRN Electronic Journal*. doi: 10.2139/ssrn.1484998.

Gujarati, D. N. and Porter, D. C. (2009) *Basic econometrics*. McGraw-Hill Irwin.

Gunter, U. and Önder, I. (2015) 'Forecasting international city tourism demand for Paris: Accuracy of uni- and multivariate models employing monthly data', *Tourism Management*, 46, pp. 123–135. doi: 10.1016/j.tourman.2014.06.017.

Gunter, U. and Önder, I. (2016) 'Forecasting city arrivals with Google Analytics', *Annals of Tourism Research*, 61, pp. 199–212. doi: 10.1016/j.annals.2016.10.007.

Gurung, B. (2013) 'An application of exponential autoregressive (EXPAR) nonlinear time-series model', *International Journal of Information and Computation Technology*, 3(4), pp. 261–266.

Haggan, V., Heravi, S. M. and Priestley, M. B. (1984) 'A study of the application of state-dependent models in non-linear time series analysis', *Journal of time series analysis*, 5(2), pp. 69–102.

Haggan, V. and Ozaki, T. (1981) 'Modelling nonlinear random vibrations using an amplitude-dependent autoregressive time series model', *Biometrica*, 68(1), pp. 189–196.

Hamilton, J. D. and Lin, G. (1996) 'Stock market volatility and the business cycle', *Journal of Applied Econometrics*, 11(5), pp. 573–593. doi: 10.1002/(SICI)1099-1255(199609)11:5<573::AID-JAE413>3.0.CO;2-T.

Hansen, B. E. (2011) 'Threshold autoregression in economics', *Statistics and its Interface*, 4, pp. 123–127. doi: 10.4310/sii.2011.v4.n2.a4.

Harrison, P. J. and Stevens, C. F. (1976) 'Bayesian forecasting', *Journal of the Royal Statistical Society. Series B (Methodological)*, 38(3), pp. 205–247. doi: 10.1016/S1574-0706(05)01001-3.

Harvey, D. I., Leybourne, S. J. and Taylor, A. R. (2009) 'Simple, robust and powerful tests of the breaking trend hypothesis', *Econometric Theory*, 25, pp. 995–1029.

Harvey, D. L., Leybourne, S. J. and Xiao, B. (2008) 'A powerful test for linearity hen the order of integration is unknown', *Studies in Nonlinear Dynamics & Econometrics*, 12(3), pp. 1–24.

Hassan, T. A. *et al.* (2016) 'Aggregate and idiosyncratic political risk: measurement and effects', *SSRN Electronic Journal*. doi: 10.2139/ssrn.2838644.

Hassani, H. *et al.* (2013) 'Forecasting before, during, and after recession with singular spectrum analysis', *Journal of Applied Statistics*, 40(10), pp. 2290–2302. doi: 10.1080/02664763.2013.810193.

Hassani, H. *et al.* (2015) 'Forecasting U.S. Tourist arrivals using optimal Singular Spectrum Analysis', *Tourism Management*, 46, pp. 322–335. doi: 10.1016/j.tourman.2014.07.004.

Hassani, H., Heravi, S. and Zhigljavsky, A. (2009) 'Forecasting European industrial production with singular spectrum analysis', *International Journal of Forecasting*. Elsevier, 25(1), pp. 103–118. doi: 10.1016/J.IJFORECAST.2008.09.007.

Hassani, H., Heravi, S. and Zhigljavsky, A. (2013) 'Forecasting UK industrial production with multivariate singular spectrum analysis', *Journal of Forecasting*, 32(5), pp. 395–408. doi: 10.1002/for.2244.

Hassani, H., Soofi, A. S. and Zhigljavsky, A. A. (2010) 'Predicting daily exchange rate with singular spectrum analysis', *Nonlinear Analysis: Real World Applications*, 11(3), pp. 2023–2034. doi: 10.1016/j.nonrwa.2009.05.008.

Hassani, H. and Thomakos, D. (2010) 'A review on singular spectrum analysis for economic and financial time series', *Statistics and Its Interface*, 3(3), pp. 377–397. doi: 10.4310/SII.2010.v3.n3.a11.

Heravi, S., Easaw, J. and Golinelli, R. (2016) 'Generalized state-dependent models: a multivariate approach', *Quaderni - Working Paper DSE No. 1067*. (Alma Mater Studiorum - Università di Bologna Department of Economics Working Paper), pp. 1–27.

Heravi, S. M. (1985) *A study of state-dependent models in non-linear time series analysis and dynamical systems*. University of Manchester Institute of Science and Technology.

Heravi, S., Osborn, D. R. and Birchenhall, C. R. (2004) 'Linear versus neural network forecasts for European industrial production series', *International Journal of Forecasting*, 20, pp. 435–446. doi: 10.1016/S0169-2070(03)00062-1.

Hinich, M. J. and Patterson, D. M. (1985) 'Evidence of nonlinearity in daily stock returns', *Journal of Business & Economic Statistics*, 3(1), pp. 69–77.

Hsieh, D. A. (1989) 'Testing for nonlinear dependence in daily foreign exchange rates', *The Journal of Business*, 62(3), p. 339. doi: 10.1086/296466.

Hsieh, D. A. (1991) 'Chaos and nonlinear dynamics: application to financial markets', *Journal of Finance*, 46(5), pp. 1839–1877. doi: 10.2307/2328575.

Hu, J. and Chen, Z. (2016) 'A unit root test against globally stationary ESTAR models when local condition is non-stationary', *Economics Letters*, 146, pp. 89–94.

Huang, C. H. and Yang, C. Y. (2015) 'European exchange rate regimes and purchasing power parity: An empirical study on eleven eurozone countries',

International Review of Economics and Finance, 35, pp. 100–109. doi: 10.1016/j.iref.2014.09.008.

Huang, X., Zhang, L. and Ding, Y. (2017) 'The Baidu Index: uses in predicting tourism flows –A case study of the Forbidden City', *Tourism Management*, 58, pp. 301–306. doi: 10.1016/j.tourman.2016.03.015.

Hyndman, R. J. and Athanasopoulos, G. (2018) *Forecasting: principles and practice*. Second Edi. OTexts.

Javed, B. K. (2019) 'Purchasing power parity (PPP) with structural break and mean reversion in real exchange rate: the case of Bangladesh Taka and US Dollar', *SSRN*.

Kalman, R. E. (1963) 'Mathematical description of linear dynamical systems', *Journal of the Society for Industrial and Applied Mathematics Series A Control*, 1(2), pp. 152–192. doi: 10.1137/0301010.

Katsiampa, P. (2015) 'Nonlinear exponential autoregressive time series models with conditional heteroskedastic errors with applications to economics and finance', *Loughborough University. Thesis*.

Kejriwal, M. and Perron, P. (2010) 'Testing for multiple structural changes in cointegrated regression models', *Journal of Business & Economic Statistics*, 28(4), pp. 503–522.

Keynes, J. M. (1936) *The general theory of output, interest and money*, *The Collected Writings of John Maynard Keynes*. London: Macmillan. doi: 10.2307/2143949.

Kim, Y. and Bang, H. (2018) 'Introduction to Kalman Filter and Its Applications', in Govaers, F. (ed.) *Introduction and Implementations of the Kalman Filter*.

Kon, S. and Turner, W. (2005) 'Neural network forecasting of tourism demand', *Tourism Economics*, 11, pp. 301–328.

Koop, G. and Potter, S. M. (1998) 'Bayes factors and nonlinearity: Evidence from economic time series', *Journal of Econometrics*, 88(2), pp. 251–281. doi: 10.1016/S0304-4076(98)00031-1.

Koop, G. and Potter, S. M. (2001) 'Are apparent findings of nonlinearity due to structural instability in economic time series?', *The Econometrics*

Journal, 4(1), pp. 37–55. doi: 10.1111/1368-423x.00055.

Kostakis, A., Magdalinos, T. and Stamatogiannis, M. P. (2015) 'Robust econometric inference for stock return predictability', *The Review of Financial Studies*, 28(5), pp. 1506–1553.

Kotzé, K. (2017) 'Purchasing power parity and the real exchange rate', in *International Financial Management*. Cambridge University Press, pp. 313–353.

Kuan, C. M. and Liu, T. (1995) 'Forecasting exchange rates using feedforward and recurrent neural networks', *Journal of Applied Econometrics*, 10(4), pp. 347–364. doi: 10.1002/jae.3950100403.

Kutan, A. M. and Zhou, S. (2015) 'PPP may hold better than you think: Smooth breaks and non-linear mean reversion in real effective exchange rates', *Economic Systems*, 39(2), pp. 358–366. doi: 10.1016/j.ecosys.2014.12.001.

Law, R. (2000) 'Back-propagation learning in improving the accuracy of neural network-based tourism demand forecasting', *Tourism Management*, 21(4), pp. 331–340. doi: 10.1016/S0261-5177(99)00067-9.

Law, R. and Au, N. (1999) 'A neural network model to forecast Japanese demand for travel to Hong Kong', *Tourism Management*, 20, pp. 89–97. doi: 10.1016/S0261-5177(98)00094-6.

Li, G. *et al.* (2006) 'Tourism demand forecasting: A time varying parameter error correction model', *Journal of Travel Research*, 45(2), pp. 175–185. doi: 10.1177/0047287506291596.

Li, G., Song, H. and Witt, S. F. (2005) 'Recent developments in econometric modeling and forecasting', *Journal of Travel Research*, 44, pp. 82–99. doi: 10.1177/0047287505276594.

Liew, V. K. (2004) 'On autoregressive order selection criteria', *Computational Economics*.

Lim, C. and McAleer, M. (2001) 'Forecasting tourist arrivals', *Annals of Tourism Research*, 28(4), pp. 965–977. doi: 10.1016/S0160-7383(01)00006-8.

Lisi, F. and Medio, A. (1997) 'Is a random walk the best exchange rate

predictor?', *International Journal of Forecasting*, 13(2). doi: 10.1016/S0169-2070(97)00001-0.

Lopes, H. F. and Tsay, R. S. (2011) 'Particle filters and Bayesian inference in financial econometrics', *Journal of Forecasting*, 30, pp. 168–209. doi: 10.1002/for.1195.

MacDonald, R. (1996) 'Panel unit root tests and real exchange rates', *Economics Letters*, 50, pp. 7–11. doi: 10.1016/0165-1765(95)00730-X.

MacKinnon, J. (2010) 'Critical Values for Cointegration Tests', *Working Paper*, (February 1990). doi: 10.22004/ag.econ.273723.

Michael, P., Nobay, A. R. and Peel, D. A. (1997) 'Transactions costs and nonlinear adjustment in real exchange rates : an empirical investigation', *Journal of Political Economy*, 105(4), pp. 862–879.

Mitchell, W. C. (1927) *Business Cycles: The Problem and Its Setting*. New York: National Bureau of Economic Research.

Mohler, R. R. (1973) *Bilinear Control Processes*. New York and London: Academic Press.

Mohler, R. R. (2005) 'Bilinear control structures in immunology', *Modelling and Optimization of Complex System*, pp. 58–68.

Newey, W. and West, K. (2014) 'A simple, positive semi-definite, heteroscedasticity and autocorrelation consistent covariance matrix', *Applied Econometrics*, 33(1), pp. 125–132. doi: 10.2307/1913610.

Nikolaou, K. (2008) 'The behaviour of the real exchange rate: Evidence from regression quantiles', *Journal of Banking and Finance*, 32(5), pp. 664–679. doi: 10.1016/j.jbankfin.2007.05.002.

O'Connell, P. G. J. and Wei, S.-J. (1997) '"The bigger they are, the harder they fall": how price differences across U.S. cities are arbitraged', *NBER Working Paper No. 6089*.

Öcal, N. and Osborn, D. R. (2000) 'Business cycle non-linearities in UK consumption and production', *Journal of Applied Econometrics*, 15(1), pp. 27–43.

Oh, K.-Y. (1996) 'Purchasing power parity and unit root tests using panel

data', *Journal of International Money and Finance*, 15(3), pp. 405–418.

Osborn, D. R., Heravi, S. and Birchenhall, C. R. (1999) 'Seasonal unit roots and forecasts of two-digit European industrial production', *International Journal of Forecasting*, 15, pp. 27–47. doi: 10.1016/S0169-2070(98)00055-7.

Ozaki, T. (1978) 'Non-linear models for non-linear random vibrations', *Technical Report No. 92, Department of Mathematics, University of Manchester Institute of Science and Technology, UK*.

Ozaki, T. (1981) 'Non-linear threshold autoregressive models for non-linear random vibrations', *Journal of Applied Probability*, 18, pp. 443–451.

Pattie, D. C. and Snyder, J. (1996) 'Using a neural network to forecast visitor behavior', *Annals of Tourism Research*, 23(1), pp. 151–164. doi: 10.1016/0160-7383(95)00052-6.

Paya, I. and Peel, D. A. (2003) 'Purchasing power parity adjustment speeds in high frequency data when the equilibrium real exchange rate is proxied by a deterministic trend', *The Manchester School*, 71(Supplement), pp. 39–53. doi: 10.1111/1467-9957.71.s.3.

Paya, I., Venetis, I. A. and Peel, D. A. (2003) 'Further evidence on PPP adjustment speeds: The case of effective real exchange rates and the EMS', *Oxford Bulletin of Economics and Statistics*, 65(4), pp. 421–438. doi: 10.1111/1468-0084.t01-1-00055.

Peel, D. and Speight, A. (1996) 'Is the US business cycle asymmetric? Some further evidence', *Applied Economics*, 28, pp. 405–415.

Pesaran, M. H. and Potter, S. M. (1997) 'A floor and ceiling model of US output', *Journal of Economic Dynamics and Control*, 21(4–5), pp. 661–695. doi: 10.1016/s0165-1889(96)00002-4.

Pfann, G. A., Schotman, P. C. and Tschernig, R. (1996) 'Nonlinear interest rate dynamics and implications for the term structure', *Journal of Econometrics*, 74(1), pp. 149–176. doi: 10.1016/0304-4076(95)01754-2.

Pippenger, M. K. and Goering, G. E. (1998) 'Exchange rate forecasting: results from a threshold autoregressive model', *Open Economies Review*, 9(2), pp. 157–170. doi: 10.1023/A:1008264302419.

Priestley, M. B. (1980) ‘State-dependent models: a general approach to non-linear time series analysis’, *Journal of Time Series Analysis*, 1(1), pp. 47–71. doi: 10.1111/j.1467-9892.1980.tb00300.x.

Rao, S. (1981) ‘On the theory of bilinear time series models’, *Journal of the Royal Statistical Society. Series B (Methodological)*, 43(2), pp. 244–255.

Rothman, P. (1998) ‘Forecasting asymmetric unemployment rates’, *Review of Economics and Statistics*, 80(1), pp. 164–168. doi: 10.1162/003465398557276.

Sarantis, N. (1999) ‘Modeling non-linearities in real effective exchange rates’, *Journal of International Money and Finance*, 18(1), pp. 27–45. doi: 10.1016/S0261-5606(98)00045-X.

Sarno, L. and Taylor, Mark P (2002) ‘Purchasing power parity and the real exchange rate’, *IMF Staff Papers*, 49(1), pp. 65–105. doi: 10.1080/09603100500389291.

Sarno, L. and Taylor, Mark P. (2002) *The economics of exchange rate*. Cambridge; New York: Cambridge University Press.

Sarno, L., Taylor, M. P. and Chowdhury, I. (2004) ‘Nonlinear dynamics in deviations from the law of one price: A broad-based empirical study’, *Journal of International Money and Finance*, 23(1), pp. 1–25. doi: 10.1016/j.jimonfin.2003.10.004.

Scheinkman, J. A. and LeBaron, B. (1989) ‘Nonlinear dynamics and stock returns’, *Journal of Business*, 62(3), pp. 311–337. doi: 10.1086/296465.

Schnatz, B. (2006) ‘Is reversion to PPP in Euro exchange rates non-linear?’, *European Central Bank Working Paper Series No.682*.

Sercu, P., Uppal, R. and Hulle, C. V. (1995) ‘The exchange rate in the presence of transaction costs: Implications for tests of purchasing power parity’, *Journal of Finance*, 50, pp. 1309–1319.

Silva, E. S. *et al.* (2017) ‘Cross country relations in European tourist arrivals’, *Annals of Tourism Research*, 63, pp. 151–168. doi: 10.1016/j.annals.2017.01.012.

Silva, E. S. *et al.* (2019) ‘Forecasting tourism demand with denoised neural networks’, *Annals of Tourism Research*, 74, pp. 134–154. doi:

10.1016/j.annals.2018.11.006.

Silva, E. S., Hassani, H. and Heravi, S. (2018) 'Modeling European industrial production with multivariate singular spectrum analysis: A cross-industry analysis', *Journal of Forecasting*, 37(1), pp. 371–384. doi: 10.1002/for.2508.

Skalin, J. and Teräsvirta, T. (1999) 'Another look at Swedish business cycles, 1861-1988', *Journal of Applied Econometrics*, 14(4), pp. 359–378.

Small, G. and Wong, R. (2002) 'The validity of forecasting', in *A paper for presentation at the Pacific Rim Real Estate Society International Conference*.

Sobreira, N. and Nunes, L. C. (2016) 'Tests for multiple breaks in the trend with stationary or integrated shocks', *Oxford Bulletin of Economics and Statistics*, 78(3), pp. 394–411.

Song, H. and Li, G. (2008) 'Tourism demand modelling and forecasting-A review of recent research', *Tourism Management*, 29, pp. 203–220. doi: 10.1016/j.tourman.2007.07.016.

Song, H., Witt, S. F. and Jensen, T. C. (2003) 'Tourism forecasting: Accuracy of alternative econometric models', *International Journal of Forecasting*, 19, pp. 123–141. doi: 10.1016/S0169-2070(01)00134-0.

Stock, J. H. and Watson, M. W. (2012) 'Disentangling the channels of the 2007-09 recession', *Brookings Papers on Economic Activity*, pp. 120–157.

Su, C. W., Chang, T. and Liu, Y. S. (2012) 'Revisiting purchasing power parity for African countries: with nonlinear panel unit-root tests', *Applied Economics*, 44(25), pp. 3263–3273. doi: 10.1080/00036846.2011.570730.

Taylor, A. M. and Taylor, M. P. (2004) 'The Purchasing Power Parity debate', *Journal of Economic Perspectives*, 18(4), pp. 135–158. doi: 10.1257/0895330042632744.

Taylor, M. P. (2003) 'Purchasing power parity', *Review of International Economics*, 11(3), pp. 436–452.

Taylor, M. P. (2006) 'Real exchange rates and Purchasing Power Parity: Mean-reversion in economic thought', *Applied Financial Economics*, 16(1–2), pp. 1–17. doi: 10.1080/09603100500390067.

Taylor, M. P., Peel, D. A. and Sarno, L. (2001) 'Nonlinear mean-reversion in real exchange rates: Toward a solution to the purchasing power parity puzzles', *International Economic Review*, 42(4), pp. 1015–1042. doi: 10.1111/1468-2354.00144.

Teräsvirta, T. and Anderson, H. M. (1992) 'Characterizing nonlinearities in business cycles using smooth transition autoregressive models', *Journal of Applied Econometrics*, 7, pp. 5119–5136. doi: 10.1002/jae.3950070509.

Teräsvirta, T., van Dijk, D. and Medeiros, M. C. (2005) 'Linear models, smooth transition autoregressions, and neural networks for forecasting macroeconomic time series: A re-examination', *International Journal of Forecasting*, 21(4), pp. 755–774. doi: 10.1016/j.ijforecast.2005.04.010.

The Japan Times (2014) *Tourism emerges as new economic driver for Japan*. Available at: http://www.japantimes.co.jp/news/2014/08/25/reference/tourism-emerges-new-economic-driver-japan/#.V2HbDTWGYtx (Accessed: 18 September 2020).

The Japan Times (2015) *Inbound Tourism boom*. Available at: https://www.japantimes.co.jp/opinion/2015/06/18/editorials/inbound-tourism-boom/ (Accessed: 18 September 2020).

The Japan Times (2018) *Japan's tourism boom is spreading economic benefits to rural areas: report*. Available at: https://www.japantimes.co.jp/news/2018/06/05/national/japans-tourism-boom-spreading-economic-benefits-rural-areas-report/ (Accessed: 18 September 2020).

Thomakos, D. D., Wang, T. and Wille, L. T. (2002) 'Modeling daily realized futures volatility with singular spectrum analysis', *Physica A: Statistical Mechanics and its Applications*, 312, pp. 505–519. doi: 10.1016/S0378-4371(02)00845-2.

Tideswell, C., Mules, T. and Faulkner, B. (2001) 'An integrative approach to tourism forecasting: A glance in the rearview mirror', *Journal of Travel Research*, 40, pp. 162–171. doi: 10.1177/004728750104000207.

Tong, H. (1978) *On a Threshold Model*. Sijthoff and Noordhoff.

Tong, H. (1980) 'A view of non-linear time series model building', *Time Series (O. D. Anderson, ed.)*., pp. 41–56.

Tong, H. and Lim, K. S. (1980) 'Threshold autoregression , limit cycles and cyclical data', *Journal of the Royal Statistical Society. Series B (Methodological)*. doi: 10.2307/2985164.

Toshinori, M. (1998) *Fundamentals of the new artificial intelligence*. New York: Springer.

Tsay, R. S. (1989) 'Testing and modeling threshold autoregressive processes', *Journal of the American Statistical Association*, 84(405), pp. 231–240. doi: 10.1080/01621459.1989.10478760.

Vanegas, M. (2013) 'Co-integration and error correction estimation to forecast tourism in El Salvador', *Journal of Travel and Tourism Marketing*, 30(6), pp. 523–537. doi: 10.1080/10548408.2013.810992.

Vellido, A., Lisboa, P. and Vaughan, J. (1999) 'Neural networks in business: a survey of applications (1992–1998)', *Expert Systems with Applications*, 17(1), pp. 51–70. doi: 10.1016/S0957-4174(99)00016-0.

Wei, Y. and Chen, M.-C. (2012) 'Forecasting the short-term metro passenger flow with empirical mode decomposition and neural networks', *Transportation Research Part C: Emerging Technologies*, 21(1), pp. 148–162.

Welch, G. and Bishop, G. (1997) 'An introduction to the Kalman Filter', *Department of computer Science, University of North Carolina at Chapel Hill Working Papers*.

Westlund, A. and Öhlén, S. (1991) 'On testing for symmetry in business cycles', *Empirical Economics*, 16(4), pp. 479–502.

Witt, S. F., Newbould, G. D. and Watkins, A. J. (1992) 'Forecasting domestic tourism demand: application to Las Vegas arrivals data', *Journal of Travel Research*, 31(1), pp. 36–41. doi: 10.1177/004728759203100108.

Witt, S. and Song, H. (2000) 'Forecasting future tourism flows', in Medlik, S. . and Lockwood, A. (eds) *Forecasting future tourism flows*. Oxford: Butterworth-Heinemann, pp. 106–118.

Woodward, W. A., Gray, H. L. and Elliott, A. C. (2017) *Applied time series analysis with R*. Second. Boca Raton: CRC Press.

Wu, Z. and Huang, N. E. (2009) 'Ensemble empirical mode decomposition:

A noise-assisted data analysis method', *Advances in Adaptive Data Analysis*, 1(1), pp. 1–41. doi: 10.1142/S1793536909000047.

Yadav, P. K., Pope, P. F. and Paudyal, K. (1994) 'Threshold autoregressive modeling in finance: the price differences of equivalent assets', *Mathematical Finance*, 4(2), pp. 205–221. doi: 10.1111/j.1467-9965.1994.tb00058.x.

Yahya, N. A., Samsudin, R. and Shabri, A. (2017) 'Tourism forecasting using hybrid modified empirical mode decomposition and neural network', *International Journal of Advances in Soft Computing and its Applications*, 9(1), pp. 14–31.

Yao, Y. *et al.* (2018) 'A paired neural network model for tourist arrival forecasting', *Expert Systems with Applications*, 114, pp. 588–614. doi: 10.1016/j.eswa.2018.08.025.

Yoon, G. (2010) 'Nonlinear mean-reversion to purchasing power parity: Exponential smooth transition autoregressive models and stochastic unit root processes', *Applied Economics*, 42(4), pp. 489–496. doi: 10.1080/00036840701604552.

Zhigljavsky, A. (2010) 'Singular Spectrum Analysis for time series: Introduction to this special issue', *Statistics and Its Interface*, 3, pp. 255–258. doi: 10.1007/978-3-642-34913-3_1.

Zhigljavsky, A., Hassani, H. and Heravi, S. (2009) 'Forecasting European industrial production with multivariate singular spectrum analysis', *International Institute of Forecasters*.

Zhou, J. (2010) 'Smooth transition autoregressive models a study of the industrial production index of Sweden', *Upsala Universitet, Sweden, Master Thesis*.